University of Venda

School of Environmental Sciences

Evaluation of Nebulas Gold Deposit in Giyani Greenstone Belt, Limpopo Province, South Africa

Name : Mbofholowo Emmanuel Mavhungu

Student No : 11582603

Supervisor : Dr. Francis Amponsah-Dacosta

Co-Supervisor : Mr. Sphiwe Emmanuel Mhlongo

A Dissertation submitted to the Department of Mining and Environmental Geology, University of Venda for fulfilment of the degree of the Master of Earth Sciences in Mining and Environmental Geology.

May 2018

DECLARATION

I, **Mbofholowo Emmanuel Mavhungu**, student no **11582603** hereby declare that the work presented in this dissertation titled “Evaluation of Nebulas Gold Deposit in Giyani Greenstone Belt, Limpopo Province, South Africa” is my own original contribution and has not been submitted to any institution or published anywhere before. Further, I have acknowledged all sources used and have cited these in reference section of this dissertation. This research is in accordance with University and School guidance on good academic conduct.

…….. ……
Mbofholowo Emmanuel Mavhungu Date

We, the supervisors recommend that this declaration is correct.

Supervisor’ signature ……. Date……
Dr. Francis Amponsah-Dacosta

Co-Supervisor’ signature ……. Date……
Mr. Sphiwe Emmanuel Mhlongo

DEDICATION

For the ancestors and great men who paved the path before me upon whose shoulders I stand. This is also devoted to all my family and relatives.

To Ndivhuwo for her everlasting support, calmness and love.

To my beloved son, Zwivhuya.

To you as a reader.

ABSTRACT

Giyani Greenstone Belt is known to host significant amount of gold of which about 10 tonnes were extracted from the belt in the 19th century. Due to increased gold price and mining practices that make it economic to mine low-grade ore deposits, major gold deposits within the belt have been the main targets for exploration while Nebulas Prospect remain unnoticed. To make the Nebulas Prospect attractive for investment, its gold mineralization potential needed to be investigated.

The main purpose of this study was to conduct assessment of the probable gold mineralization in the Nebulas Prospect and its economic viability. The specific objectives were to establish the gold mineralized zones within the Nebulas Prospect, develop a geological model showing the geometry and placement of gold in the subsurface, establish gold grade distribution and its economic implication, and select the most appropriate and practical mining method for exploitation of the established gold deposit. The research approaches used in achieving these objectives comprised of knowledge driven predictive modelling of Nebulas Prospect to derive prospectivity map demarcating the area with the potential of hosting gold mineralization. Magnetic survey was conducted in geological permissive areas, thereby establishing boundaries of mineralization, both lateral and vertical. Geological and subsurface gold grade distribution were carried out by means of trenching and pitting. The integration of the geological, geophysical and geochemical data using Geosoft 8.5 and ArcGIS 10.5 assisted in development of a gold deposit model that model illustrates distribution and concentration of gold.

Results of the investigation reveals that Banded Iron Formation (BIF) dominates the southern part of the study area while quartz vein and schist dominate the northern part. The application of knowledge driven predictive modelling established mineral prospectivity map for Nebulas Prospect, which narrowed the potential area for further investigation. The area located outside the boundary of prospective area indicated low mineralization potential compared to highly mineralized zone within geological permissive boundary.

The two mineralize zones which exits in the Nebulas Prospect are separated by pegmatite intrusion which is observed from magnetic data presentation. The gold is hosted within BIF, schist and quartz vein. The highest concentration observed value of 10.65 g/t is hosted in serpentine schist and lowest significant of 1.24 g/t in BIF. The gold grades are higher in schists than in BIF and quartz veins. The Nebulas Prospect present significant measured

gold mineral resource with substantial economic potential. The evaluation of the technical aspects of the Nebulas Gold Deposit, which include grade and tonnage was estimated through longitudinal vertical section method. The gold hosted within Banded Iron Formation (BIF) comprise a measured gold resource of 6957.6 t at an average weighted grade of 2.22 g/t Au. However, the gold mineralization hosted within tremolite-mica schist, serpentine schist and quartz veins comprise a measured gold resource of 3919.37 t with average grade of 3.8 g/t Au. The Nebulas Gold Deposit contain a significant grade and tonnage.

At an assumed currently economically mineable cutoff grade 1 g/t Au, Nebulas Prospect has a measured resource of 10877 t at a weighted average grade of 2.79 g/t Au. Analytical hierarchy process (AHP) was used to prioritize the factors affecting mining method selection and ranking of potential mining method, technically appropriate for the established gold deposit in Nebulas Prospect. Open pit mining method was identified as appropriated for extraction of the Nebulas Gold Deposit.

Keywords: Gold mineralization, Predictive modelling, Analytical hierarchy process

ACKNOWLEDGEMENT

Foremost, I would like to express my sincere gratitude to my supervisors Dr. Francis Amponsah-Dacosta and Mr. Siphiwe Emmanuel Mhlongo for the continuous support of my Masters study and research, for their patience, motivation, enthusiasm, and immense knowledge. Their guidance greatly helped me conducting this research and writing of this Dissertation. I could not have imagined having a better supervisors and mentors for my Masters study.

I would like to extend my thanks to those who offered collegial indisputable support and friendly motivation over the years: Ms. Ndivhudzannyi Rembuluwani (Sister-Boss), Mr. Confidence Muzerengi, Mr. Nndanduleni Muavhi (Knova), Mr. Khuthadzo Nndwambi, Mr. Thakhani Ramuhulu, Ms. Gudani Thanyani and Mr. Matamela Mudanalo.

The following sponsors are acknowledged for their funding contribution in making this research successful; Kusile Investments (Pty) Ltd, Council for Geoscience, National Research Foundation (NRF) and University of Venda's Research and Publication Committee (RPC).

I beg to express my very profound gratitude to my parents and to my dearest Ndivhuwo Nemangani, for providing me with unfailing support and continuous encouragement throughout my years of study and during the research process and the write-up of this dissertation. This accomplishment would not have been possible without them. Finally, I thank God almighty for his endless blessings and leading me all the way until the completion of this research project.

TABLE OF CONTENTS

LIST OF FIGURES

LIST OF TABLES

GLOSSARY OF ABBREVIATION AND ACRONYM

3D	- Three Dimensional
AHP	- Analytical Hierarchy Process
ALS	- Australian Laboratory Services
Au	- Gold
BIF	- Banded Iron Formation
CI	- Consistency Index
CR	- Consistency Ration
ESRI	- Environmental Systems Research Institute
GGB	- Giyani Greenstone Belt
GIS	- Geographic Information System
GPS	- Global Positioning System
ICP-AES	- Inductively Coupled Plasma Atomic Emission Spectroscopy
IDW	- Inverse Distance Weighting
mA	- Mining Alternative Method
MCDM	- Multi-criteria Decision Making
MDD	- Mineral Deposit Database
NNS	- Nebulas North Sector
NSS	- Nebulas South Sector
pH	- Potential of Hydrogen
RTP	- Reduction to Pole
SAMREC	- South African Code for the Reporting of Mineral Resources and Mineral Reserves
SI	- Structural Index
USA	- United State of America
USBM	- United States Bureau of Mines
USGS	- United States Geological Survey
UTM	- Universal Transverse Mercator
WGS 84	- World Geodetic System of 1984

GLOSSARY OF UNITS OF MEAUREMENTS

%	- percent
°	- degree
°C	- degree Celsius
µm	- micrometer
g	- gram
g/m^3	- gram per cubic meter
g/t	- gram per tonne
kg	- kilogram
km	- kilometer
m	- meter
m^2	- square meter
m^3	- cubic meter
mm	- millimeter
nT	- nanotesla
ppm	- parts per million
Sp. Gr.	- specific gravity
t	- tonne

CHAPTER ONE

INTRODUCTION

1.1 Background of the Research

The Giyani Greenstone Belt (GGB) has been for many years a mining region for gold (Au). There are 55 known gold occurrences in the belt, 20 of them are inactive mines and 35 are prospects (Billay et al., 2014). About 10 tonnes of gold were produced from the belt between 1886 and 1990 (Steenkamp and Clark-Mosterrt, 2012). Almost 97% of gold recovered from the GGB come from six of the currently inactive mines, namely; Klein Letaba, Louis Moore, Osprey, Fumani, Franke and Birthday (Carranza et al., 2015).

The GGB has been subjected to intense tectonic events which are suspected to have led to gold mineralization in the belt (Kröner et al., 2000). The mineral potential of the belt has been documented by many authors and the general findings where that, gold mineralization in the GGB is associated with quartz veins with minor sulphides, quartz-sulphide replacement veins, carbonate (calcite) veins or Banded Iron Formation (BIF) (Kramers et al., 2014; Kröner et al., 2000; McCourt and van Reenen, 1992; Sadeghi et al., 2015; Steenkamp and Clark-Mosterrt, 2012).

Exposed outcrops of BIF have previously been used as a guide in gold explorations in the belt (Steenkamp and Clark-Mosterrt, 2012). This is because BIF is considered the main host rock for gold mineralization in the area. Nevertheless, most of the known prospects and deposits are hosted by mafic rocks (Sadeghi et al., 2015). The lithological domains of the GGB hardly outcrop due to superimposed thick younger gravels, restricting the potential to correlate the various sections across the belt (Kröner et al., 2000). This has resulted to limited availability of consistent prospective lithological map of the GGB.

According to Carranza et al. (2015), the limited exposure, patchy deposits, poor metal recovery, weak market viability and environmental requirements has led to exploration and mining companies abandoning the GGB, thus leaving it underexplored. However, Steenkamp and Clark-Mosterrt (2012) suggests that the discovery of continuous, well defined reefs offering easier mining in the Witwatersrand Goldfields at approximately the same time as the Sutherland Goldfields (now Giyani Greenstone Belt) was a major contributor for abandoning the belt by exploration companies. Even though the GGB has not been mined for many years now, there is a renewed interest in mining companies to re-evaluate gold deposits within the GGB (Giyani-Gold, 2010). Some of the factors responsible

for this interest are the changes in gold prices and mining practices that make it economic to mine the low-grade deposits. Furthermore, the revived interest of the mining companies to explore for low grade deposits is that there is a decrease in the inventory of high-grade; high-quality deposits. Consequently, at the current discovery rates, the industry is struggling to meet the future demand for the metal (Schodde, 2011).

With regards to prospectivity, there are preserved historic workings (such as trenches and pits) that exists in various prospects within the GGB (including Nebulas Prospect). This gives an indication that trenching and pitting were the foremost gold exploration techniques employed in the GGB. There is limited indication and information which relates to other prospecting work that were previously carried out in the belt (including drilling).

Small to large-scale underground mining techniques were previously used to exploit the gold in the GGB. Small-scale operations done in the past targeted free gold which was recovered through gravity separation methods. On the other hand, recovery of refractory gold during the period when most mines were operational in the belt proved to be difficult due to the absence of advanced processing and recovering methods (Steenkamp and Clark-Mosterrt, 2012).

Small-scale mining offers several potential benefits such as mining of sub-economic resources (Saldarriaga-Isaza et al., 2015). The reason being that it is mobile, flexible, and requires little capital compared to large-scale operations (Danielson, 2003). The adoption of small-scale mining may offer rural employment which has a potential to reduce rural migration to urban areas. Furthermore, small-scale operations tend to be locally owned, which retains capital in the community. Finally, it is complementary to existing social structures in developing countries (Marin et al., 2015). In view of these, detailed exploration of the Nebulas Prospect was conducted to fill the gap of missing exploration and mining information. This may warrant development of small-scale mining to extract gold once again in this part of the GGB.

1.2 Statement of the Problem

The Giyani Greenstone Belt (GGB) has not been explored to a satisfying extent. Increasing gold price in recent decade has attracted few exploration companies to explore the portion of the belt with more interest on previously recognized deposits around the abandoned mine such as Klein Letaba and Louis Moore. Despite that, this has left potential gold prospects such as Nebulas Prospect unnoticed. Previous exploration activities such as trenches and pits which date to 1955 exist in the Nebulas Prospect. However, there is paucity of

information regarding gold distribution and concentration based on these activities. Feasibility sampling of the site, conducted as part of this research indicated significant occurrence of gold concentration ranging from 0.05 – 6.5 ppm. This required more detailed studies to establish the extent of the gold occurrence and its economic significance, thus the current research was conducted.

1.3 Objectives of the Research

The main aim of this research was to conduct assessment of the probable gold mineralization in the Nebulas Prospect and its economic significance.

The specific objectives were to:

- Establish the gold mineralized zones within the Nebulas Prospect.
- Develop a 3D geological model to illustrate the geometry and placement of gold in the subsurface.
- Asses the distribution of the grade of gold and its economic implications.
- Select the most appropriate and practical mining method for the exploitation of the gold deposit.

1.4 Research Questions

This section presents questions to be answered to fulfill the objectives of this research. These questions are:

- Which are the prospective areas for gold mineralization at Nebulas Prospect?
- What is the grade of the gold and its distribution in the study area?
- Which are the host rocks for gold mineralization within the study area?
- What is the economic potential of the Nebulas Prospect?
- Which mining method would be practically appropriate for mining of the gold deposit?

1.5 Justification of the Study

South Africa was once the largest producer of Gold in the world and large amount of this mineral has been exploited from the Witwatersrand Basin. However, gold resources in this basin are slowly depleting, thus there is a need to refocus attention to other gold bearing localities. One of the prospective areas in the country is the GGB. This study aims to provide the baseline information regarding the gold distribution within the Nebulas Prospect in the GGB.

Few mines within the GGB have been rehabilitated while others are not. In abandoned mine site where mine shaft was not treated to prevent access to underground mine workings, illegal miners take the opportunity to conduct their illegal activities within the old pits and underground mine working. It is important to note that these illegal miners have no intention of discontinuing such activities due to lack of job opportunities in the area. According to Steenkamp and Clark-Mosterrt (2012), GGB host economic sized gold deposits, but these are currently not being exploited. Evaluation of such deposits may prove to be economic, thus warranting chances of developing a mining operation in the area.

Responsible small-scale mining requires a certain amount of investment which is less compared to those of large-scale operations. However, there are challenges of obtaining capital investments from investors because of the absence of a guarantee of return and financial success of these projects. Investors require reserve/resource information of the commodity of interest which assist them in their decisions on whether to invest or not. It is therefore through this study that the nature of the gold resource in the study area can be established.

Small-scale mining operations are mostly conducted without prior geological exploration. This study will establish more detailed information required for planning process rather than only relying on previous operation and instinct. Furthermore, it will reduce the level of uncertainty and restore credibility and positive image in small scale sector to the investors. Knowledge of the gold deposit gained in this research will assist in identification of suitable mining method for the deposit. Developing a gold mine in the area will also boost the local economy of the Giyani area through job creation. Techniques used in the evaluation of Nebulas Gold Deposit will also be used for exploration of similar deposit in the belt.

1.6 Description of the Study Area

This section provides the description of the study area in terms of the geographical setting, climatic condition, topography, drainage and land use.

1.6.1 Location

Nebulas Prospect shown in Figure 1.1 is part of the Giyani Greenstone Belt (GGB), located 15 km north east of Giyani Town and 5 km north of Nsami Dam in Limpopo Province of South Africa. It falls within the Greater Giyani Municipal council area of the Mopani District. Nebulas Prospect lies in the northwestern part of the Giyani Greenstone Belt that is located at the northern edge of the Kaapvaal craton where prograde metamorphism is known to have occurred.

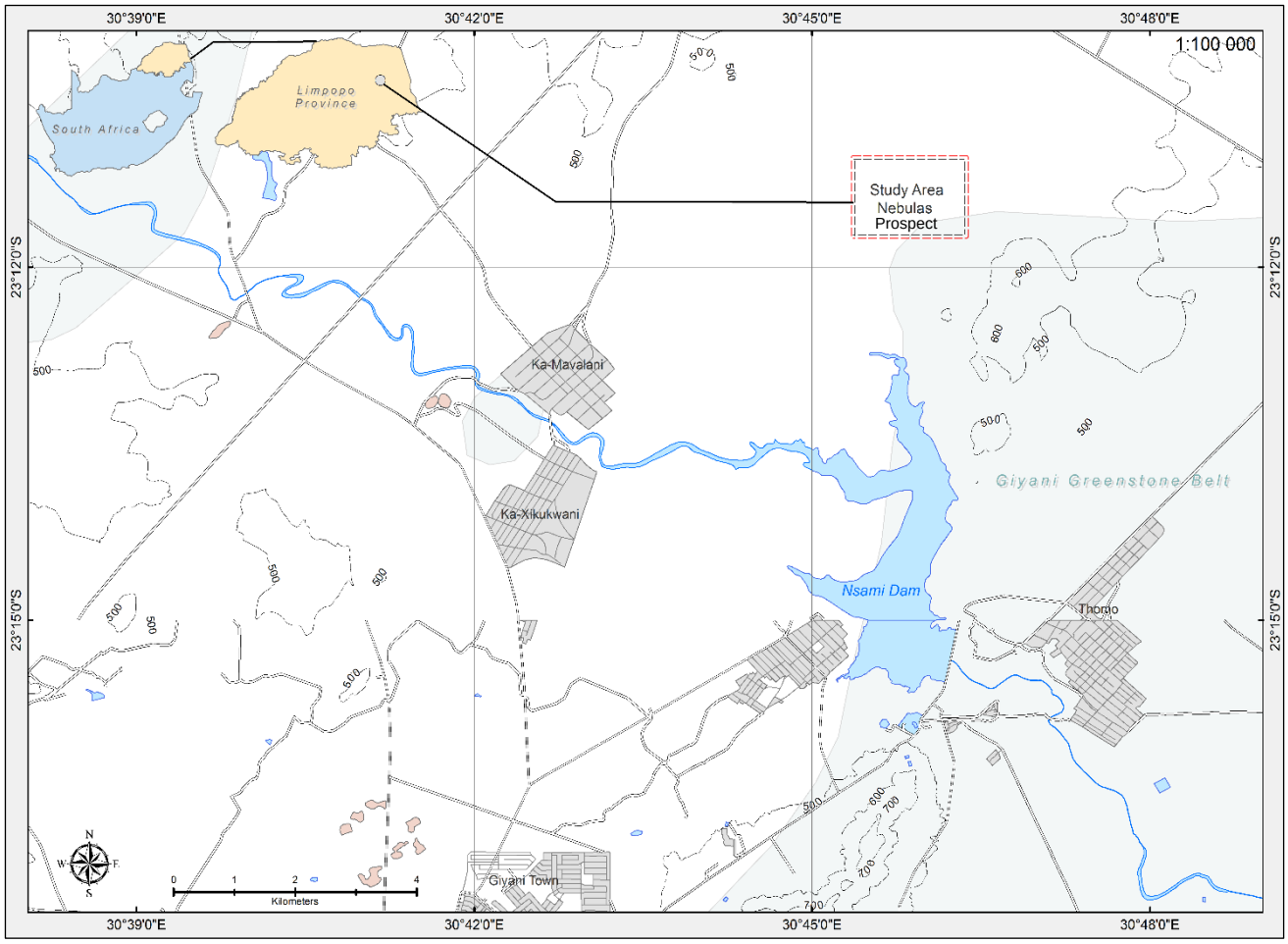

Figure 1.1: Location of the Nebulas Prospect area within the Giyani Greenstone Belt.

1.6.2 Climatic condition

The Nebulas Prospect is situated within the subtropical zone. The climate setting comprises of two predominant seasons, namely summer and winter. It is characterized by summers temperatures that exceeds 36°C and winters which go to the maximum of 22°C (Du Plessis, 2012). Summers are hot during the day and night, winters are mild during the day and cold during the night. Rainfall season is between September and March, while the winter season starts from April to August. In 2000 the area received extensive rainfall leading to flooding which lasted for more than 3 months and contributed to burial of some mining activities (trenches and pits) and subsidence to some abandoned mines within the belt (Du Plessis, 2012).

1.6.3 Topography and drainage

The topographic relief varies from zones of high mountains to zones of low mountains with prominent hills trending from east of Nsami Dam to Giyani Town. The area is dominated by dendritic pattern of non-perennial and perennial channels with non-perennial pools.

1.6.4 Land use

The Giyani area was known for gold mining. However, there are no mining activities taking place at the present. The area has been (in the past) a low-level producer of gold, base and industrial minerals (Du Plessis, 2012). Some mine and plant infrastructure can still be found in the area (Steenkamp and Clark-Mosterrt, 2012). The magnesite dumps are prominent on the northwestern margin of the belt. There are also agricultural practices which take place in the area. The land in the study area is now used for grazing. Exploration activities in the area are known to exist, but no evidence of this can be shown in the recent past.

1.7 Organization of the Dissertation

The research focus on identifying potential mineralized areas within the Nebulas Prospects through application of geological, geochemical and magnetic methods of investigation. Trenching and pitting were considered as techniques for data collection for evaluating of mineralization potential of the Nebulas Prospect area in the GGB.

The work presented in this section is divided into six chapters. Chapter One gives a brief introduction of the study. Literature which is aligned to the research is presented in Chapter Two. Chapter Three describes material and methods implemented as part of the research methodology. In Chapter Four, presentation and interpretation of field data is accomplished for characterization of Nebulas Prospect. Gold evaluation and selection of mining methods for the Nebulas Gold Deposit is presented in Chapter Five. Chapter Six focuses on discussing the findings of research and give recommendations for further research and development.

CHAPTER TWO

LITERATURE REVIEW

Evaluation of gold for a disregarded prospect such as Nebulas Prospect required detailed analysis of literature pertaining to the geology and mineralization of gold in the belt. This Chapter focuses on the issues interrelated to this research including history of exploration, mining and mineralization of gold (Au) in the belt. To provide a description, summary and critical evaluation, literature on exploration techniques, mineral evaluation methods and mining selection methods was broadly reviewed in relation to the research problem.

2.1 Archean Greenstone Belts

Archean greenstones are rocks approximately greater than 2.5 Ga in age and are exposed in small areas on all continents. There are three rock associations in Archean provinces, which are classified in order of relative abundance; the granite-greenstone association, the high-grade association, and the cratonic basin association (Lelubre, 1982).

The granite greenstone association is characterized by supracrustal successions, comprised dominantly of mafic volcanic rocks, known as greenstone belts, immersed in a sea of granitic rocks. This association is dominant in Archean provinces in North America, southern Africa, and Australia (Lelubre, 1982). The high-grade association, dominates in Archean provinces in central and northern Africa, Greenland, and in the Russian Federation, is characterized by gneiss-migmatite-granulite complexes, layered igneous intrusions, and high-grade supracrustal remnants (Metelka et al., 2011; Ugarkar et al., 2016). The cratonic basin association has thus far been defined only in the Kaapvaal province in South Africa by Anhaeusser (2014) and is characterized by a succession composed dominantly of quartzites, shales and carbonates with smaller amounts of volcanic rock. The Giyani Greenstone Belts is characterized by supracrustal association and high-grade association (Kröner et al., 2000).

Archean granite-greenstone terranes are composed in large part of granitic and gneissic rocks (80 - 90%) which surround and, in part, intrude greenstone belts which comprise the remainder. The most prominent feature of these terranes is their world-wide resemblances. Archean mineral deposit of nickel, silver, gold, copper and chrome occur in or closely associated with greenstone belts (Lelubre, 1982).

2.1.1 Giyani Greenstone Belt

The Giyani Greenstone Belt shown in Figure 2.1 is located on the Northern Kaapvaal Craton immediately adjacent to the Hout River shear zone (Kramers et al., 2014) close to the contact with the Limpopo Belt. The GGB is contiguous in its eastern region, but to the west of the Klein Letaba River, it consists of a northern (Khavagari) and a southern (Lwaji) arm, which are separated by a granitoid-gneiss zone (McCourt and van Reenen, 1992; McCourt and Vearncombe, 1992). Gravity and geoelectric profiles across the belt show a 4 km down dip extension into the crust for the Lwaji, and a mere 1 km depth for the Khavagari arm, whereas the central portion of the belt is very shallow (de Beer and Stettler, 1992; Kramers et al., 2014). The GGB is mainly made up of supracrustal rocks of the Giyani Group which consists mainly of mafic-ultramafic rocks. The mafic rocks dominate over ultramafic rocks, with felsic and sedimentary with minor intercalations of metasedimentary rocks and felsic lavas rocks playing only a minor role (Kröner et al., 2000).

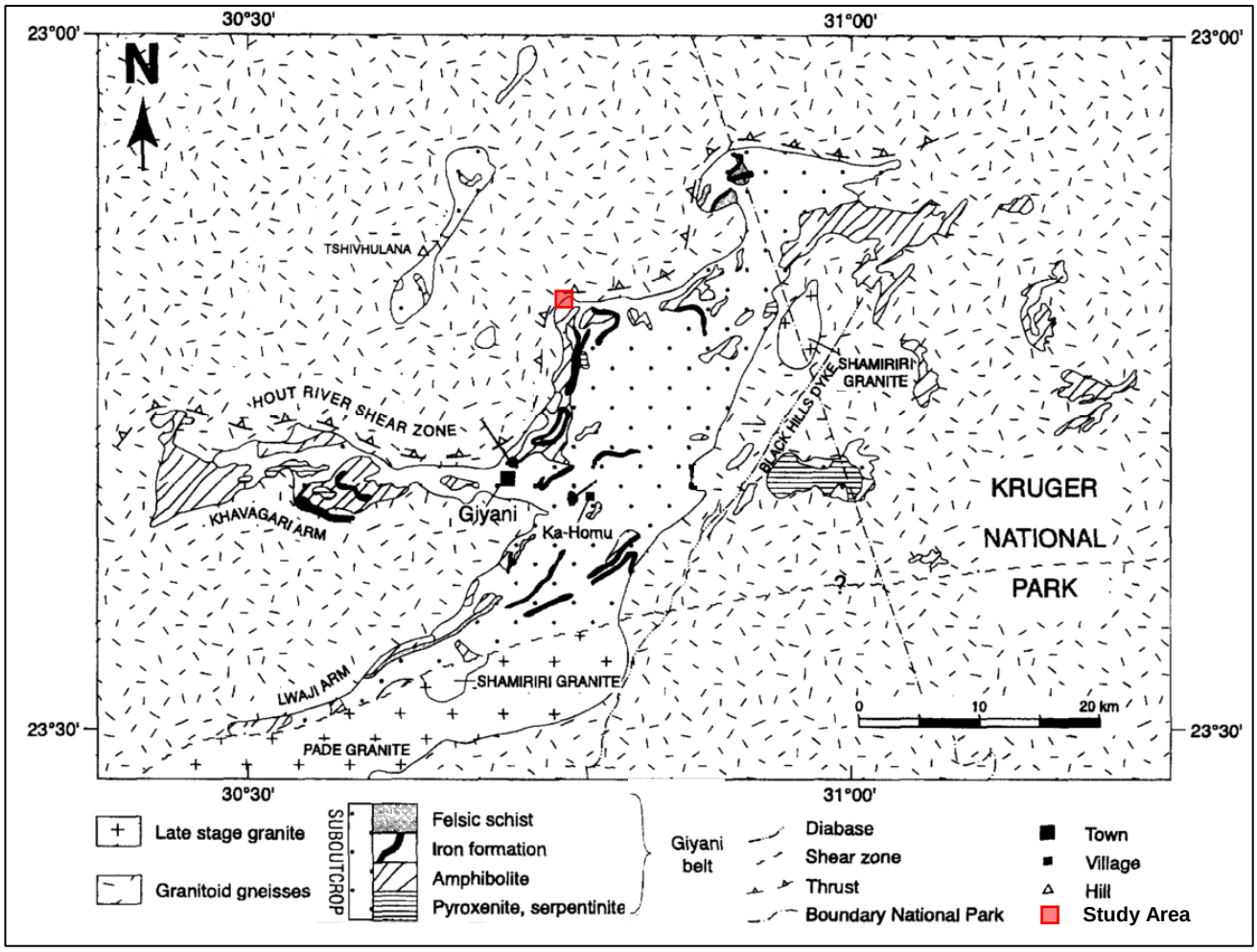

Figure 2.2: Geological map of Giyani Greenstone Belt and surrounding granitoids areas (Source: Kröner et al., 2000).

Central

In the central part of the belt, the succession commences with ultramafic schists containing tremolite, talc, chlorite or hornblende in varying proportions. These are followed by a thin unit of felsic to mafic volcanics and sedimentary rocks (Kröner et al., 2000). There is interactions of rocks and iron formation with schists which are followed by thin unit made up of mafic volcanic felsic volcanic and sedimentary rock which includes quartz, sericite-schist, rhyolite, ferruginous quartz and iron formations (McCourt and van Reenen, 1992). This unit overlain by succession is characterized by repeated cycles of ultramafic and mafic rocks capped by iron formation which grades into a ferruginous dolomite at the top (Kröner et al., 2000). Mafic rocks are presented by the massive and pillowed hornblende bearing amphibole (Kröner et al., 2000; McCourt and van Reenen, 1992; McCourt and Vearncombe, 1992). The Nebulas Prospect is located at the central part of the belt as shown in Figure 2.1.

Khavagari arm

Khavagari arm is located on the south west part of the Giyani group, characterized by large body of altered dunite as structural base of succession (Kröner et al., 2000). The base represents cumulus basal part of a layered differentiated ultramafic complex. In the ultramafic body, magnesite is well developed, and it is covered by thick siliceous crust of birbirite. The body of dunite is followed by thick sequence of ultramafic schists, overlain by metasedimentary rocks (McCourt and van Reenen, 1992).

Lwaji arm

Lwaji arm is comprised of ultramafic rocks in varying proportions, which include tremolite, talc, chlorite and amphibolite schists. Various mafic units include massive and pillowed hornblende-amphibolite (de Beer and Stettler, 1992; Kramers et al., 2014).. The structural base of Lwaji arm is formed by ultramafic schists which pass upwards into a succession of meta-sediments including phyllite, quartz-sericite-chlorite schist and quartzite (de Wit et al., 1992; Kröner et al., 2000).

2.2 History of Gold Exploration and Mining in Giyani

The Sutherland Greenstone Belt now known as the called Giyani Greenstone Belt (GGB) was discovered by prospectors, Sutherland and Button in 1870. The gold rush in the area started in 1886 (Steenkamp and Clark-Mosterrt, 2012) and can be related to the gold rush in the Barberton greenstone belt. The second Anglo-Boer War interrupted mining activities within

the belt. After the war focus of the world and attention of pioneers shifted to the rich gold field of Witwatersrand leaving the belt under-explored (Steenkamp and Clark-Mosterrt, 2012).

Few prospects were developed into full-fledged mines and these include Giant Reefs (Fumani), Louis Moore, Klein Letaba, Franke, Golden Osprey and Birthday. The rest of the sites were never developed beyond small-scale operations. A series of factors contributed to the decline in exploration and mining activity in this goldfield. The factors are related to market viability, recovery and environmental constraints (Carranza et al., 2015; Sadeghi et al., 2015).

The old trench exploration workings focused on quartz, schist and Banded Iron Formation (BIF) outcrops. Steenkamp and Clark-Mosterrt (2012) indicated that prospects which yielded encouraging results from trenching were further developed using open pit or underground operations on the small to medium scale, developed on-reef.

Gold recovery was focused on free gold through gravity separation methods. Free gold is contained in small amounts in the outcrops and surrounding oxidized zones, but the deeper gold mineralization is mainly refractory (Steenkamp and Clark-Mosterrt, 2012). The processing and treatment of the refractory ore required ultra-fine milling, cyanidation at controlled pH, dissolved oxygen and cyanide concentration which were not developed at the time and could have been too expensive for small scale operations (Swash, 1988).

2.3 Gold Ore Deposit Classifications

Gold deposits classifications are an essential framework for designing exploration strategies, evaluating prospects and performing resource assessment of selected areas (Robert et al., 1997). Different authors have developed schemes to subsets gold deposits and this include epithermal, intrusion-related, bulk-mineable or epigenetic Archean. Lode gold deposits are associated with formation of mountains, which are accompanied by tectonism. The few globally recognized types of lode gold deposit include paleo-placer, skarn, greenstone-hosted quartz-carbonate vein, porphyry gold and iron formation hosted (Goldfarb et al., 2001; Liu et al., 2016; Ren et al., 2016; Vaughan, 2004). Gold in Giyani is associated with mafic to ultramafic rocks, banded iron formations and quartz veins (McCourt and van Reenen, 1992)

2.3.1 Gold deposit and mineralization within the GGB

Gold mineralization occurs in lager parts of the GGB. The characteristics and genesis of gold mineralization in the GGB have been studied mainly from six gold mines namely; Klein Letaba, Louis Moore, Osprey, Fumani, Franke and Birthday and from four prospects which are

Doornhoek, West-59, Nsuku Hill and Gemsbok (Carranza et al., 2015). Information about gold mineralization styles in the Nebulas Prospect is limited.

Gold mineralization in the GGB is associated with quartz veins with minor sulphides, BIFs, quartz-sulphide replacement veins or carbonate (calcite) veins and mafic metavolcanics (McCourt and van Reenen, 1992). Gold in most deposits is closely associated with sulphides in quartz veins. However, in some areas it occurs as free-milling inclusions (Carranza et al., 2015). The sulphides mainly comprise pyrrhotite, chalcopyrite, pyrite and arsenopyrite, with the last being the most predominant in BIF-hosted deposits. However, the sulphide mineralogy of the six major mines and the Doornhoek Prospect is similar despite the clear differences in host lithology.

The deposits are structurally controlled with mineralization at the Fumani, Klein Letaba and Birthday Mines as well as several abandoned deposits unequivocally linked to the occurrence of north-dipping oblique to reverse sense ductile shear zones (McCourt and van Reenen, 1992; McCourt and Vearncombe, 1992). Mineral assemblages in auriferous metapelites suggest that the gold mineralization is late and related to the retrograde metamorphism of amphibolite and granulite facies rocks by fluid movement along ductile shear zones (de Wit et al., 1992; McCourt and van Reenen, 1992; Smit et al., 2014; Van Reenen et al., 2014).

2.4 Mineral Exploration Techniques

Mineral exploration is a strategic activity to locate and define an economic mineable mineral commodity. It endeavors to find commercially viable concentrations of mineral deposits for mining purposes (Carranza, 2009). A Prospect may be defined as a restricted volume of ground that is considered to have the possibility of directly hosting an ore body (Marjoribanks, 2010). The Nebulas Prospect is characterized by old exploration activities such as trenches and pits with the anomalous gold concentration.

There are various stages in mineral exploration and these include; area selection, target generation, resource evaluation and reserve definition. These require enormous capital investments that can only be recovered through the discovery of large deposit (Marin et al., 2015; Seccatore et al., 2014). However, the GGB comprise patchy gold deposits (Carranza et al., 2015).

2.4.1 Remote sensing and GIS in gold exploration

Systematic evaluation, interpretation and identification of key elements from photographs have multidimension applications in mineral exploration. The key information includes soil

and rock types, structures like fold closure, faults, shears and lineaments, and surface indicators like presence of old mining activities. This information contributes toward conceptualizing the existence of minerals and possible exploration targets. The approach is more significant particularly for mineral deposits occurring at remote inaccessible areas (Haldar, 2013). The Giyani Greenstone Belt (GGB) is dominantly covered with soil limiting exposure of outcrops on the surface (Billay et al., 2014). However, surface indicators like old exploration activities including pits and trenches within the belt can be observed from aerial photographs indicating possible exploration targets.

With the development of computers, multispectral sensors and sophisticated analysis software, mineral exploration complexities and risks are minimized. Remote sensing allows that target generation based on the analysis of various spectral band of images which meet the spectral signatures related to mineralization parameters such as alteration zones to be conducted (Kirilin et al., 2015).

Geographic information system applications in mineral exploration is being widely used internationally. GIS platform is a great tool in establishing Mineral Deposit Database (MDD) for an area, region or country by integration of all available geoscientific data into digital single and unified database (Haldar, 2013). Geoscientific data includes various data sets such as geological, geochemical, geophysical and remotely sensed data which can be integrated to determine spatial association between them and generate exploration target influenced with such data sets (Prol-Ledesma, 2000). Formation of mineral deposit within the Giyani Greenstone Belt is too complex to permit the application of mathematical analytical models alone; therefore, the knowledge of an expert is required to provide the proper weighing of the available evidence and their integration in a predictive map of mineral deposit potential (Porwal and Carranza, 2015; Prol-Ledesma, 2000).

2.4.2 Geological mapping in mineral exploration

The preparation of a geological map is one of the key elements in exploration of a prospect. It is invariably the first step in any mineral exploration project and it remains an important control document for all subsequent stages of exploration and mining, including, trenching, drilling, geochemistry, geophysics and mine planning (Marjoribanks, 2010).

Maps and sections are essential tools in visualizing spatial, three dimensional, and geological relationships. They allow theories on ore deposit controls to be applied and lead to predictions to be made on the location, size, shape and grade of potential ore bodies (Zoheir and Emam, 2012). Geologic mapping involves plotting the position and attitude of the various rock units,

faults, and folds on a base map. Geologic maps are useful in investigation of mineral resources (Matthew, 2004).

The quality and scale of the geological map vary with the importance of the program and the finance available. The process of geological mapping of mineral prospects is similar to that of general geological mapping, but is more intensive (Moon et al., 2009). During the geological mapping of a mineral prospect, every significant rock outcrop in the area is identified and outlined on the map. The substantial rock outcrop associated with gold mineralization in the GGB include mafic to ultramafic rocks, banded iron formations and quartz veins (Billay et al., 2014; Carranza et al., 2015; Kröner et al., 2000 and Sadeghi et al. 2015). According to Billay et al. (2014) and Carranza et al. (2015) most the GGB covered with soil restricting exposure of outcrops on the surface, consequently leading to limited stratigraphic correlation in the GGB.

2.4.3 Geophysical methods in gold exploration

Various geophysical methods are used in mineral exploration stages depending on the physical characteristics of the target deposit. Geophysical studies are always quantitative and involve real measurements based on the variation of response pattern or contrast of propagating waves passing through non-homogeneous medium (Telford et al., 1990). The propagation parameters are seismicity, density, magnetic susceptibility, electrical conductivity, resistivity, electromagnetic and radiometric radiance. The measures of variation are with respect to either position of the object such as strength of magnetic field along a profile or function of time such as propagation of seismic waves (Haldar, 2013; Telford et al., 1990).

Magnetic survey as a tool for gold exploration

Many authors such as Carranza et al. (2015), Kramers et al. (2014), Kröner et al. (2000), Sadeghi et al. (2015) and Steenkamp and Clark-Mosterrt (2012) indicated that gold mineralization within the GGB is associated with BIFs and sulphide minerals which are generally magnetic. Investigation of such rocks which are not exposed to the surface maybe accomplished by carrying out a magnetic survey.

Magnetic survey is mostly applied in investigating the physical properties of geological formation based on the contrast in the magnetic susceptibility of the rocks (Carbonel et al., 2013; Metelka et al., 2011). BIF and ultramafic rock of the GGB which may host gold are expected to be having a significant magnetic susceptibility contrast, thus making it easily to

recognize them from magnetic anomaly maps. A magnetic approach is therefore useful to constrain associated gold mineralization host rocks.

The collection, processing, interpolation and interpretation of complex geophysical data are cumbersome with computing limitations (Haldar, 2013; Hoover et al., 1994). Development of information systems such a Geosoft Oasis Montaj allowed improved efficiency and faster data processing. Various mathematical techniques, such as Fourier analysis, convolution, cross-correlation, digital filtering, are applied to maximize the signal content useful for geological interpretation (Geosoft, 2004; Plessis and Joubert, 2009). The digital data processing and interpretation simulate an image or model of the subsurface structure. Analytical signal and Euler 3D convolution tools can be applied to determine depth and type of the geological structure present in the area of investigation (Telford et al., 1990).

The Nebulas Prospect is characterized by few opened trenches and pits, however there are possibilities of some existing but buried as the prospect date to 1955. Sarris et al. (2004) showed that magnetic methods are best suited for finding features that contrast with the surrounding soils in the concentration of the magnetic minerals they contain. Features such as pits, trenches, hearths, kilns, burned soils, habitation structures, and ditches filled with organic remains alter the magnetic susceptibility of the soil and are good targets for magnetic surveys.

2.4.4 Predictive modeling of mineral exploration targets

In searching for mineral deposit, mainly of economic interest, different techniques are employed in various stages of exploration. Phases of exploration include but not limited to area selection and target generation (Carranza, 2009). Area selection allows characterization of permissive regions within the Nebulas area, target generation demarcates within permissive, prospective area within the Nebulas area for further investigation until gold deposit is discovered based on exploration models for gold and relevant thematic geoscience data sets such as geological, geochemical and geophysical anomalies.

Target generation involves collection, analysis and integration of various thematic geoscience data sets to extract pieces of spatial geo-information, geological, geochemical and/or geophysical anomalies associated with gold deposits and prospective areas defined by intersections of such anomalies. The process of analyzing and integrating such pieces of spatial geo-information is called predictive modeling (Carranza, 2009; Carranza et al., 2015).

Application of Boolean logic modelling

In the application of Boolean logic to mineral prospectivity mapping, classes of attributes of spatial data that meet the condition of a prospectivity recognition criterion are labelled TRUE (or given a class score of 1), otherwise, they are labelled FALSE (or given a class score of 0). Thus, a Boolean evidential map contains only class scores of 0 and 1. Class scores of 0 and 1 in a Boolean evidential map are only symbolic and non-numeric (Cheng and Thompson, 2016; Iza et al., 2016). Giyani Greenstone Belt comprise of different rock types and intense geological structure, and classing of lithology and structures associated with gold mineralization is significant to effectively delineate prospective area.

Boolean evidential maps are combined logically according to a network of steps (inference network), which reflect inferences about the inter-relationships of processes that control the occurrence of a mineral deposits and spatial features that indicate the presence of that mineral deposits (Carranza, 2009). Every step, whereby at least two evidential maps are combined, represents a hypothesis of inter-relationship between two sets of processes that control the occurrence of a sits and/or spatial features that indicate the presence of the mineral deposit (Prol-Ledesma, 2000; Žalik et al., 2017).

A Boolean inference network makes use of set operators such as (AND) and (OR). The (AND) (or intersection) operator is used if it is considered that at least two sets of spatial evidence must be present together to provide support to the proposition under examination (Iza et al., 2016). The OR (or union) operator is used if it is considered that either one of at least two sets of spatial evidence are sufficient to provide support to the proposition under examination. Boolean logic modeling is not exclusive to using only the (AND) and (OR) operators, although the other Boolean operators (NOT and XOR) are not commonly applied in GIS-based knowledge-driven mineral prospectivity mapping. The output of combining evidential maps via Boolean logic modeling is a map with two classes, one class represent locations where all or most of the prospectivity recognition criteria are satisfied, whilst the other class represents locations where none of the prospectivity recognition criteria is satisfied (Carranza, 2009).

Binary index overlay modeling

In binary index overlay modeling, attributes or classes of attributes of spatial data that satisfy a prospectivity recognition criterion are assigned a class score of 1; otherwise, they are assigned a class score of 0. Therefore, a binary index map is like a Boolean map, except that the values in the former are both symbolic and numeric. Binary index map is amenable to arithmetic operations (Sten et al., 2016). Consequently, each binary evidential map B_i ($i =$

$1,2,\ldots,n$) can be given (multiplied with) a numerical weight W_i based on expert judgment of the relative importance of a set of indicative geological features represented by an evidential map with respect to the proposition under examination (Asadi and Hale, 2001). The weighted binary evidential maps are combined using equation (2.1), which calculates an average score, S, for each location.

$$S = \frac{\sum_i^n W_i B_i}{\sum_i^n W_i} \qquad (2.1)$$

Where: W_i is weight of each B_i ($i = 1,2,\ldots,n$) binary evidential map. In the output map S, each location or pixel takes on values ranging from 0 (i.e., completely non-prospective) to 1 (i.e., completely prospective). Even though the input maps only have two classes, the output map can have intermediate prospectivity values, which is more intuitive than the output in Boolean logic modeling.

Assignment of meaningful weights to individual evidential maps is a highly subjective exercise and it may involve a trial-and-error procedure, even in the case when real expert knowledge is available particularly from different experts. The difficulty lies in deciding objectively and simultaneously how much more important or how much less important is one evidential map compared to every other evidential map (Carranza, 2009).

2.4.5 The use of trenches and pits in mineral exploration

According to Marjoribanks (2010), pits and trenches can be a quick and cheap way of obtaining lithological, structural and assay information in areas of shallow cover. Trenches which exist within the Giyani Greenstone Belt were used as a method of exploring shallow deposit. Trenches are usually employed to expose steep dipping bedrock buried below shallow overburden and are normally dug across the strike of the rocks or mineral zone being tested.

Trenches are an excellent adjunct to drilling programs, where the structural data from trench mapping are needed to complement the lithological information obtained from the drill cuttings. To ensure safer and convenient subsequent mapping and sampling, the following attentions outlined by Marjoribanks (2010) was adopted during trenching;

- Cut back both sides of the top of the trench for one bucket width and to a depth of 50–100 cm to prevents loose unconsolidated surface material from falling into the trench and on to the head of any geologist below.

- Stack all topsoil and any loose surface material from the trench on one side of the opening; stack all bedrock material to the other side. This will facilitate in making a quick assessment of the trench material from the bedrock spoil heaps and permit a bulk sample to be taken if required. When re-filling the trench (a normal environmental requirement) the spoil should be replaced in reverse order so that the topsoil is preserved on top.

- When the trench becomes deeper and more than 50 m long, an access ramp will be provided at its midpoint.

Pitting is usually employed to test shallow, extensive, flat-lying bodies of mineralization. Pitting offers advantage over pattern-drilling program on the same deposit by providing a very large volume sample (Haldar, 2013; Marjoribanks, 2010). Large sample sizes are necessary to overcome problems of variable grade distribution, which are a characteristic feature of such deposits.

2.4.6 Geostatistical modelling in mineral exploration

There is no objective way to measure the reliability of the estimation. This shortcoming is however maneuvered by borrowing techniques from formal statistical theory. These include sample mean, range, standard deviation, variance, frequency distribution, histogram plot, correlation coefficients, analysis of variance, t-test, and f-test, trend analysis and distance inverse for univariate and multivariate elements (Bohling, 2005; Johnston et al., 2003).

According to ESRI (2017), Geostatistics is a class of statistics used to analyze and predict the values associated with spatial or spatiotemporal phenomena. Many geostatistical tools were originally developed to predict probability distributions of ore grades for mining operations as a practical means to describe spatial patterns and interpolate values for locations where samples were not taken. Geostatistics is the most efficient and powerful framework to characterize, estimate and manage mineral resource (Geovariance, 2017). It can be used at all stages of the mine life cycle, from exploration (to quantify mineral resources and evaluate the project's economic feasibility) to development, production and even for site remediation. It can be applied to a deposit modelling and its delamination, resource/reserve calculation assessment of uncertainty of resources/reserves estimation, optimal drill holes and samples spacing (Kokesz, 2006). Geostatistics offers a wide range of methodologies adapted to all commodities and styles of deposits (Clark and Harper, 2007; ESRI, 2017; Geovariance, 2017) and include but not limited to interpolation (kriging) and simulation (variogram).

2.5 Evaluation of Mineral Resource and Reserve

Mineral resources and ore reserves are defined by the quantity and quality of in situ concentration of material in or on the Earth's crust. The resources and reserves exist within well-defined 3D mineralized envelopes (Haldar, 2013). A mineral reserve, which is a modified subset of a measured or indicated mineral resource, needs consideration of all factors affecting extraction, including mining, metallurgical, economic, marketing, legal, environmental, social, and governmental factors, and should in most instances be estimated with input from a range of disciplines (Gandhi and Sarkar, 2016). The boundaries are drawn between ore and waste or between several grades of ore of all possible bodies within overall framework of mineralized horizon.

2.5.1 Mineral resource and reserve definition

The mineral resource is the in situ natural concentration or occurrence of mineralization within a geologically defined envelope. The geological characteristics (quantity, grade, and continuity) are partly known, estimated, or interpreted from broad base evidences and regional knowledge. The presence of mineralization is inferred without programmed framework of verification and cutoff concept (Haldar, 2013).

The mineral reserve or precisely ore reserve is that well defined part of the deposit at specific cutoff after completion of detailed exploration. The reserve is estimated with a high level of confidence based on detail and reliable information. The sample locations are spaced closely enough to confirm geological and/or grade continuity. This reserve must be techno-economically viable (Haldar, 2013; Huleatt and Jaques, 2005; Macdonald, 2007; SAMREC, 2007).

2.5.2 Estimation of reserve/resource

The quality or grade of mineral resources and ore reserves is the relative concentration of minerals and metals. The unit of measurement is expressed as percent (%) for base metals and gram per ton (g/t) or parts per million (ppm) for precious metals (Haldar, 2013). The purpose of mineral resource/reserve estimation is to first assist in determining if a property is worth mining, and, if so, to guide its later development. The ore deposit models are the underlying foundation for numerous consequent economic decisions and the correctness of those decisions will be directly dependent upon the accuracy of resource/reserve estimation (Gandhi and Sarkar, 2016; Seccatore et al., 2014).

The conventional and geostatistical methods have been developed to estimate resource/reserve. The conventional methods involve the use of section and plan maps, while geostatistical methods involve complex, computer-driven 2D and 3D statistical techniques to estimate tonnage and grade (Bustillo Revuelta, 2018). The calculation of grade and tonnage in a mineral deposit by the conventional methods is usually made by the analysis of sample data found in a polygonal, triangular, cross-sectional, contour, and longitudinal vertical sectional (LVS) pattern. These techniques are not particularly reliable but can offer an order of magnitude resource calculation (Bustillo Revuelta, 2018; Haldar, 2013). Moreover, they are applicable in many situations and can produce an end result superior to that possible by a geostatistical method (Bustillo Revuelta, 2018). The choice of method depends upon the shape, dimensions, and complexity of the mineral deposit and the type, dimensions, and pattern of spacing of the sample information (Gandhi and Sarkar, 2016; Macdonald, 2007).

Triangular method

The triangular method is employed for the flat type, near surface deposits having better continuity such as laterite and bauxite. Triangles are formed by joining three adjacent positive intersections defining a block (Haldar, 2013). The horizontal area of each block is measured and multiplied by the thickness of the mineralization to get the volume. The reserve is obtained by multiplying the volume with bulk specific gravity ore. The grade is computed by averaging the three corner values of the triangle. This method has the advantage in that the three drillholes are considered in the calculation of the thickness and grade parameters for each triangular reserve block (Bustillo Revuelta, 2018). The problems with this method are that it is possible to construct the triangles in several ways on the samples depending on the interpretation and the problem of closure at the boundary of a deposit which depends on the interpretation and the experience of the interpreter (Gandhi and Sarkar, 2016).

Longitudinal Vertical Section method

Longitudinal vertical section (LVS) is the creation of a vertical image along the elongated direction presenting features like lithology, ore geometry categorization and ore reserve. The trace of the surface profile and subsurface position of mineralized information gathered by trenches, drill holes and underground workings are plotted in the vertical plane (Gandhi and Sarkar, 2016; Haldar, 2013). The total mineralized envelope on the longitudinal vertical section is divided into sub-blocks around the positive intersection with the principle of halfway influence. The merits of this method that it portrays graphically the geology of a deposit, while the general procedure is simple and rapid (Gandhi and Sarkar, 2016). The LVS method is convenient in computing reserves of uniform mineral deposits. The method is applied in many

tabular deposits. Furthermore, the LVS method is flexible for the simultaneously use with other conventional methods (Bustillo Revuelta, 2018). The methods have an advantage over the triangular method in that it is easy to observe variations in the shape and grade of mineralization.

Inverse Power of Distance

Inverse Power of Distance (IPD) is the most accepted computerized extension functions applied in the mining industry for computation of mine production blocks and sub-blocks are based on the principle of gradual change for making value estimates (Haldar, 2013). The technique uses straightforward mathematics for weighting the influence of all surrounding samples upon the block being estimated. The method provides a gradual change in values between multiple sample points rather than an abrupt and unnatural change at the boundary between adjacent polygonal blocks (Bustillo Revuelta, 2018; Haldar, 2013). The IPD is a smoothing technique and as such is unsuited to deposits that have sharply defined boundaries and very sudden drop in grade. In these situations, the methods tend to produce larger tonnages at a lower grade than actually exist, which can thus seriously affect the results of any economic feasibility study (Bustillo Revuelta, 2018; Carranza, 2009).The IPD works best for mineralization that displays a gradual decline in grade across its economic fringes. It is ideal for porphyry deposits, some alluvial or eluvial deposits, and for limestones (Bustillo Revuelta, 2018).

2.5.3 Mineral resource and ore reserve classification

Mineral resources are classified based on the degree of geological knowledge of continuity and consideration of techno-economic parameters. The classification is regulated by laws, norms, and industry standards. Mineral resource and ore reserve classification system and reporting code have been evolved over the years by different countries exclusively on the basis of geological confidence, convenience to use and investment need in mineral sector (Gandhi and Sarkar, 2016; Haldar, 2013). Classification schemes include USGS/USBM reserve classification scheme, Joint Ore Reserve Committee (JORC) code, Canadian Institute of Mining, Metallurgy and Petroleum (CIM) classification, South African Code for the Reporting of Mineral Resources and Mineral Reserves (SAMREC) and Conventional reserve classification system (CRCS) (Haldar, 2013; Moon et al., 2009).

USGS/USBM reserve classification scheme

The USGS/USBM reserve classification system conveys a common classification and nomenclature, more workable in practice and more useful in long-term public and commercial

planning. The objectives are based on the probability of discovering new deposits, developing economic extraction processes for currently unworkable deposits and knowing immediately available resources (Haldar, 2013). It believes in continuous resources reassessment with new geological knowledge, progress in science and technology, research and development and changes in economic and political conditions. The system can be used to report the status of mineral and energy-fuel resources for the nation or for specific areas (Bustillo Revuelta, 2018; Haldar, 2013; Moon et al., 2009)

Joint Ore Reserve Committee (JORC) code

The strengths of JORC classification are its clarity, transparency, materiality, and competency. The reporting system for exploration results, mineral resources, and ore reserves is exhaustive with checklist at each level. The database format includes the increasing levels of geological knowledge acquired during successive exploration phase attaining higher confidence. It also considers the rational reflection of mining, metallurgy, technical, economic, marketing, legal, social, environment and governmental issues (Gandhi and Sarkar, 2016). The reporting domain is a complete documentation of exploration input, mineability, extraction recovery and economic viability supported by the essence of pre-feasibility or feasibility study, whichever is possible. It provides a clear vision and mission of the project under consideration for an investment decision. All global exploration and mining companies listed in standard Stock Exchanges, particularly in Australia (ASX) and New Zealand (NZX), are required to comply resource-reserve reporting with JORC Code (Joint Ore Reserves Committee, 2012).

Conventional reserve classification system (CRCS)

Conventional reserve classification system (CRCS) is plain and simple representation of the status of mining and other category of reserve and resources. It is more of qualitative depiction of reserves and easily understandable by small mine owners and common users without having advance knowledge of the trade (Haldar, 2013). CRCS categorize resource/reserve into Developed, Proved, Probable and Possible.

Developed resource/reserve present part exposed by trial pit and trenches or drilling on the surface at a small spacing of 15 - 30 m (confidence of estimate is ~ 90%), Proved or Measured reserves are estimated based on samples from outcrops, trenches, development levels and drilling intervals between 200 - 400 m (confidence of estimate is ~ 80 %). The Probable or Indicated reserve estimate is essentially based on wide-spaced sampling, surface and underground drilling at 100 - 400 m interval depending on the complexity of the mineralization

(confidence of estimate is ~ 70 %). The opening of the deposits by trial pit or underground levels is not mandatory to arrive at this category (Gandhi and Sarkar, 2016; Haldar, 2013; Seccatore et al., 2014).

2.5.4 Economic potential of gold mineral resources

A detailed work done by Schodde (2011) from over 49000 mineral deposits from around the world indicated a downward trend of ore grades over time, from over 2 g/t in the 1960s to 1980s to less than 1 g/t Au at present. This is due to a range of factors, including changes in gold prices and mining practices that make it economic to mine low-grade ore. Most important finding was that inventory of high-grade high-quality deposits is being depleted. Subsequently, at current discovery rates, the industry is struggling to meet the future demand for metal.

Large scale mining requires large volumes of resource to be proved to make the operation viable (Basu et al., 2015; Mathibe, 2012; Ravengai et al., 2005). The smallest gold deposit estimated since 2008 by large-scale mining is the Bell Mountain (USA), consisting of 1.07 million ounces of Au (about 33.6 tonnes of Au) (Schodde, 2011). In comparison, the volume that needs to be proved to make the operation viable, in terms of the order of magnitude, is 1/1000 in favor of the small scale operation (Marin et al., 2015; Seccatore et al., 2014).

2.6 Selection of Mining Method for Extraction of Minerals

Once existence of valued mineral is established with confidence, mine design phase may commence. During mine design phase, method of ore extraction is established as well. Extraction of ore can either be surface, underground or combination of both mining methods. Selection of appropriate mining method is dependent on geological, geotechnical, geographical and economical factors (Ataei et al., 2008).

Karimnia and Bagloo (2015), further discuses and expands factors affecting mining selection method into physical and mechanical characteristics of deposit such as local geological conditions, the strengths of the hanging and footwall, ore thickness, general shape of the deposit, slope, overburden thickness, grade distribution, and quality. The main geological conditions include shear strength of the intact rock, natural fractures, shear strength of the discontinuities, the orientation, length, spacing and locality of the geological structures, in-situ stresses and hydrological conditions. Economic factors include operating cost, capital cost, mineable ore tonnes, orebody grades and mineral value, while technical include factors such as annual productivity, applied equipment, environmental considerations, mine recovery, flexibility of methods, machinery and mining rate (Bogdanovic et al., 2012).

2.6.1 Overview of mining methods

There are various mining methods devised to suit a particular ore deposits. They are grouped into underground (such as room and pillar, shrinkage stoping, sublevel stopping and cut and fill) and surface (open pit) methods and are discussed in the following section.

Room and pillar

This is an underground mining method. In this method, a grid of rooms is developed, leaving pillars to support the back. The rooms and pillars may or may not be uniform in size, and the pillars may or may not be extracted at a later date (Gupta and Kumar, 2012; Hartman and Britton, 1992). It is applicable for flat lying deposits and usually not practiced in very thick (450 m) deposits. The size of the rooms and pillars depends on the depth of the working and the strength of the ore/host rock (Bogdanovic et al., 2012; Gupta and Kumar, 2012). There are no reported application of room and pillar mining method within the Giyani Greenstone Belt (GGB).

Shrinkage stoping

In this stoping method, the ore is drilled and blasted, and most of the blasted muck remains (with only a part being drawn out) in the stope, to provide support for the walls and working platform until the whole stope has been blasted. The broken ore is drawn out afterwards. (Gupta and Kumar, 2012; Hartman and Britton, 1992). This method is appropriate for narrow, steep deposits where incompetent host rock cannot stand without support (Gupta and Kumar, 2012;Musingwini and Minnitt, 2008). The shrinkage stoping method was used to extract gold ore at Swartkoopies, Gemsbok and Birthday mines within the GGB (Billay et al., 2014; Steenkamp and Clark-Mosterrt, 2012).

Sublevel caving

This is an induced caving method. Operations in the orebody are undertaken in headings developed at comparatively small vertical intervals (Brady and Brown, 2013). The ore is blasted by ring drilling from sublevel drifts. The overlying and the hanging wall are expected to cave in as the ore is drawn out (Brady and Brown, 2013; Gupta and Kumar, 2012; Hartman and Britton, 1992). It is suitable only for steeply dipping orebodies, with reasonably strong orebody rock enclosed by weaker overlying and wall rocks. The method produces significant disturbance of the ground surface, imposing some possible limitations on its applicability from considerations of local topography and hydrology (Brady and Brown, 2013). The method was used to extract gold ore at Klein Letaba mine within the Giyani Greenstone Belt (Du Plessis,

2012). The sublevel caving is declining in industrial popularity because of the low ore recovery (rarely greater than 65%) and high costs of production (Brady and Brown, 2013)

Cut and fill

The Cut and fill is an underground cyclic stoping method where each slice of ore is removed after blasting and replaced with fill material (Gupta and Kumar, 2012; Hartman and Britton, 1992). There are a multitude of variations, such as overhand cut and fill, underhand cut and fill, rill stoping and post-pillar cut and fill, which can be selected to suit the conditions. Mostly overhand cut and fill is practiced(Gupta and Kumar, 2012). It is applicable for narrow, steeply dipping ore deposits. The ore can be moderately to highly competent. The cost of the fill must be less than the cost of leaving pillars. The cut and fill method can be employed for irregular ore bodies.

Open pit/open cast mining

These are surface mining techniques in which the overburden is removed to uncover the ore. This category includes strip mining and quarrying (Nicholas, 1992). The equipment used to extract the waste and ore is generally mechanical but differs somewhat for each of these methods. The parameters of stripping ratio and slope angle are critical to all in determining whether the method is applicable. Open pit usually refers to metal mines, open cast or strip mining generally refers to coal, and quarrying refers to construction materials and dimension stone such as limestone and granite (Nicholas, 1992; Yamatomi and Okubo, 2009). The method is appropriate for shallow mineral deposits.

While most mineral deposits can be mined by either surface or underground methods, some minerals can only be recovered in a hybrid manner, usually by initial extracted by open pit mining, followed by underground methods (Yamatomi and Okubo, 2009). The gold ore in Frankie mine located north of the Klein Letaba was extracted using both open pit and underground method (Billay et al., 2014; Du Plessis, 2012; Steenkamp and Clark-Mosterrt, 2012). Surface mining is generally considered to provide better recovery, grade control, flexibility, safety, and working environments than underground mining.

2.6.2 Approaches for selection of mining methods

Mining method selection is an important part for mine design and tend to be very complicated decision-making process. For a deposit, usually two or more mining methods are appropriate, with each method carrying some intrinsic problems (Ataei et al., 2008; Brady and Brown, 1985). The selected method should be flexible enough to adapt to the nature of the deposit,

petrology, financial implications, surface structures, dilution of extracted ore, and health and safety issues (Gupta and Kumar, 2012). Several methodologies have been developed in the past for mining method selection (Bustillo Revuelta, 2018) and are discussed in the following section.

Two phases approach method

In this approach, procedure for mining method selection include two phases, preliminary mining method selection and the selection of the most suitable mining method from a group of applicable methods. The selection of the most suitable method from a group of applicable methods is made by the techno-economic model procedure. This model is based on the estimation of expected financial effects, which can be acquired by the implementation of each method from a group of applicable methods. The mining method with the best financial effects is selected (Bogdanovic et al., 2012).

Numerical modeling approach method

Nicholas (1992) proposed a numerical approach for mining method selection. This methodology rates different mining methods based on the rankings of specific input parameters. The mining method with the highest sum result is selected. Nicholas has suggested some modifications that involve the weighting of various categories, such as that of ore geometry, ore zone, hanging wall and footwall. Miller et al (1995) have established the University of British Columbia (UBC) selection method. The UBC mining method selection is a modification of the Nicolas. Selection involves summation and ranking of numerical values associated with orebody characteristics that reflect the suitability of a method.

Multi-criteria decision-making method

Multi-criteria decision making (MCDM) is an updated approach used in selection of mining method. In this approach a finite number of alternatives must be ranked considering many different and conflicting criteria. MCDM include, the most popular scoring models, analytic hierarchy process (AHP), and Preference Ranking Organization Method for Enrichment Evaluation (PROMETHEE) (Bogdanovic et al., 2012).

Saaty (1980), developed a method to support multi-criteria decision making (MCDM) called analytical hierarchy process (AHP). This method combines qualitative and quantitative factors in the selection process and is used in setting priorities in complex, unanticipated, multi-criteria problematic situation. Various authors (Ataei et al., 2008; Bitarafan and Ataei, 2004; Bogdanovic et al., 2012; Gupta and Kumar, 2012; Kassim et al., 2016; Musingwini and Minnitt,

2008; Yavuz, 2015) have demonstrated effective application of AHP in mining selection method. The AHP method has been accepted by international scientific community.

This is an outranking method for a finite set of alternatives. These options include the choice of an appropriate preference function and the weighting given to each variable (Gupta and Kumar, 2012). The preference function defines how one object is to be ranked relative to another and translates the deviation between the evaluations of two samples on a single parameter into a preference degree. The criteria weights, obtained by AHP, have a higher level of coherence, correlation, consistency and accuracy than weights determined on the basis of intuition, which is mostly used in the PROMETHEE method (Bogdanovic et al., 2012)

CHAPTER THREE

RESEARCH METHODOLOGY AND MATERIALS

This chapter discusses the techniques that were used in the collection of data and procedures followed in data processing and analysis techniques. The adopted methods in this research are shown in Figure 3.1. The approaches used in this research comprise of literature review, fieldwork (data collection), identification, characterization and evaluation of the potential mineralized area within the Nebulas Prospect and modelling studies.

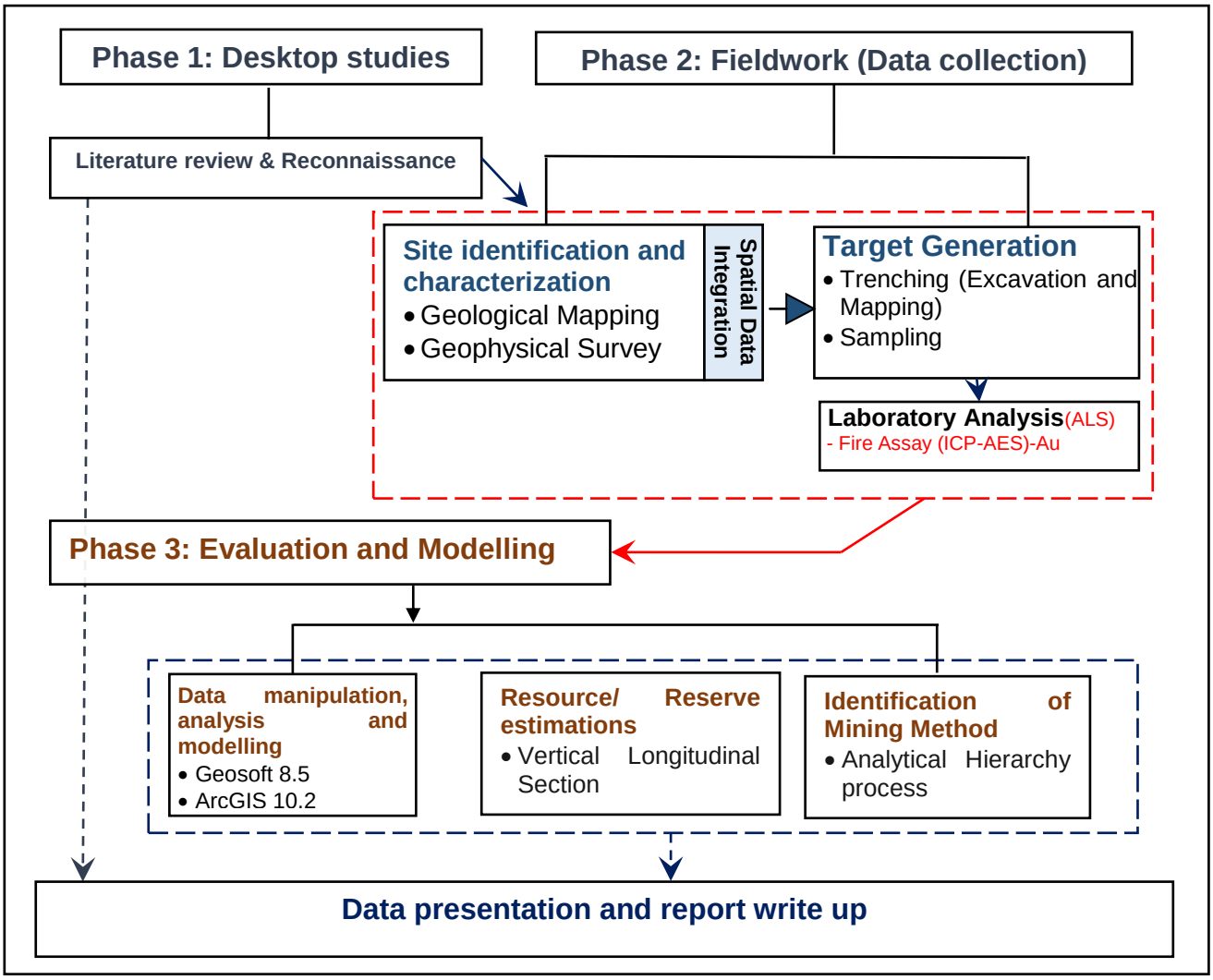

Figure 3.1: An illustration of the research methodology.

During the reconnaissance study of the Nebulas Prospect, 16 randomly located soil samples were collected for gold analysis as part of feasibility study. The gold analysis results from reconnaissance study were used to develop evidential gold anomaly map for the study area.

3.1 Classification of Mineralized Area

Different exploration techniques are employed in saving costs associated with searching of economic minerals. This section lists and discusses data collection and analysis methods for each data collection technique used in this research to generate significant prospective targets for detailed mineral evaluation. Geological mapping is limited to identification of lithologies from outcrops. However, lithologies in the area hardly outcrops and this lead to the consideration of the use of magnetic survey. Data collection included geological mapping and magnetic survey which helped to generate area for further exploration using trenches and pits.

3.1.1 Geological field mapping

Detailed geological field mapping at a scale of 1:10 000 was conducted to map out all the exposed outcrops of rocks in the study area. The design of the geological work comprised 9 traverses which are of 440 m in length. The spacing between the designed traverse lines was maintained at 90 m. The design of the traverse lines in the study area is shown in Figure 3.2. During the mapping design, the existing orthophoto maps were used as a base map.

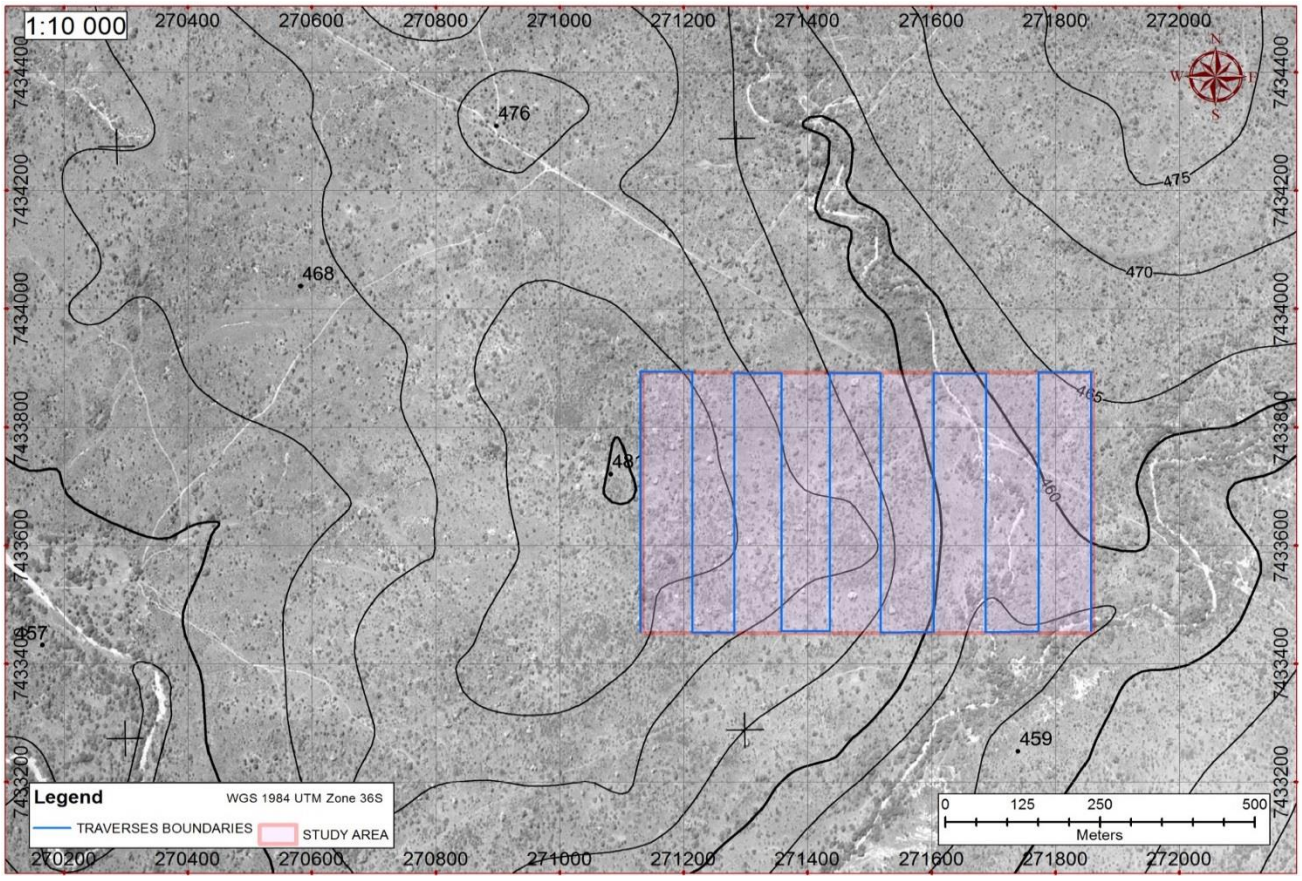

Figure 3.2: An illustration of traverses adopted in geological mapping.

Geological features (such as rock type, dips, strikes and structures) and location data were recorded on field note book and presented on a plan map of the study area. Translation of raw field data into digital geologic data was accomplished using a computer and spatial modelling software (ArcMap 10.2.2). Unique colors, patterns, and labels were used to differentiate the mapped features on the map. Structural information describing rock layers tilting was also collected during the field work. The tilt (dip) of layered rock units provided key information to understand whether non-horizontal units were deformed by faulting or folding.

3.1.2 Knowledge driven geological characterization of the deposit

The developed geological map covering the Nebulas Prospect and its surrounding showed structures and lithology found in the area. However not all lithologies and structures identified during the field work are known to host or control gold mineralization. To enhance the depiction of formations associated with gold mineralization, computer techniques for geological interpretation, geostatistical prediction and graphical visualization of geological conditions were employed. A geological map was transformed to a compatible spatial format (raster data model) to allow Local Functions (f) to the map which includes conditional, logical and mathematical operations on a pixel-by-pixel basis to generate geologically permissive areas.

Based on information related to gold mineralization in Giyani described by various authors (Carranza et al., 2015; Kramers et al., 2014; Sadeghi et al., 2015; Steenkamp and Clark-Mosterrt, 2012) the prospectivity recognition criteria shown in Table 3.1 was developed. The criteria present the knowledge of gold (Au) prospectivity developed for Nebulas Prospect with reference to other areas (such as Klein Letaba, Frankie, Louis Moore and Birthday mines) which have very similar geological settings as the research study area. The gold analysis results from reconnaissance study were used to develop evidential gold anomaly map for the study area. Prospectivity recognition criteria were represented by input spatial data of continuous (C_{s3}) and discrete (C_{s1} & C_{s2}). Fields Classification operation results in an evidential map of multi-class discrete geo-objects (classes of association and proximity).

Table 3.1: Prospectivity recognition criteria for Au in the Giyani Greenstone Belt

Group	Criteria
Class 1 (C_{s1})	Association with BIFs or quartz veins
Class 2 (C_{s2})	Association with Schists (Biotitic, tremolitic and serpentinic composition)
Class 3 (C_{s3})	Presence of gold concentration anomaly

Prospectivity recognition criteria were represented by input spatial data of continuous (C_{s3}) and discrete criteria (C_{s1} & C_{s2}). Fields Classification operation results in an evidential map of multi-class discrete geo-objects (classes of association and proximity). Geological mineral prospectivity map was obtained by integrating evidential maps using computational functions mathematically shown in Equation 3.1. Where f represent logical functions (AND and/or OR Boolean operators). Boolean evidential maps were prepared from the individual spatial data sets according to the prospectivity recognition criteria presented in Table 3.1.

$$\text{Geological permisive map} = \text{f}\,(\text{class evidential maps}) \tag{3.1}$$

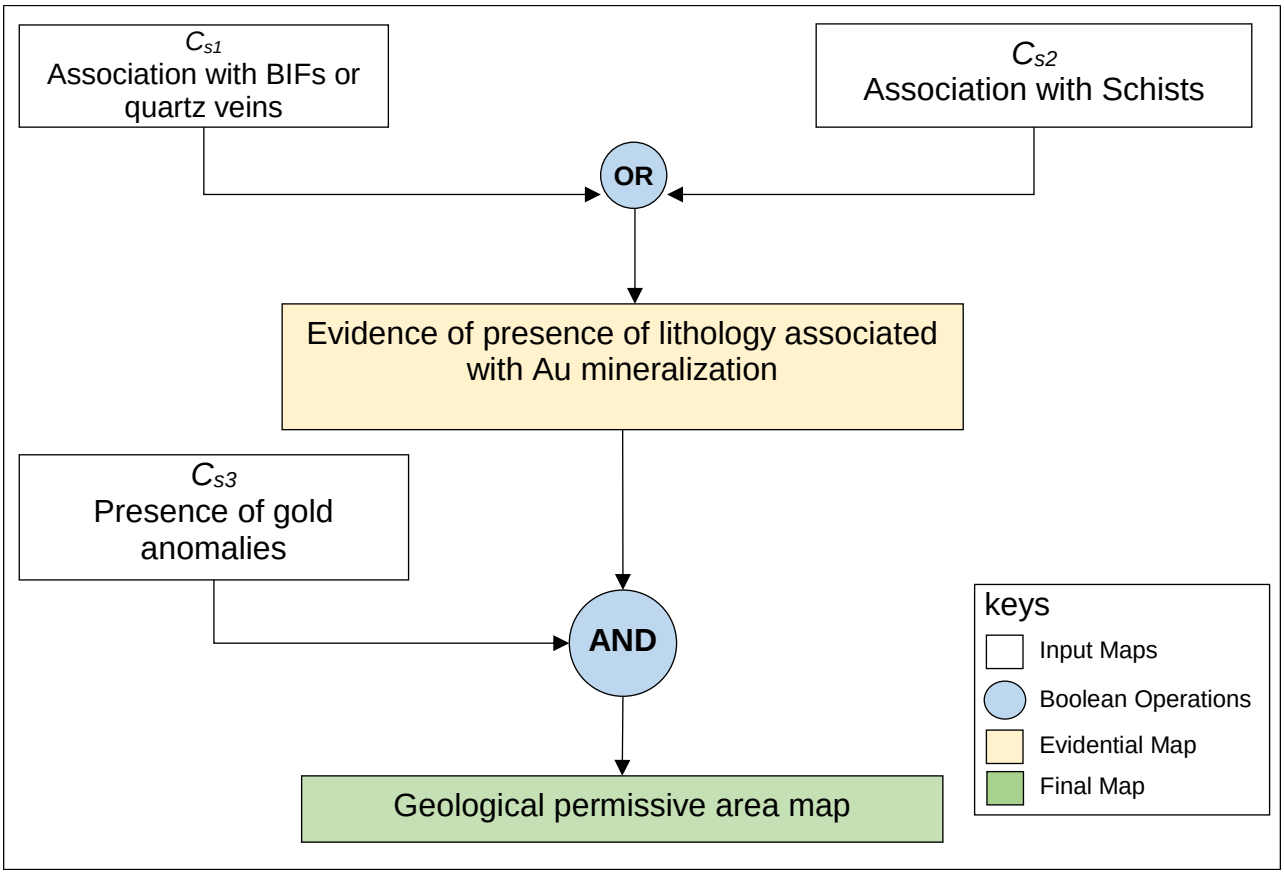

Figure 3.3: Boolean inference network for combining the Boolean evidential maps for given spatial data sets.

The Boolean evidential maps of association with BIFs or quartz veins and association with schists were firstly combined using (OR) operator to show the presence of lithology and structures associated with gold (Au) mineralization in the study area. The (OR) operator was used because it is believed that at certain locations a set of rocks can be a predominant host for gold mineralisation. The intermediate Boolean evidential map was combined with Boolean evidential map of Au anomalies in the area using an “AND” operator. The “AND” operator was used because the presence of BIF or quartz veins and variety of schist does not necessary indicate the presence of Au mineralization. Moreover, the presence of gold

anomalies does not indicate the presence of mineral deposit occurrence. However, the existence of both types of evidence would be more indicative of the potential of mineral deposit in the area. The geological characterization of the area assisted in identification of area requiring further magnetic investigation.

3.1.3 Acquisition of magnetic data

Following the completion of the geological characterization, target area measuring 600 m x 140 m was demarcated for ground magnetic survey to locate the magnetic bodies and geological structures that are present but buried by quartz rubble and clay soil. 12 parallel profiles of 100 m length were adopted, and survey details are listed in Table 3.2. A magnetometer was tuned using International Geomagnetic Reference Field to ensure that data collected from the filed correspond to the study area.

Table 3.2: Listing survey system and parameters

Acquisition systems	
Survey type	Ground Magnetic survey
Survey navigator	Spyglass & Garmin
Magnetometer	Geometrics G856 Proton precision
Resolution & sensitivity	0.1 nT
GPS	Garmin eTrex 30x & Broadcom BCM47734
Survey parameters	
Line direction	North – South
Coordinates system	WGS84 UTM zone 36S
Line spacing	20 meters
Station spacing	10 meters
Data collected	Total field magnetics and terrain elevation data

3.1.4 Magnetic data processing

The collected data was transferred from the G856 magnetometer into the computer. Raw magnetic data was visually inspected for spikes, gaps, instrument noise and other irregularities in the dataset. Location data X (longitude), Y (latitude) and Z (elevation) were merged to magnetic data as observed to locate magnetic data as shown in Appendix A. Magnetic data was processed using Geosoft Oasis Montaj computer software and resultant total field magnetic grids, analytical signal grid, structural index (SI) grids, structural complexity grids and derivative grids were produced for interpretation and integration. The stepwise procedure followed in the processing of magnetic data is shown in Figure 3.4 and later discussed.

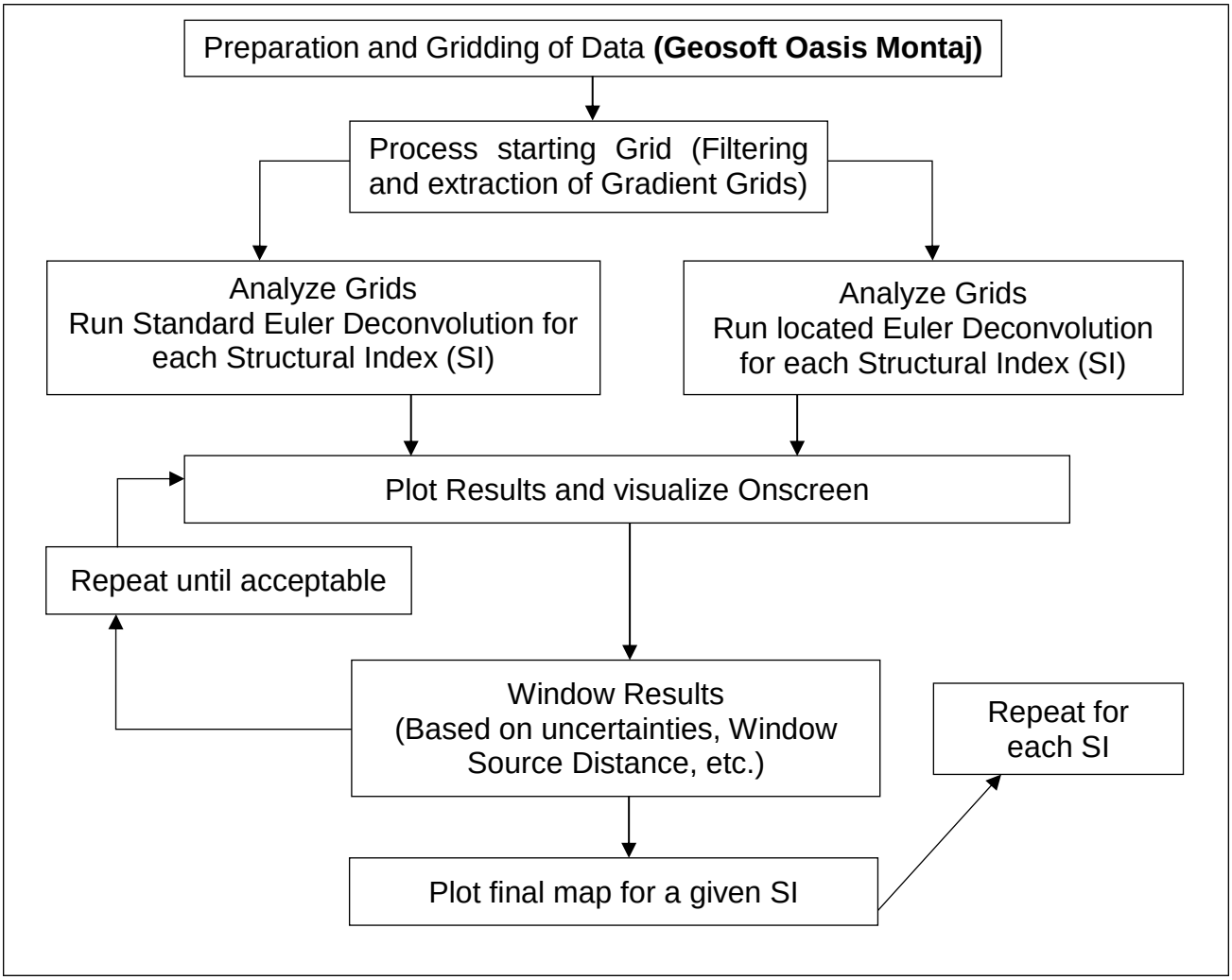

Figure 3.4: Euler 3D Processing sequence adopted in the processing of magnetic data.

Gridding, processing and filtering of magnetic data

The magnetic data grid was done using the bidirectional gridding tool Oasis Montaj software. The tool is effective in interpolation of roughly parallel line-based data with high sample density. Location of the ridges and peaks of magnetic anomaly directly over the causative geological body was assimilated through analytical signal processing. This works regardless of structural dip that may be present, and independently of the direction of magnetization.

An analytic signal is a direct measure of the total gradient of the magnetic field. The calculation of analytical signal is defined as the square root of the squared sum of the vertical and horizontal derivatives of the total magnetic field. In view of this, equation 3.2 was used to calculate the analytical signal from the total magnetic field grid.

$$|A(xy)| = \sqrt{\left[\left(\frac{dT}{dx}\right)^2 + \left(\frac{dT}{dy}\right)^2 + \left(\frac{dT}{dz}\right)^2\right]} \quad (3.2)$$

$|A(xy)|$ is the amplitude of the analytical signal and (T) is the observed magnetic field at (xy). This is naturally a function of the distance to the magnetic source and the intensity of magnetization.

The reduction to pole (RTP) filtering technique was applied to magnetic intensity data to transform anomaly occurring at a low magnetic latitude which may be dipolar and are offset from their causative body. RTP recalculates total magnetic intensity data as if the inducing had a 90-degree inclination using equation 3.3. The RTP assumes that all magnetization is parallel to the Earth's magnetic field.

$$L(\theta) = \frac{1}{(\sin(i_a) + \cos(i) \cdot \cos(D - \theta)^2} \quad (3.3)$$

Where: (i) is the geomagnetic inclination, (i_a) inclination of amplitude correction (never less than 1) and (D) geomagnetic declination.

Euler 3D deconvolution

The soil cover in the Nebulas Prospect limits the outcrop exposure, thus difficulty in linking the magnetic source and their depth from magnetic intensity map. To enhance the depiction of the magnetic source and depth estimates, Euler 3D deconvolution was applied. Euler 3D deconvolution technique locate magnetic sources and estimate their depths by mathematically solving Euler's homogeneity using equation 3.4.

$$(x - x_0)\frac{\delta T}{\delta x} + (y - y)\frac{\delta T}{\delta y} + (z - z_0)\frac{\delta T}{\delta z} = N(B - T) \quad (3.4)$$

Where (x_0, y_0, z_0) is the position of the magnetic source whose total field (T) is detected at (x, y, z), (B) is the regional magnetic field and (N) is the measure of the fall-off rate of the magnetic field and may be interpreted as structural index (SI). Structural index (N) is defined as a measure of the rate of change of a field with distance and assumes different values for diverse types of magnetic sources.

Properly selected structural indices for specific geological bodies of interest results in closer clustering of Euler solutions for both location and depth of magnetic sources. Selection of improper structural indices yields Euler solutions that are widely scattered horizontally and have inaccurate depths. Table 3.3 indicates proper structural indices for specific magnetic geological bodies that results in accurate Euler solutions. This method requires prior little knowledge about the magnetic source geometry causing magnetic anomaly, as the attainment of accurate Euler solutions depends on proper selection of structural index.

Table 3.3: Structural indices for Euler solutions of specific geologic models (Geosoft, 2004)

Structural index	Geologic model
0	Contacts/faults
1	Thin dykes and sills
2	Kimberlite pipes
3	Massive spherical bodies

3.2 Evaluation of Potential Mineralization in the Nebulas Prospect

The magnetic, geological and gold anomaly processed data were all integrated to produce a gold prospectivity map of Nebulas Prospect to support development of exploratory trench plans used in gold evaluation. Trenching and geochemical sampling was done based on gold prospectivity map developed with potential targets for investigation. The advantages trenches are that they permit the accurate sampling of mineralized horizons and they facilitate the collection of very large samples, which is particularly important in the evaluation deposits such as gold deposits (Bustillo Revuelta, 2018). Trenches were used earlier in the Giyani Greenstone belt expose steep-dipping rocks buried below shallow overburden.

3.2.1 The development of trenches and pits

Existing 5 trenches (denoted as TH1, TH2, TH5, TH9 & TH10) were reopened and 5 new trenches (denoted as TH3, TH4, TH6, TH7 and TH8) were excavated, mapped and sampled. The exaction of trenches was done manually using pickaxes and shovel as shown in Figure 3.5. Old trenches (TH1, TH9 and TH10) are located outside the geological permissive except TH2 and TH5. On the other hand, new trenches were located within geological permissive area. Design parameters for new trenches were guided by the strikes of the lithology in the area which varies from east-west and northwest-southeast. Trench parameters for both old (reopened) and new trenches are listed in Table 3.4.

Two old exploration pits one on the southern part with depth of ± 12 m and other on north with depth of ± 8 m were recognized. Both pits fall within geological prospective area and were used as guides for depth continuity of lithology and mineralization. A minimum length of 5 m and a maximum of 50 m was adopted during digging of trenches. The depth of trenches was set to 50 cm (0.5 m) for the areas with outcrops exposed to the surface and ± 1.2 m where outcrops are buried with regolith. This was aided using depth model from magnetic data. To ensure safer and convenient subsequent mapping and sampling, safety and logistics requirements outlined by Marjoribanks (2010) were used.

Figure 3.5: Manual excavation of trenches using pickaxe and shovel.

Table 3.4: The design parameters for new and reopened trenches.

Trench ID	Length (m)	Azimuth (°)	X (Start)	Y (Start)	Elevation	Depth (m)
TH1	15	56	271576.7	7433700	465.9	1.5
TH2	6	171	271507.6	7433690	468.1	0.5
TH3	5.5	157	271481.2	7433682	470.6	1.5
TH4	20	158	271438.9	7433687	472.8	1
TH5	9	165	271411.6	7433677	473.6	1.5
TH6	35	51	271555.7	7433711	466.2	1.5
TH7	49	51	271525.9	7433718	466.6	1.5
TH8	21	38	271522.3	7433751	466.7	1
TH9	30	47	271504.1	7433764	468.4	1.5
TH10	31	48	271481.7	7433787	469.5	1

3.2.2 Trench mapping

The mapping of trenches was done to develop a vertical longitudinal section map showing lithology map of the trenches. The scales of 1:100 to 1:350 were applied during trench mapping. Trenches were mapped in a plan view, with information seen on the walls of the trench projected on the plan. Where a good vertical profile can be seen in the trench wall, a vertical plan of the wall was made as well as a horizontal plan. Trench mapping data was digitized using Geosoft Target software and integrated with digital geological map and geophysical data to develop a geological model (lithology, structural, and magnetic).

3.2.3 Sampling and sample analysis

During sampling, several rock chips and soil were collected along channels in the trenches and from two pits (at pits opening and bottom). Intervals for sampling were marked out on the exposed and such intervals reflected natural geological boundaries that were regarded as control of gold mineralization as shown in Figure 3.6. Horizontal channels along the trench floor and pit walls were used for trench and pit sampling.

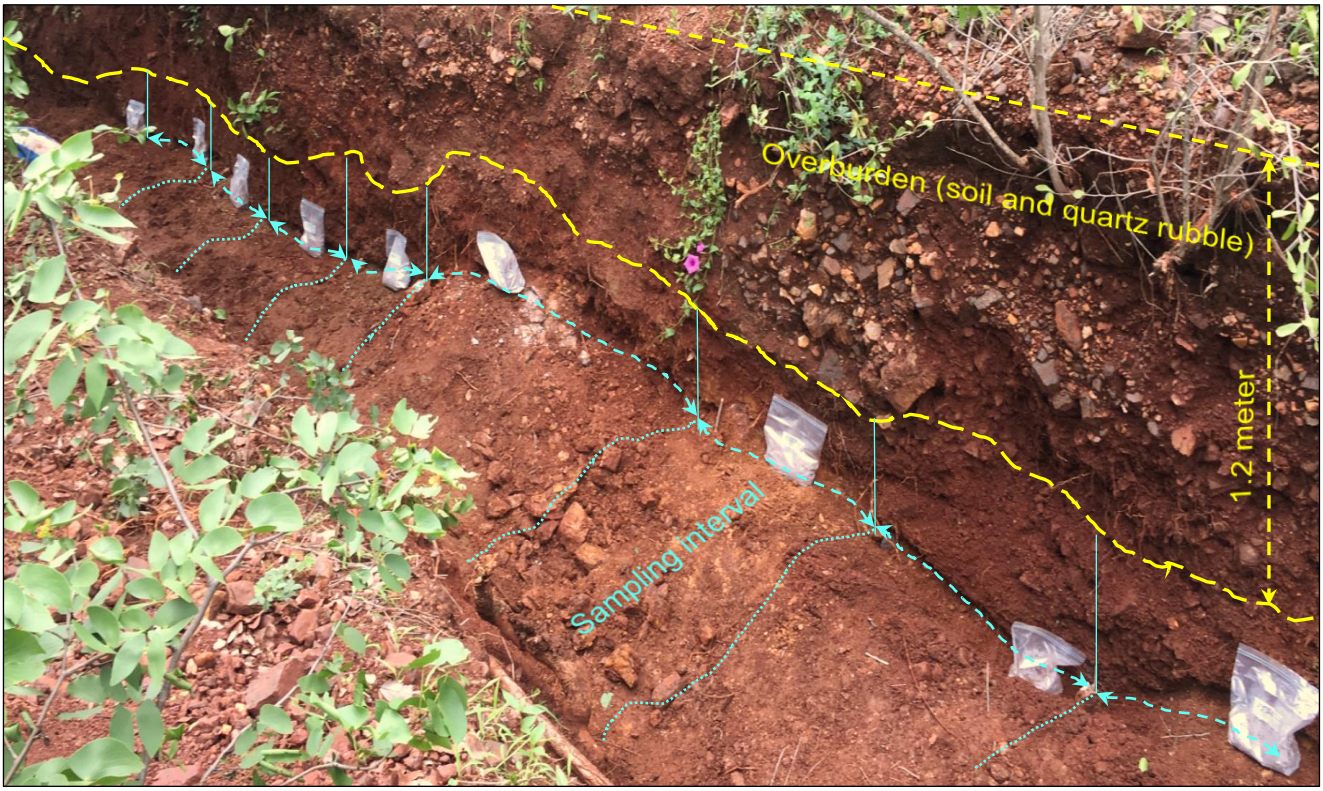

Figure 3.6: Soil and rock chip sampling from trench TH7.

Fire assaying analysis for gold

Samples (representative portion ± 1.5 kg/sample) were taken to ALS Laboratory in Johannesburg, South Africa for assay. At ALS facilities, samples were crushed to 70% of

particles less than 2mm and dried at 120°C. Sample was then split using riffle splitter. A sample split of up to 250 g was pulverized to 85% of particles less than 75µm to produce a representative sub-sample for gold analysis. The prepared sample was fused with a mixture of lead oxide, sodium carbonate, borax, silica, litharge and flour. The gold concertation was then analyzed by Fire Assay and ICP-AES methods with detection level of 0.005 ppm. Internal laboratory cross checking methods and standards were implemented by ALS.

3.2.4 Three Dimensional (3D) geological Modelling

Three-dimensional (3D) geoscience information (geological, magnetic and geochemical) for the Nebulas area was integrated for understanding subsurface structures, lithology and mineralization. The lithology model was constructed using longitudinal geological sections of 10 trenches with a scale of 1:315 followed by 3D inversion of magnetic data (magnetic intensity and structural index (S=0)) for identification of anomaly zones which are associated gold mineralization.

3.3 Mineral Resource/Reserve Evaluation

Mineral resource/reserve evaluation provide a basis on which economic decisions can be taken. At least, four aspects can be identified if a mining project is evaluated, technical, economic/financial, social, and political (Bustillo Revuelta, 2018). The study focuses on technical aspects which include geological setting of the deposit and characteristics of the mineralization (grade, tonnage). The technique adopted for estimation of grade and tonnage of Nebulas Gold Deposit is discussed in the following sections.

3.3.1 Longitudinal vertical section (LVS) grade estimation and weighting

This method has an advantage in it portrays graphically the geology of a deposit, and the procedure is swift and not complicated (Gandhi and Sarkar, 2016). The method is applied in many tabular deposits. Furthermore, this method is flexible for the simultaneously use with other conventional methods (Bustillo Revuelta, 2018). Longitudinal vertical section was created along the elongated direction presenting features (lithology, structures, ore geometry and categorization). The trace of the surface profile and subsurface position of mineralized information as gathered by trenches was plotted in the vertical plane. The section sub-block area around each trench was demarcated by halfway influence. The estimation of resource and grade for the section with bulk specific gravity is given by;

Volume = Area x Halfway influence
Block tonnage (t) = Volume x Bulk Specific Gravity
Total section tonnage (T) = Sum of all block tonnes = $\sum(t_1 + t_2 + \cdots + t_n)$

Simplified equation:

$$T = \sum_{i=1}^{n} t_i \tag{3.5}$$

Weighting was implemented in calculation of average grade of trench section and block from assay intervals of different lengths and on the average grade of a deposit from the combined grades of individual, unequal blocks using equation 3.5.

$$\overline{G}_w = \frac{G_1 a_1 + G_2 a_2 + G_n a_n}{a_1 + a_2 + \cdots a_n} = \frac{\sum_{i=1}^{n} G_i a_i}{\sum_{i=1}^{n} a_i} \tag{3.6}$$

Where: G_1 to G_n are the values (gold grade in g/t) whose weighted average is to be determined, a_1 to a_n are the weighting factors (mineralization length, volume or block tonnage), $\overline{G}_w$ is the weighted average Grade.

3.4 Identification of Potential Mining Method for the Deposit

Recovery of mineral from subsurface rock involves the development of physical access to the mineralized zone, liberation of the ore from the enclosing host rock and transport of this material to the processing area. Excavations of various shapes, sizes, orientations and duty functions are required to support the series of operations which comprise the complete mining process (Brady and Brown, 1985). The size of the established deposit limits the type of operation to either large scale or small scale. The selection of a mining method is a complex multi attribute decision making process. Depending on the dip, depth, size and shape of the deposit, strength of the ore and host rock, various technically feasible mining methods may be adopted for a particular deposit (Gupta and Kumar, 2012). The section below present mining method selection process.

3.4.1 The factors influencing the selection of a mining method

Factors influencing the selection of mining methods were identified and categorized as intrinsic as listed on Table 3.5. Intrinsic comprise of those factors which are driven by nature and are uncontrollable, dictated by the deposit itself and the host rock. On the other hand, extrinsic include extended factors not directly associated with the deposit which include capital investment, the market and the dilution of the extracted ore, as well as the availability of labour, and health and safety.

Table 3.5: Parameters influencing the choice of mining method (Source: Gupta and Kumar, 2012).

Intrinsic factor affecting selection method	Description
C_1 - Dip of the deposit	Can be flat (<15°), moderate (15° - 45°) or steep (> 45°)
C_2 - Strength of the ore	Can be Weak, Moderate or Strong
C_3 - Strength of the host rock	Can be Weak, Moderate or Strong
C_4 - Depth of the deposit	shallow (< 450 m), moderate (450-1200 m) or deep (>1500)
C_5 - Shape of the deposit	Categorized into irregular, tabular or massive
C_6 - Grade of the ore	Categorized as uniform, gradual or erratic
C_7 - Thickness of the deposit	Narrow (< 10 m), intermediate (10 – 45 m) or Thick (>45 m)

3.4.2 Application of an Analytical Hierarchy Process

The Analytical hierarch process (AHP) was selected over other Multi-Criteria Decision Methods (MCDM) because it has the ability to detect inconsistent in judgments. Moreover, it provides estimates on degree of inconsistency in the judgements and can rank alternative mining methods in the order of their effectiveness when conflicting criteria have to be met (Ataei et al., 2008; Bogdanovic et al., 2012; Gupta and Kumar, 2012; Kassim et al., 2016; Musingwini and Minnitt, 2008).

The hierarchy developed in this study consist of three levels as shown in Figure 3.5. Level 1 represent the goal of the selection process of which the outcome is the most suitable mining method. The second level presents factors affecting the selection of mining methods and were used as criteria (denoted as C_1, C_2,…, C_7) for weighting and prioritizing of 3 alternatives (mining methods denoted as mA_1, mA_2, & mA_3) constituted in level 3 of the hierarchy. The mining alternative was compared pairwise with the other at the same level with respect to criterions at level 2 following equation 3.7. The pairwise comparison was established based on nine-point scale of importance developed by Saaty in 1980 shown in Table 3.6.

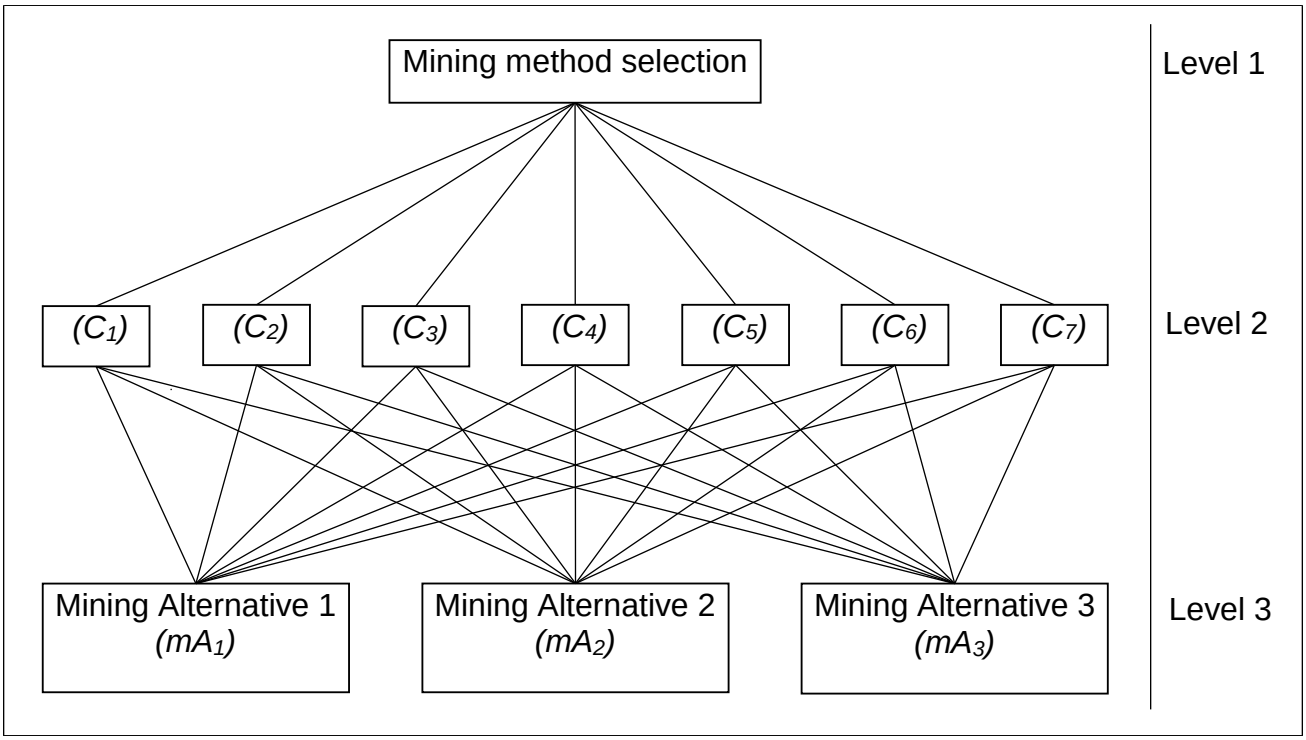

Figure 3.7: Analytical hierarchy tree diagram adopted for selection of the method for mining of Nebulas Gold Deposit

Table 3.6: Pairwise comparison scale (Source: Saaty, 1980)

Comparison Index	Score
Equally preferred	1
Moderately preferred	3
Strongly preferred	5
Very strongly preferred	7
Extremely preferred	9
Intermediate values between two adjacent judgments	2, 4, 6, 8

From pairwise comparison, matrices of comparison were created. The normalized relative weights at each level (priority vectors) for each element of the hierarchy was computed using equation 3.8 and 3.9. The consistency ratio was estimated to check the consistency of the judgment (consistency index – CI and consistency ratio – CR) (Eq. 3.10 & 3.11).

$$A = a_{ij} \tag{3.7}$$

Equation 3.7 present matrix pairwise comparison and represent the value of preference among individual pairs of alternatives (A_i versus A_j for all $i, j = 1, 2, \ldots, n$). Equation 3.8 present normalization of elements while equation 3.9 shows the computation of weight w_i of elements.

$$a_{ij}^{*} = \frac{a_{ij}}{\sum_{i=1}^{n} a_{ij}} \tag{3.8}$$

$$w_i = \frac{\sum_{i=1}^{n} a_{ij}^*}{n} \quad (3.9)$$

$$CI = \frac{\lambda_{max} - n}{n - 1} \quad (3.10)$$

$$CR = \frac{CI}{RI} \quad (3.11)$$

Where λ_{max} is an important validation parameter in AHP and is used as a reference index to screen information by calculating consistency ration (CR). RI is the random consistency index obtained from a randomly generated pair-wise comparison matrix (see Table 3.7).

Table 3.7: Random Consistency Index ($\mathbf{RI}$) (Source: Saaty 1980)

n	1	2	3	4	5	6	7	8	9	10
RI	0	0	0.58	0.9	1.21	1.24	1.32	1.41	1.45	1.49

Consistency ratio of less than 0.1 (<10%) is acceptable as an indication of consistency in judgment. Overall priority for each decision alternative and overall ranking of decision was achieved through synthesizing the results over all levels and the technically appropriate mining method was recommended.

CHAPTER FOUR

CHARACTERIZATION OF NEBULAS PROSPECT

The identification of the potential mineralized area within the Nebulas Prospect included the integration of geo-thematic data layers. Each of the layers was representing theory which relates to gold mineralization in the belt and the layers are described as evidential spatial data or evidential maps. This chapter presents such evidential spatial data sets (geological, geochemical and geophysical) which are key inputs in establishing mineral prospectivity map of the Nebulas Prospect. The results presented in this chapter were accomplished based on the methodologies which were described in detail in Chapter Three. These assisted in defining and identification of the prospective areas in the Nebulas Prospect. The results obtained were discussed and presented in form of Figures and Tables.

4.1 Geology and Geochemistry of the Nebulas Prospect

The geological evidential spatial datasets were produced through the application of the Boolean logic model. The main aim of the characterization was to develop a prospective map of Nebulas Prospect indicating areas which may require further exploration. Geochemical and geological spatial data sets were used to achieve this anticipated outcome.

4.1.1 Geological mapping of Nebulas Prospect

The aim of conducting geological mapping was to establish the presence of lithological units favorable in hosting gold mineralization and structural units that may be responsible in controlling gold mineralization in the study area. Following a successful geological mapping, observed data was used to construct geological map shown in Figure 4.1. It can be seen from the map that about 70 % of the area is covered with clayey soils and quartz rubble.

The outcrops of Banded Iron Formation (BIF) shown in Figure 4.2a exists on the southern part of the Nebulas Prospect and are to some extent exposed. The BIF is deformed show indication of deformation through discontinuous bands of iron and silica. The iron (hematite and magnetite) are the dominate minerals within the BIF while siliceous bands are minor. As indicated by Billay et al. (2014) exposed outcrops BIF were used earlier as guides for gold exploration within the Giyani Greenstone Belt (GGB).

Poorly exposed amphibolite shown in Figure 4.2b exists in the central part of the Nebulas Prospect with the general strike of east-west, truncated by northeast; north-west trending

faults. The amphibolite in the study exhibits dark color and weakly foliated structures. It is composed dominantly of hornblende, minor feldspars, and it is truncated by a 5 cm quartz vein. The Schists of different compositions (mica and tremolite) exist in the study area and are patchy as perceived from the surface as shown in Figure 4.2c. However, their recorded locations were buffered and overlain on the geological map. The exposed tremolite-mica schists are weathered, and the dominant minerals include tremolite muscovite and biotite. The gold mineralisation within the belt is associated with mafic to ultramafic rocks (Sadeghi et al., 2015) and these comprise tremolite-mica and serpentine schists, thus a useful guide for the development of prospectivity map for the Nebulas Prospect.

The southeast-northwest trending pegmatite shown in Figure 4.2d is well exposed and is composed dominantly of plagioclase feldspar and quartz minerals. The migmatised-gneiss covers about 15 % of the study area to the east and extend northwards, and are composed of quartz, biotite and feldspar. The dolerite dykes shown in Figure 4.2f are well exposed on the southwest part of the Nebulas Prospect. According to Billay et al. (2014), Carranza et al. (2015) Kramers et al. (2014) and Kröner et al. (2000) the dolerite, migmatised gneiss and pegmatite within the Giyani Greenstone Belt have no association with the gold mineralisation.

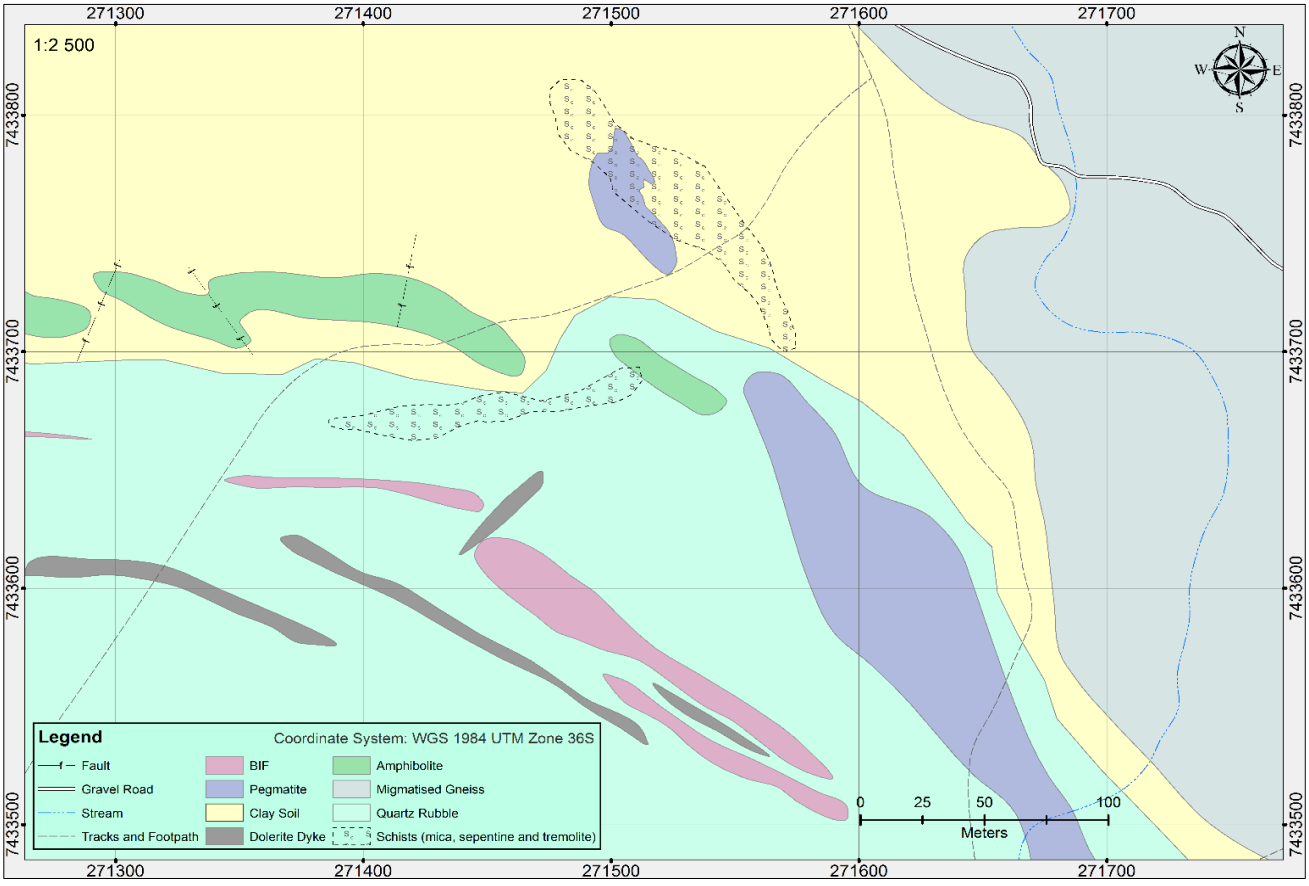

Figure 4.1: Geological map of the Nebulas Prospect

(a) Banded Iron Formation (BIF)

(b) Amphibolite

(c) Tremolite-mica schist

(d) Pegmatite

(e) Migmatised gneiss

(f) Dolerite

Figure 4.2: Exposed outcrops of various rocks in the Nebulas Prospect.

4.1.2 Distribution of gold concentration on surface soils

The soil sample results for gold analysis were used to generate surface gold anomaly map. Due to randomness of locations of samples, Inverse Distance Weighting (IDW) methods for gridding was adopted to produce the anomaly map shown in Figure 4.3. The gold concentration shown in Table 4.1 ranges from 0.063 to 6.03 ppm in the Nebulas Prospect. The concentration values of gold in the soils from the other areas within the belt such as West-59 ranges from 0.03 to 0.08 ppm (Billay et al., 2014; Muzerengi, 2013)

High concentration of Au was found to be visible towards the northeast of the study area. However, its distribution was trending northwest, showing relationship with strike direction of exposed schists in the area. The low concentration values of Au were found to be trending east-west in the southern part of the study area which could be influenced by the strike direction of BIF in the study area. The gold anomalies in the northeast of the Nebulas Prospect are associated with tremolite-mica schist, quartz veins and serpentine schist. The existence of gold anomalous values was not indication of presence of gold deposit, but prospectivity potential of the area.

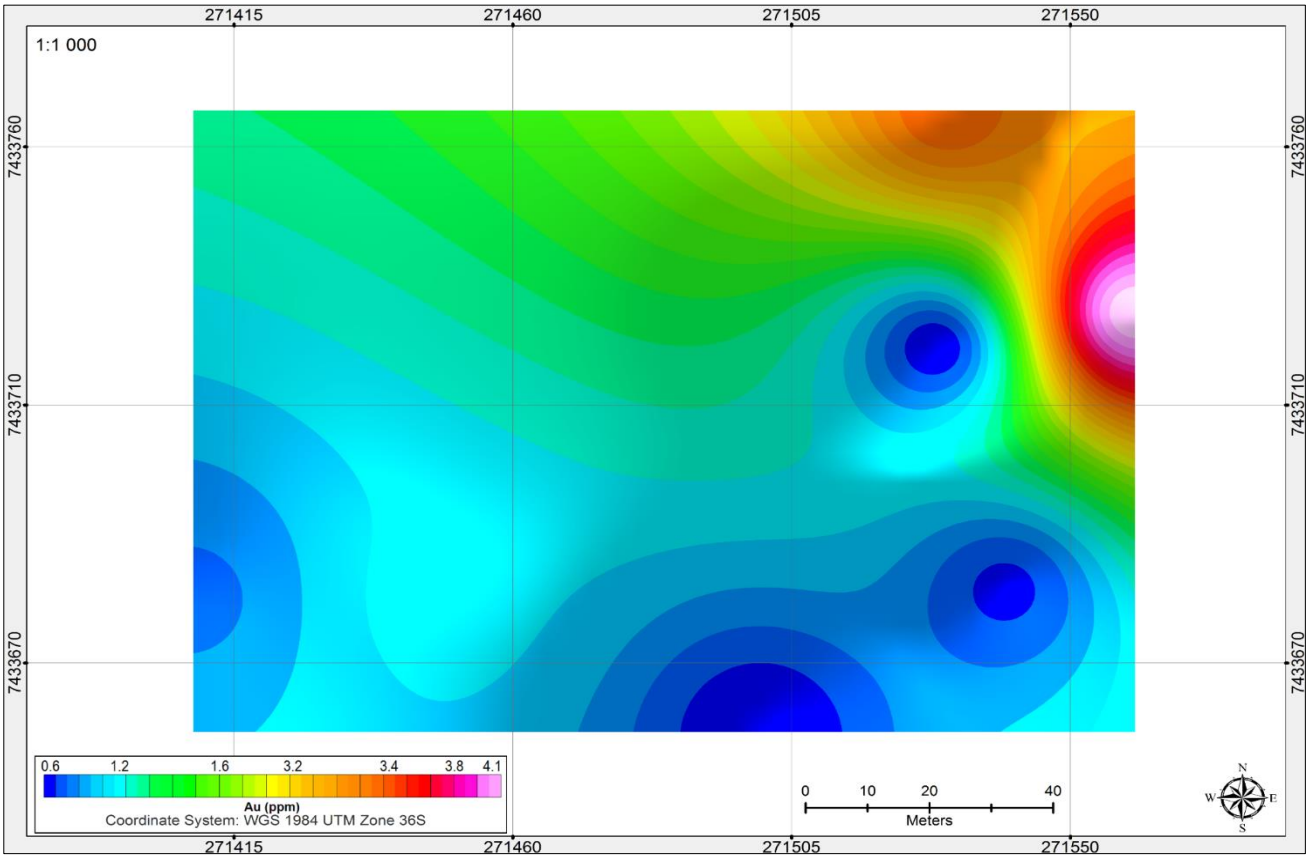

Figure 4.3: Gold distribution map on surface for randomly collected sample.

Table 4.1: Gold assay results for randomly collected soil samples during reconnaissance survey

SAMPLE-ID	Au PPM	Sample location superimposed on Au anomaly map
NBS1	6.03	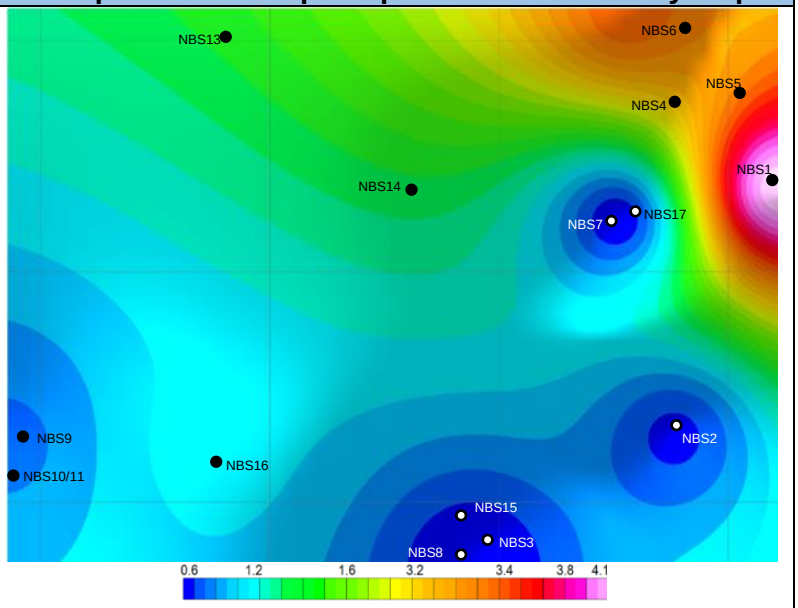
NBS2	0.133	
NBS3	0.094	
NBS4	3.19	
NBS5	5.41	
NBS6	5.07	
NBS7	0.16	
NBS8	0.063	
NBS9	0.442	
NBS10	0.391	
NBS11	0.43	
NBS12	0.316	
NBS13	1.09	
NBS14	1.335	
NBS15	0.355	
NBS16	1	
NBS17	0.401	

Mean: 1.524118
Standard Deviation: 2.045824
Sample Variance: 4.185397
Minimum: 0.063
Maximum: 6.03

4.1.3 Surface lithological indication

In order to develop lithological evidential map, prospectivity recognition criterion shown in Table 3.2 of chapter three was used. The geological map was converted to a raster data model to enable Boolean operations. The developed prospectivity criterion (C_{s1} and C_{s2}) specifies that gold within the belt is associated with BIFs and Schist. The association of gold mineralization with BIF and schist within the GGB has been indicated by Billay et al. (2014), Carranza et al. (2015), Kröner et al., 2000 and Sadeghi et al. (2015). The presence of either BIF or schist indicated existence of hosting potential and were labeled TRUE (assigned class score of 1) and all other areas with absence of BIF, schist or quartz veins were assigned class score of 0 (FALSE) and shown in Figure 4.4. The OR operator was used since it was probable that at certain settings either BIF, schist or quartz vein can be a predominant host of gold mineralization. The integration accepted all lithological (BIFs, schists) and structural (quartz veins) criterion and rejected all lithology (amphibolite, migmatised-gneiss, dolerite-dyke and pegmatite) not in the prospectivity criterion.

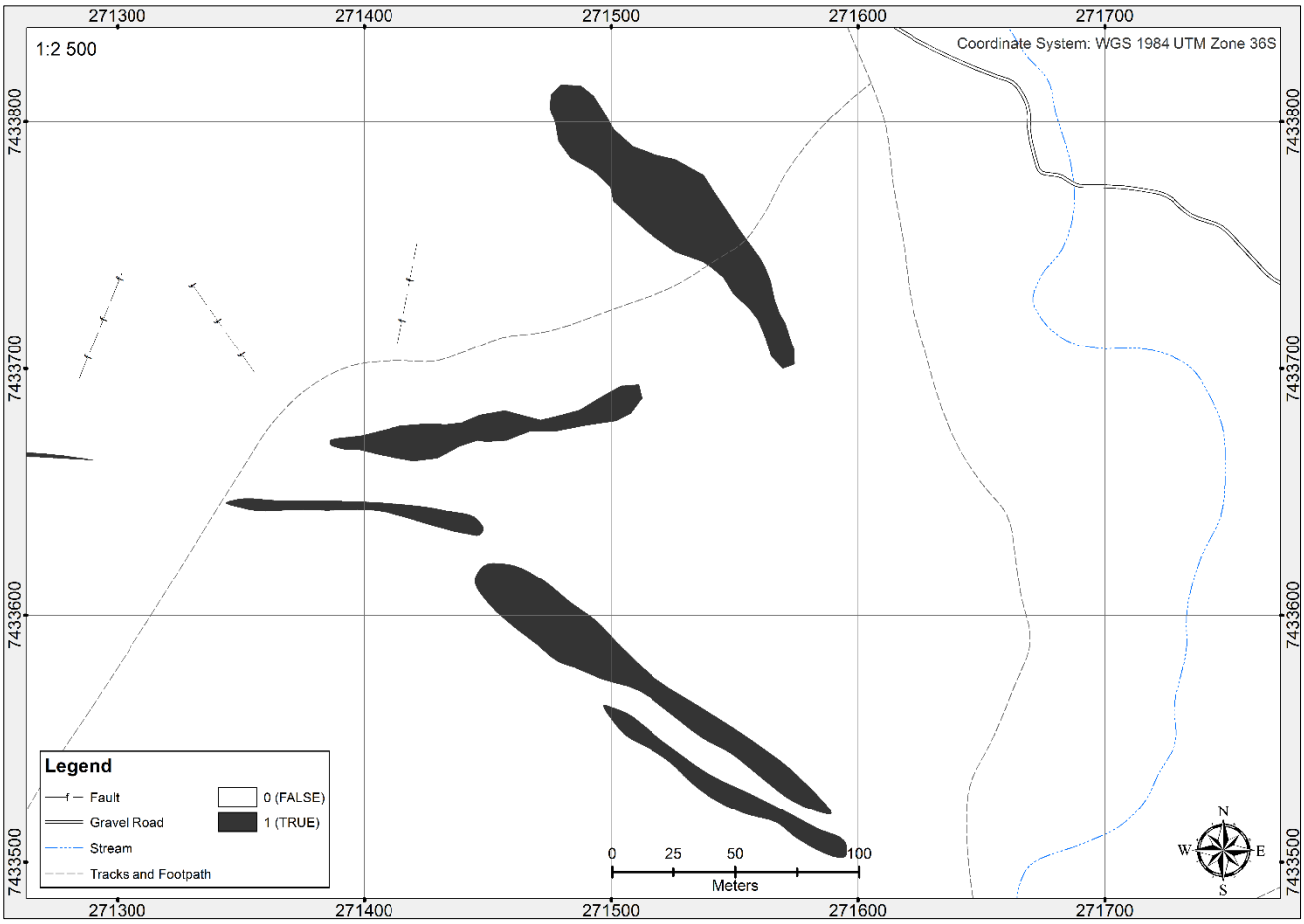

Figure 4.4: Boolean evidential map of lithology, indicating areas (TRUE) with lithology with potential of hosting gold mineralization.

4.1.4 The development of prospectivity map

Boolean evidential map of lithology was combined with evidential map of Au distribution map using (AND) operator to establish prospectivity map of Nebulas Prospect. The (AND) operator was used because the presence of BIF and schist, essentially does not confirm presence of the gold mineralization and the existence of gold concentration anomaly was not a validation of the presence of mineral deposit occurrence. Nevertheless, the existence of both types of evidence would be more indicative of possible mineral deposit in the area. The results of Boolean inference network are shown in Figure 4.5.

About 5% of the Nebulas Prospect was found to be highly prospective. The geologically permissive (high prospectivity potential) areas assigned a class value of 1, comprised of both BIFs, quartz veins and schists with association of gold occurrence anomaly. From the integration, BIFs, quartz veins and schists with no association with the gold anomaly were excluded and assigned a class value of 2 (low prospectivity potential). The Low prospective area covers about 10 % of the Nebulas Prospect.

The remaining 85 % of the Nebulas Prospect was classified as non-prospective. The non-prospective area assigned a class value of 0, comprise pegmatite, migmatised gneiss, aplite, dolerite dykes and amphibolite. The rocks existing in non-prospective area have no association with gold mineralization in the Giyani Greenstone Belt and this have been indicated by Billay et al. (2014), Carranza et al. (2015) Kramers et al. (2014) and Kröner et al. (2000).

Prospectivity map of Nebulas Prospect showed the areas which are geological permissive for further detailed evaluation for gold by trenching and pitting. The nature of the study area present limited outcrop exposure, thus developed prospectivity map was based on limited evidence that was collected from the surface. Magnetic survey was therefore conducted to provide information about the surface formation in the study area.

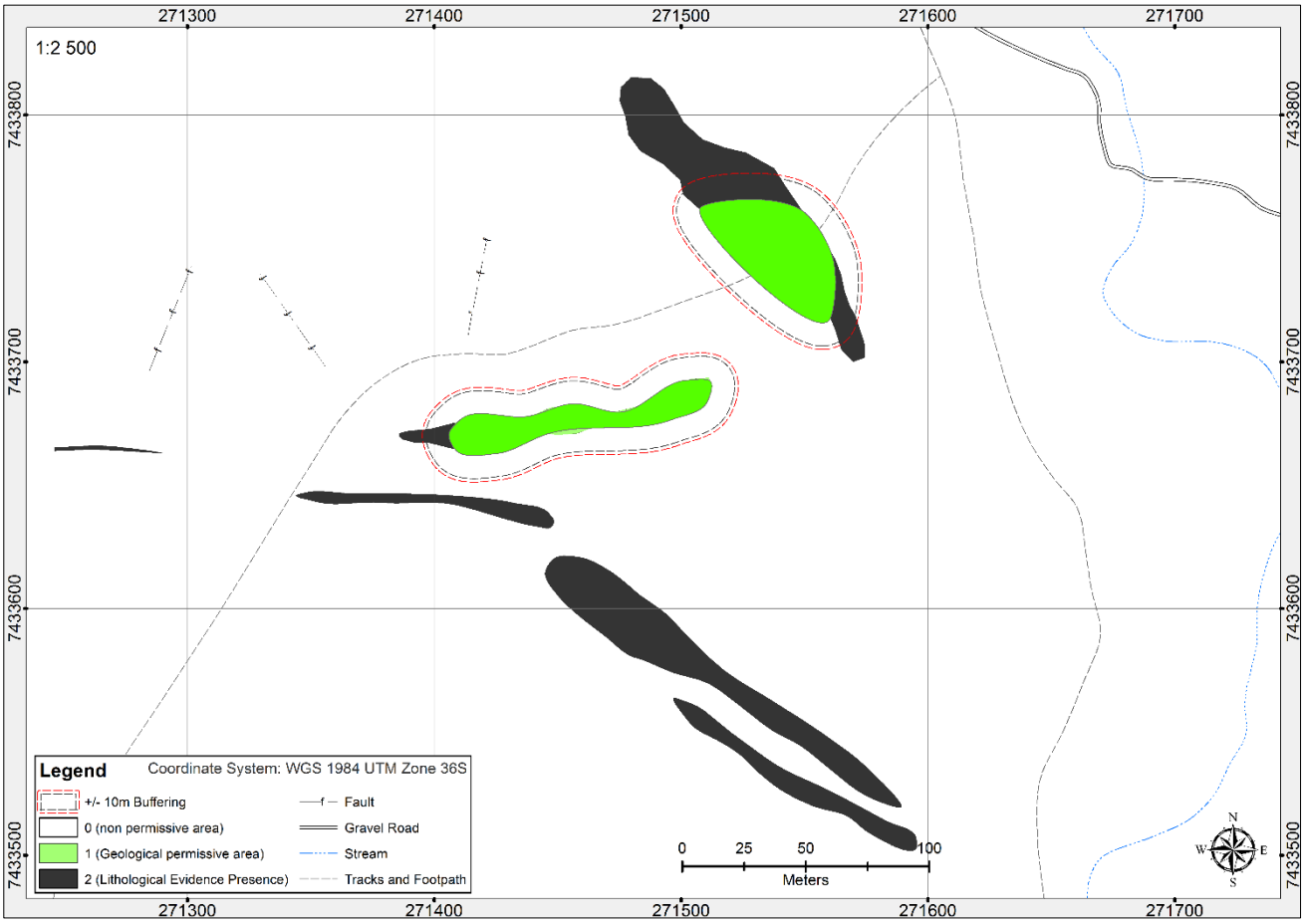

Figure 4.5: Prospectivity map of Nebulas Prospect, derived through Boolean inference network from gold anomaly map and Boolean evidential map of lithology.

4.2 The Presentation of Magnetic Data

The total magnetic field data is shown in Figure 4.6 and interpreted with guidance from the developed geological map. The total magnetic intensity map shows area of magnetic high and magnetic lows. The relationship between magnetic intensity and gold mineralization

was not recognized, rather the relationship between magnetic intensity and rocks associated with gold mineralization. The high magnetic values (>3000 nT) were found protruding in the southern part of the study area, in areas where BIF and dolerite dykes are dominant. Therefore, the magnetic highs in the south confirm the presence of BIF which is highly magnetic due to its mineral composition, namely iron. The low magnetic values (<2900 nT) were prominent in the northern part which is almost entirely overlain by felsic pegmatites and migmatised-gneiss, and such rocks have no association with gold mineralization within the belt. The intermediate magnetic values of between 29400 and 29600 nT were associated with schists (including tremolite-mica schist and serpentine schist).

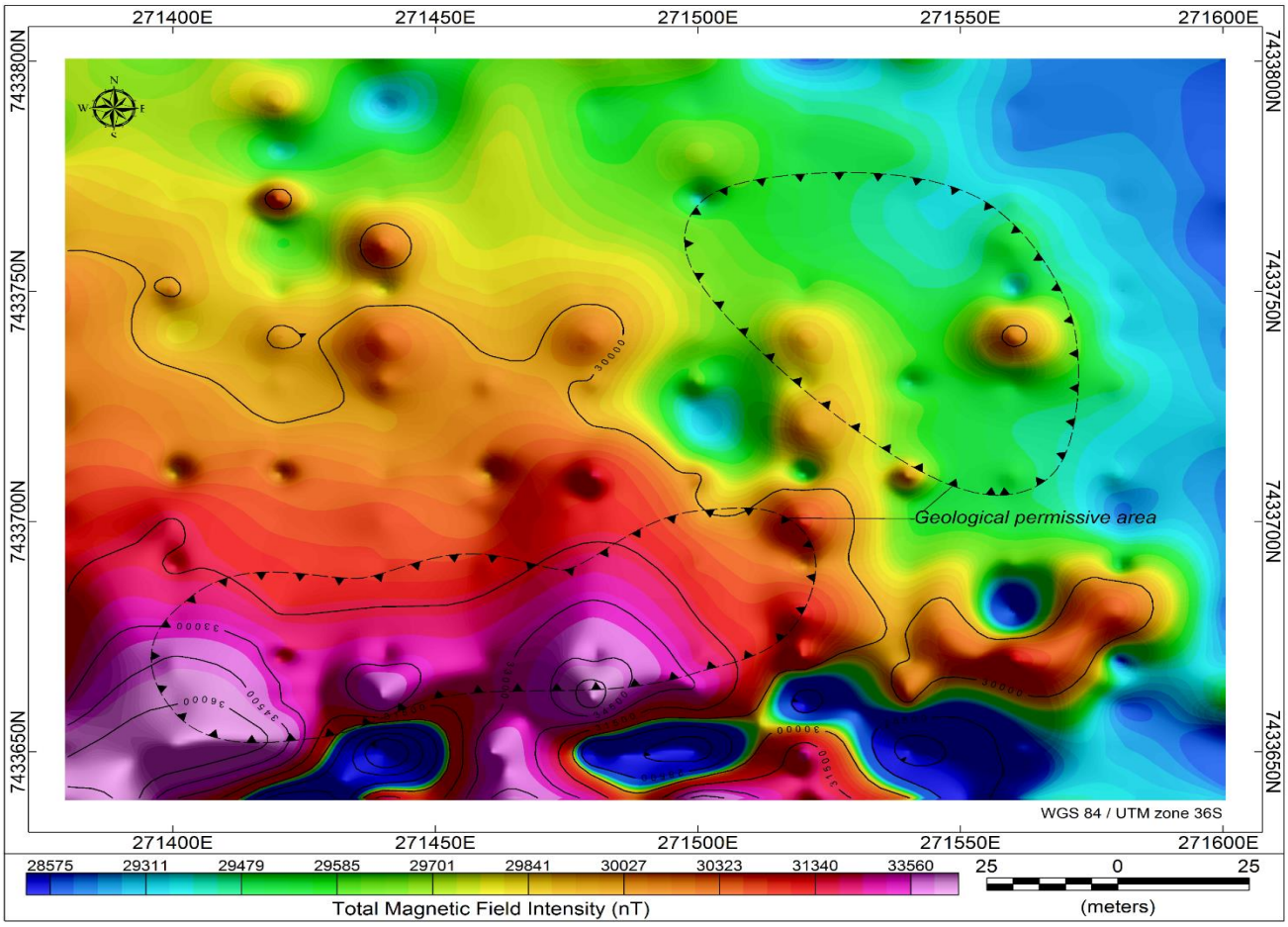

Figure 4.6: Total magnetic field intensity map of Nebulas Prospect. Prospectivity Layer of geological permissive areas from Boolean inference network is draped on the map.

Magnetic data enhancement techniques (including analytical signal processing and reduction to pole) were applied on the total magnetic field data to improve the quality of the data for better understanding. Implementing Equation 3.2, calculation of analytical signal was derived from three orthogonal gradients of the total magnetic field (x, y, z) and gridded as shown in Figure 4.7. This was done to locate the edges and peaks of magnetic source bodies. Numerous anomaly peaks were identified which could not be identified on total field

magnetic intensity map. The edges and peaks triggered by BIFs and dolerite dyke on the southern part of the study are well pronounced on the analytical map. Low analytical signal to the north of the study are associated with pegmatite and its edges are well defined.

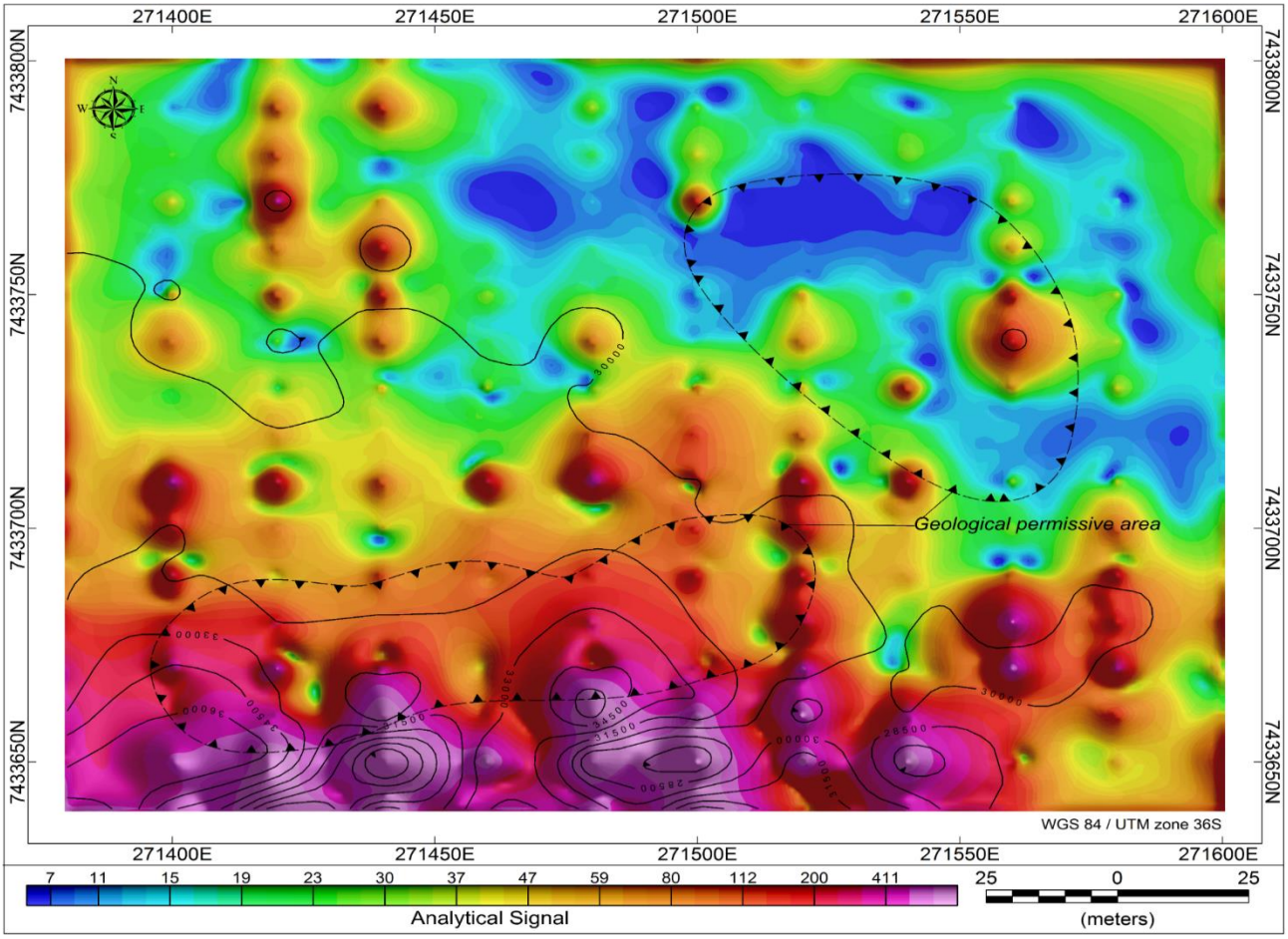

Figure 4.7: Analytical signal map derived from total field magnetic intensity Grid. Magnetic contours and prospectivity layers are overlaid on the map.

4.2.1 Reduction to pole

Magnetic intensity data was transformed using reduction to pole (RTP) filtering technique. The values of geomagnetic inclination (-60), geomagnetic declination (-15.27) and default amplitude correction of 20 were used to derive reduction to the pole magnetic intensity map shown in Figure 4.8. Geomagnetic declination and inclination values corresponds with the dates which magnetic survey was conducted (2017/08/22). Anomaly previously occurring at a low magnetic latitude shown by red delineations in Figure 4.8 were filtered and refined to their respective causative bodies. The low magnetic latitude which were concealed by high anomaly in total magnetic field intensity map are noticeable purely shown by yellow delineations in Figure 4.8. The refined magnetic low within the yellow box in Figure 4.8 were associated with (a) tremolite-mica schist and (b) pegmatite concealed by quartz rubble and clayey soil. The magnetic high within the red box suggest a concealed, highly weather basic

dyke. To the northeast, magnetic lows (28800 nT - 29500 nT) represent a migmatised gneiss which correlates with observed surface geology. The magnetic high (> 31500 nT) on the southern part of Nebulas Prospect indicate BIF with an east-west strike direction which compares with geological map.

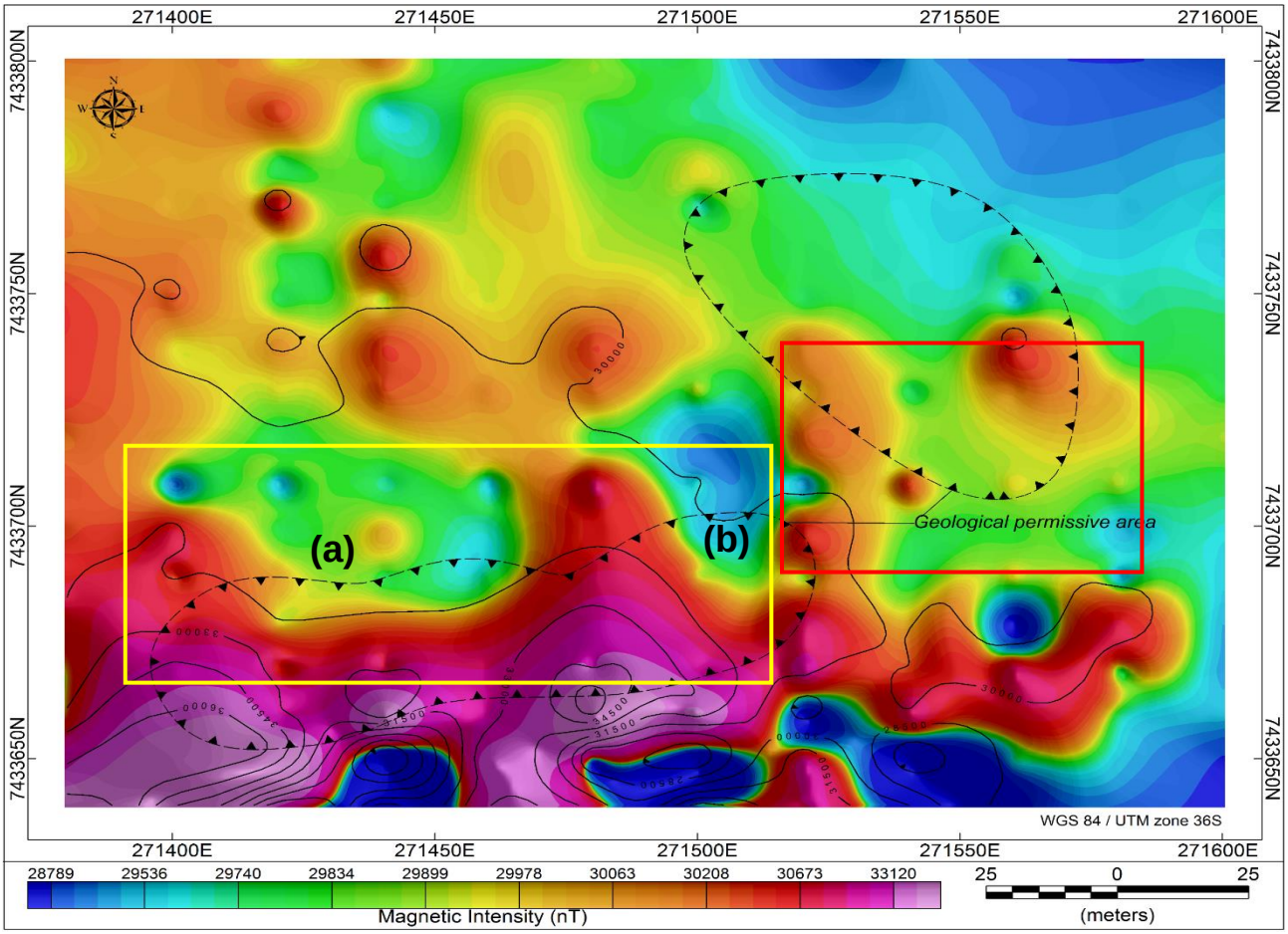

Figure 4.8: Reduction to pole magnetic intensity map. Magnetic contours and prospectivity layers are overlaid on the map.

4.2.2 Magnetic source depth modelling

The Nebulas Prospect structures (faults, contacts and dykes) and rock masses in the geological permissive area are mostly covered by soil. To locate the source and depth of magnetic anomaly, Euler 3D deconvolution method was used. A window size of 10 m was used to calculate the standard Euler solutions. Based on the geometry of magnetic targets being sought, structural index of 0 shown in Figure 4.9 was used for geological faults, contacts and joints. The clusters of solutions produced both structural index of 0 and window size of 10 as observed are closely scattered.

The dominating linear structures (faults, contacts or boundaries) which are associated with magnetic intensity were identified to be located at depth falling between 5 and 10 m.

However, few linear structures are located at depth exceeding 20 m. The contact between BIF and schist on the southern part is evidently delineated from the depth model, and this was not visible from surface geological map due to superimposed gravels and soil. This depth modelling indicates that pegmatite related contacts are shallowly located. According to Steenkamp and Clark-Mosterrt (2012), the shallow steeply dipping rocks in the GGB were evaluated using trenches, and if proven to be economic, surface mining method was employed to extract the deposit.

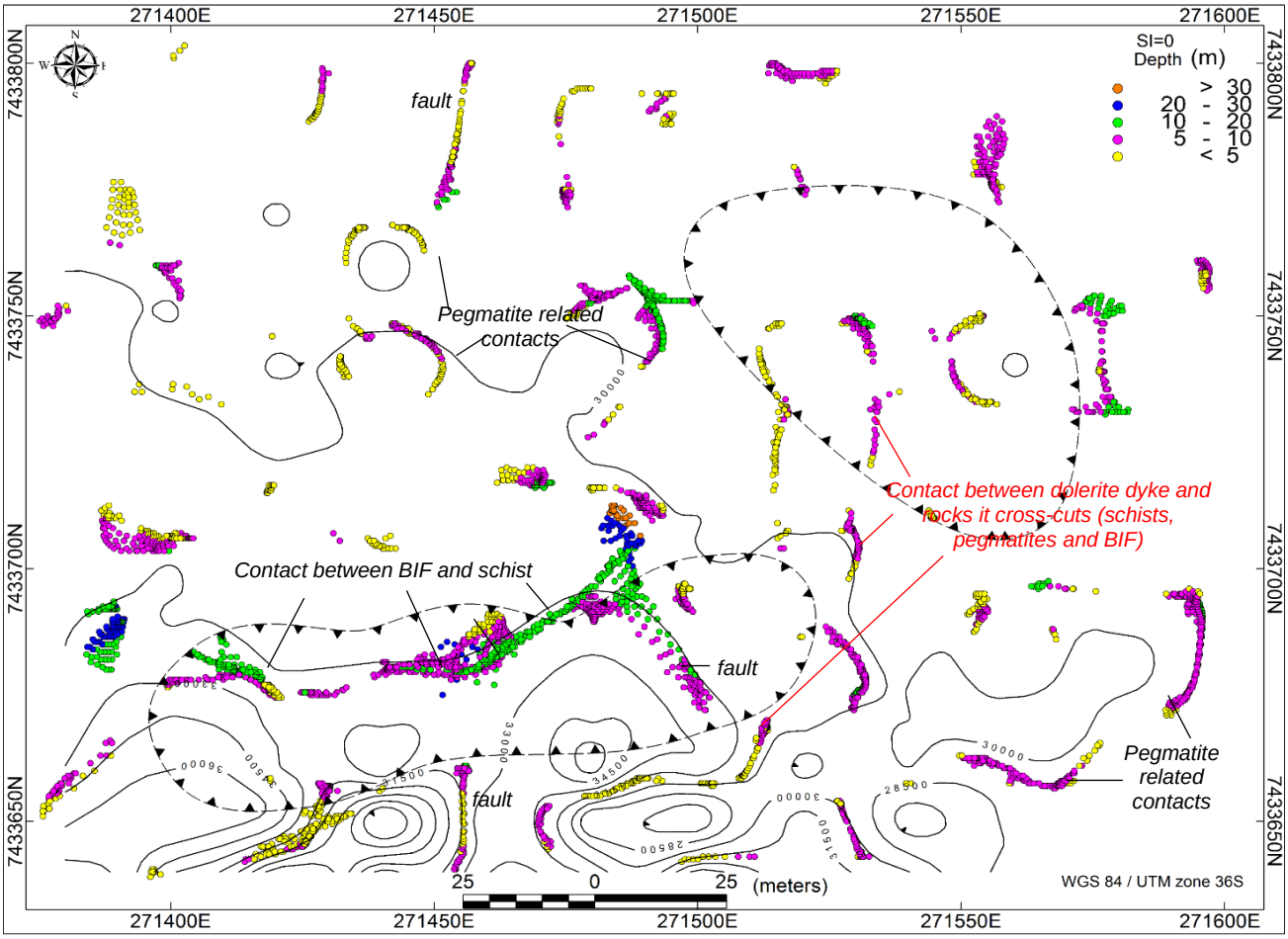

Figure 4.9: The depth model map for structures (faults and contacts) with structural index of zero.

4.3 The Sub-Surface Characteristics of the Deposit

A total of 221.7 m cumulative of trenching was completed in a series of 10 trenches as shown in Figure 4.10. Vertical longitudinal view of each trench is presented from Figure 4.11 to 4.12. Trench mapping data (lithological and structural) was used to deduce extrapolation to a depth of about 10 m. The scale of 1:315 was adopted for clear presentation of various sections.

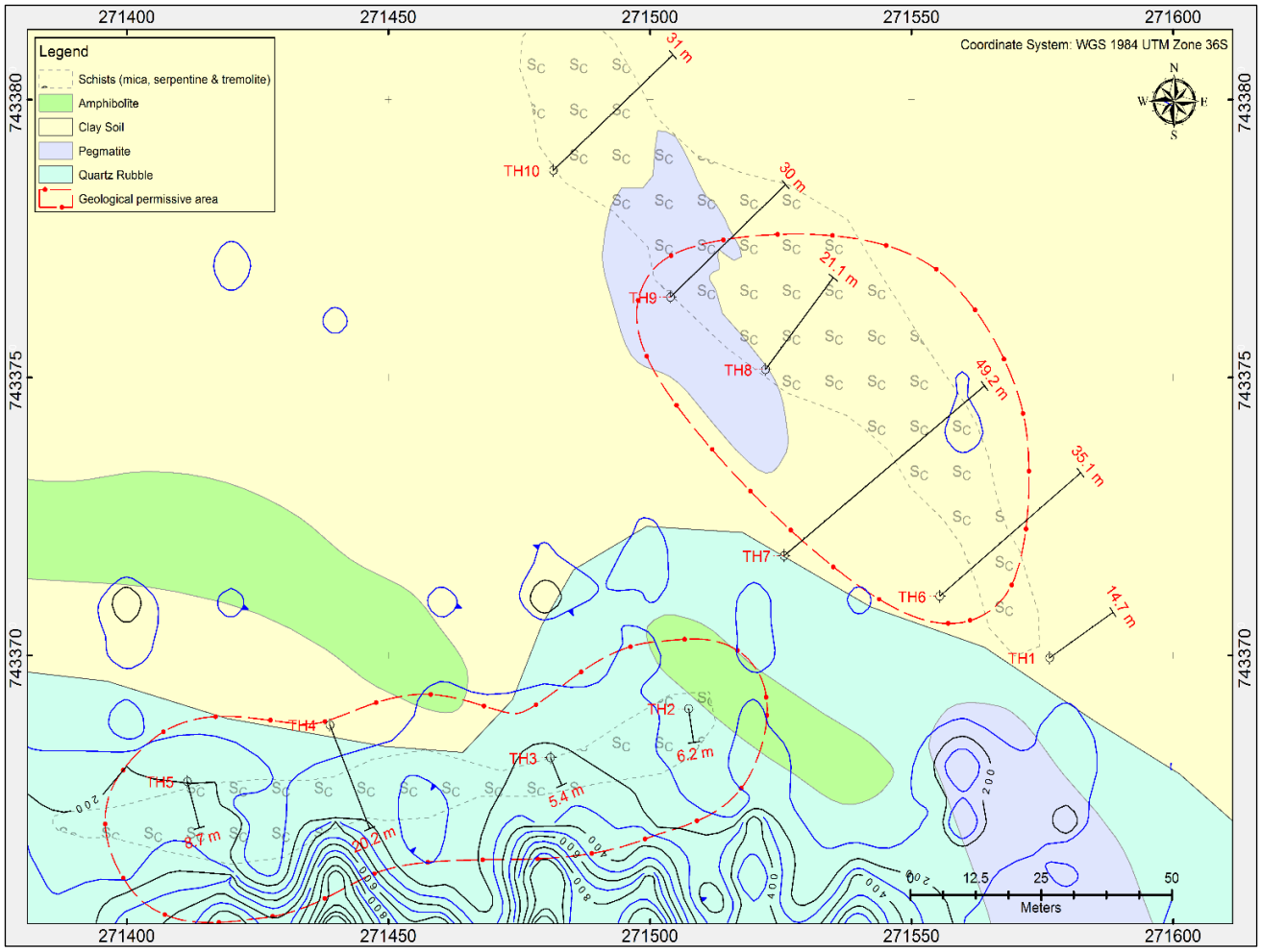

Figure 4.10: The locations of trenches superimposed on the geological map (geological permissive layer in red and analytical signal contours in blue and black).

4.3.1 Geological presentation of trenches

Trench TH1 shown in Figure 4.11a intersects massive pegmatite extending southward and weathered aplite striking northwest-southeast. Large volume of quartz rubble covers aplite to the north to a depth of more than 5 m. Southwest of trench TH1, trenches TH2 to TH5 intersected BIF and tremolite-mica schist trending on east-west direction with dips between 87° and 90°. The units intercepted in trenches TH2,3,4 and 5 are shown in Figure 4.11b - e

Old exploration pit located between trench TH4 and TH3 supports east-west continuity of BIF and tremolite-mica schist. From the pit, both BIF and tremolite-mica schist continue dipping at 90° to a measured depth of 12 m. The BIF is composed dominantly of haematite with thin siliceous bands. Tremolite and the micas minerals dominate the tremolite-mica schist. The mica minerals included muscovite and minor biotite.

Trench TH6 shown in Figure 4.12a uncovered pinkish weathered aplite and basic dyke which both extended to the southeast direction. Trenches TH7 to TH10 exposed mica-

tremolite schist, serpentine schist and quartz veins with strike of northwest-southeast (see Figure 4.12b - e). Pegmatite intrudes both lithology of trenches TH6 to TH9 but did not extend towards trench TH10 which is dominated by tremolite-mica schist and serpentine schist. The weathered basic dyke of dolerite composition with strike of North 15° East was found crosscutting all the rocks extending from trench TH7 to TH8 which obtrude in trench TH9. The old exploration pit located between trench TH6 and TH7 reveals northwest-southeast continuity tremolite-mica schist. From the pit, tremolite schist continue with a dip of 87° south to a measured depth of 7 m. The area is extensively covered by quartz rubble which extend to a depth of ± 1.2 m.

Figure 4.11: An illustration of cross-sectional view of trenches (TH1 to TH5)

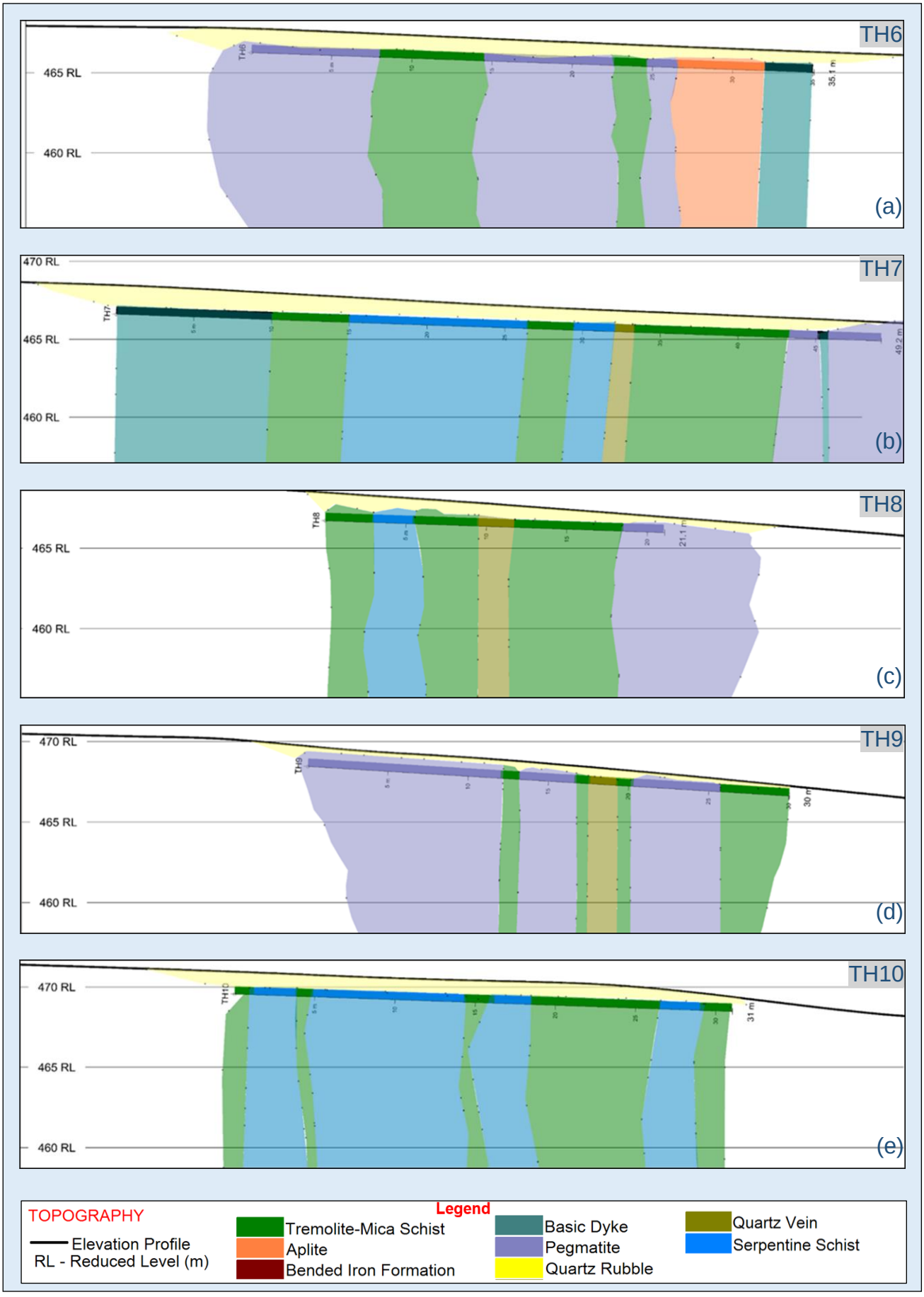

Figure 4.12: An illustration of cross-sectional view of trenches (TH6 to TH10)

4.3.2 Subsurface gold concentration and distribution

Total of 117 samples were analyzed for gold, 111 from trenches and 6 from old exploration pits. The gold assay results (Appendix B) were used to generate bar graph along trenches for different intervals as shown in Figure 4.22. Sample results located within the geological prospective areas indicated a significant concentration of gold (Au) that ranges from 0.34 g/t to 10.65 g/t. Trench TH1 located south-east of the old exploration pit includes 1.8 m grading 0.93 g/t Au (8.5 – 10.3 m) and 1.9 m grading 0.47 g/t Au (10.3 – 12.2 m) which is trending north west towards trench TH6 with grade ranging from 0.16 – 0.78 g/t Au for various interval (5.5 - 6.7m, 11.3 – 14 m, and 27 – 30.1 m). Dominating rocks in trench TH1 and TH6 include pegmatite, aplite and some thin layers of tremolite mica schists. The thin layers of tremolite-mica schist in trenches TH1 and TH6 appear to be hosting gold especially on the contacts with pegmatite.

Trench TH2 exposed BIF which cover 0.3 m grading 2.49 g/t Au (3.7 – 4 m). Moving towards the southwest part of TH2, TH3 with 1.8 m grading 1.24 g/t Au (1.8 – 3.6 m) and TH4 with 2.1 m grading 1.3 g/t Au (9.8 – 11.9 m) were identified. Significant assay results from trench TH5 showed 4.9 m long mineralized zone with maximum of 6.07 g/t Au over 0.7 m (4.2 – 4.9 m). Gold grade values between 0.46 g/t and 1.3 g/t on the opening and bottom of old south exploration pit walls showed overall strong potential of the gold trend (lateral and vertical) from trench TH2 towards TH5. Trenches (TH2 – TH5) comprise steeply dipping BIF and tremolite-mica schist. BIF contained much of the gold compared to the tremolite mica schist in the south of the area.

The best gold intersection was found in Trench TH7 which had a 7.9 m wide mineralisation interval (26.5 – 34.4 m) with a maximum of 10.65 g/t gold (Au) over 0.9 m and between 2 – 6.45 g/t Au for various intervals. The old exploration pit located next to TH7 showed a significant concentration between 3 and 4 g/t of Au at the opening and bottom (depth 6 m). Significant amount of gold is hosted by serpentine schist, tremolite schist and quartz veins which dominates trench TH7 and TH8.

Highlights for Trench TH8 included 1.4 m grading 2.34 g/t Au (2 – 3.4 m), 1.9 m grading 4.44 g/t Au (4.1 – 6 m) and another 1.6 m grading 2.93 g/t Au (12.1 – 13.7 m). These gold values confirm continuing gold trend from old north exploration pit through trench TH7. However, the trend continuation is limited on Trench TH9 with low grade values of 0.16 to 0.62 g/t Au over 4 m and a distinct 1.2 m grading 2.18 g/t Au (12.1 – 13.7 m). Truncated gold grade values between 0.16 – 0.93 g/t Au for 29 m have been intercepted along trench TH10 which confirms the overall strong potential of the gold trend.

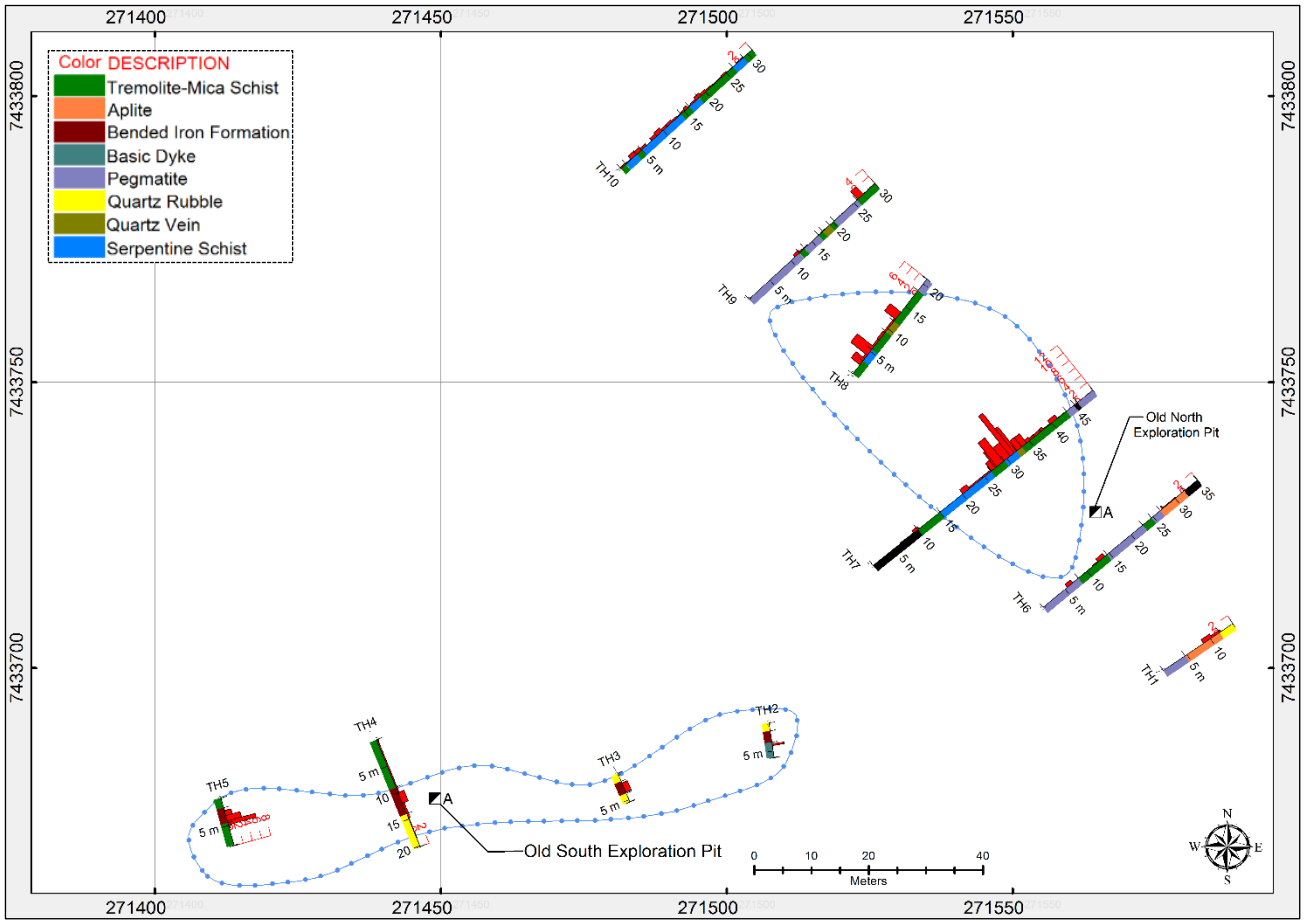

Figure 4.13: Gold grade variation (red bar graph Au (g/t)) for all trenches at depth ± 1.5 m for different sampling intervals. Geological prospective (blue) layer overlain.

4.4 The Geological Model of the Nebulas Gold Deposit

The geological and mineralized zone model was developed by joining generated series of trench sections and integrated with magnetic processed data and gold assay data. The 3D inversion of structural evidence (lithology contacts), derived from structural index data (depth model) shows depth continuity for rock hosting gold. The observed depth of tremolite-mica schist and serpentine schist on the northern part of the Nebulas Prospect was found to be about 10 m. However, the BIFs on the southern part of the study area extends to a depth of about 30 m.

The magnetic isosurface 30700 nT demarcates highly magnetic area on the south which is controlled by iron (Fe) content of the BIFs and displayed a positive response to the east-west strike direction and dip of 90°. Structural index data showed that there is a clear contact between BIF and tremolite-mica schist as observed from west side of the model as shown in Figure 4.14. Based on Figure 4.15, it can be seen that gold mineralization (red wireframe blocks) is not associated with specific magnetic anomaly, although, the host rocks of various composition have association. Tremolite mica schist and serpentine schist are associated

with magnetic intensity less than 29800 nT, which is seen from isosurface 29800 nT responding to northwest-southeast strike directions of the schists. Magnetic response of basic dyke striking northeast-southwest is not uniform as it decreases from south to north as shown in Figure 4.14 (BDmG Trend).

The Nebulas Prospect is comprised of two mineralised areas which are of different rock types, namely, east-west BIF hosted, and northwest-southeast schist hosted. The east-west steeply dipping BIF formation host a narrow (< 3 m) gold mineralisation on the south. The similar deposit of this mineralisation style in the Giyani Greenstone Belt (GGB) has been mined out using shrinkage stopping (in Birthday Mine and Swartkoopies) and cut and fill stopping (in Gemsbok mine) (Billay et al., 2014). However, the BIF hosted gold in West-59 and Frankie mine was mined out using open pit mining.

The northwest-southeast steeply dipping tremolite-mica schist, serpentine schist and quartz vein host a narrow (< 8 m) and shallow (about 5 m deep) gold mineralisation. The gold mineralization in this part of the study area followed the trend of rocks. The steeply dipping schists hosting gold in the Giyani Greenstone Belt has been mined using underground stopping methods (in Klein Letaba and Louise Moore mines) in the past (Billay et al., 2014). However, the gold mineralisation in this part of the study area is too shallow. The shallow deposits within the GGB were previously mined by open pit method (Steenkamp and Clark-Mosterrt, 2012).

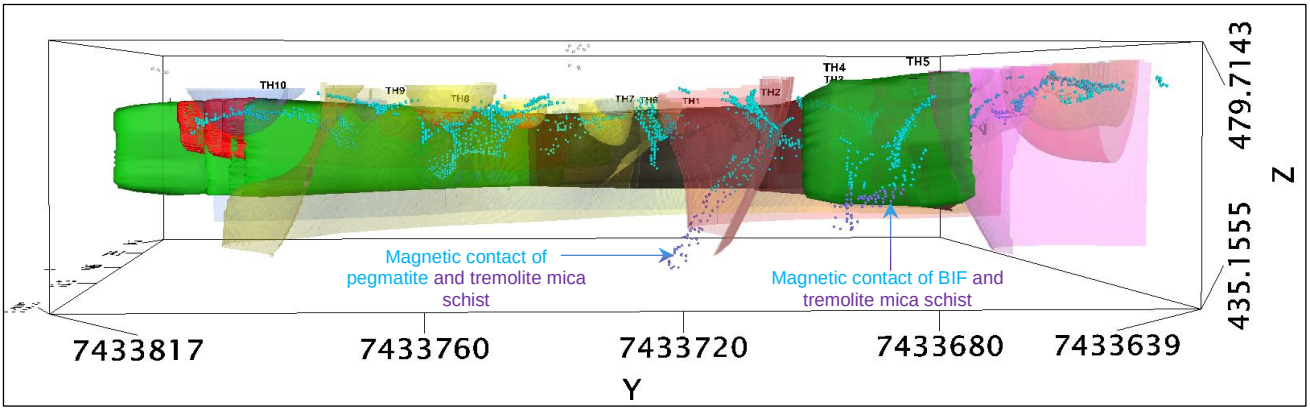

Figure 4.14 : West to east view of structural index data (cyan and purple dots). Rotated from 3D geological model.

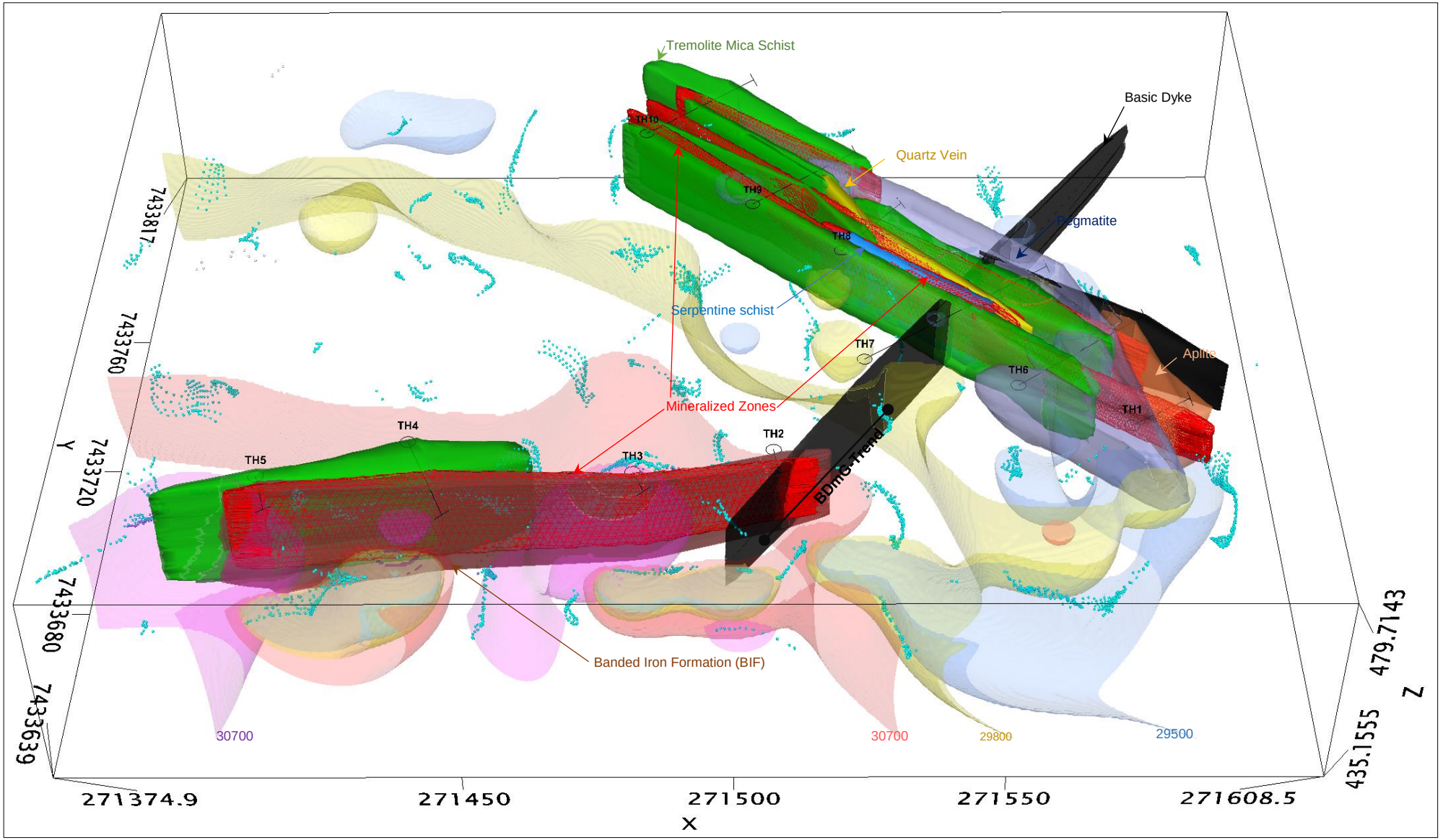

Figure 4.15: 3D geological model of the Nebulas Prospect, integrated with magnetic intensity (multiple isosurface layers) and structural index (SI=0) data. Mineralized zone marked with red mesh polygon.

CHAPTER FIVE

GOLD VALUATION AND SELECTION OF MINING METHODS

This Chapter presents the outcome of the adoption of vertical longitudinal section method for estimation of the resource/reserve. Existence of different mineralized area controlled by lithology of two different strike directions led to the classification of the Nebulas Prospect into two sectors, Nebulas North Sector (NNS) and Nebulas South Sector (NSS). Gold was quantified in relation to grade and tonnage to establish its economic significance. Appropriate mining methods were identified and ranked in relation to factors influencing the selection process.

5.1 Gold Resource Evaluation of Nebulas Prospect

Gold resource evaluation was conducted to establish gold grade and tonnage of the mineralized area, which is substantial in the economic valuation of mineral deposit. To estimate the quantity (tonnage) and the quality (grade) of gold in a definite 3D mineralization envelope, longitudinal vertical sections method was used for each trench section. The evaluation was based on the information generated and validated through geological model. Through application of the method explained in Chapter 3, an average weighted gold grade per trench section for precise mineralized length was calculated.

The dominant host rocks for gold in the area included BIF with bulk specific gravity (Sp. Gr.) of 3.99, tremolite-mica with bulk specific gravity of 2.39 and serpentine schist with bulk specific gravity of 2.42. Confirmed maximum depth of mineralization is 6 m for the area dominated by schists (trench TH1, TH6 to TH10) and 10 m for southern part area which is dominated by BIF (TH2 – TH5). The processing of data generated specific block tonnage per trench section with a maximum of halfway influence of 35 m which represent maximum spacing between successive trenches. Established block tonnage with average weighted grade per trench were used to establish the average gold grade of the gold resource presented in Table 5.1.

5.1.1 Average weighted gold grades for trenches

Trenches TH1 covered 3.7 m length of weighted 0.69 g/t of gold (Au), TH2 contains 2.49 g/t Au weighted over 0.3 m, TH3 comprise 1.8 m grading 1.24 g/t Au. Trench TH4 covers a total of 18 m with grade of 0.37 g/t, however, significant zone contains 1.3 g/t over 2.1 m (9.8 – 11.9 m). Total weighted grade average for trench TH5 is 2.75 g/t over 3.2 m, though

with decrease of mineralization intervals grade increase from 3.32 – 4.33 g/t Au for 2.3 – 4.9 m interval. Trench TH5 contains the highest grade within the BIFs domain striking east-west on the western part of the area. Through trenches TH2 to TH5 gold mineralization continuity was detected.

Trench TH6 holds 2.7 m average weighted grading of 0.5 g/t Au (11.3 – 14 m) which is one of the significant zones in the trench. Trench TH7 hold the highest grade per interval (10.65 g/t Au over 0.9 m (30.7 -31.6 m) compared to all trenches. Trench TH8 presents 4 m grading 3 g/t Au (2 – 6 m), which indicates mineralization continuity from trench TH7. Trenches TH9 and TH10 contains less than 1 g/t Au overall weighted grade. However, a significant 1.2 m grading 2.18 g/t Au (25.9 – 27.2 m) was detected in trench TH9. In each trench different sub-block were marked out representing different grade categories (< 1 g/t Au and > 1 g/t Au).

5.1.2 Average block tonnage with weighted gold grades for trenches

Two classes (class 1 and class 2) of blocks with significant mineralization were established. Class 1 present blocks with average weighted grade of greater or equal to 1 g/t Au and class 2 includes average weighted grade between 0.4 – 0.99 Au g/t. Trench blocks for trenches TH2 – TH5 are grouped and classified as Nebulas South Sector (NSS), which present east-west mineralization trend. Trench blocks of trench TH1, TH6 – TH10 are grouped and classified as Nebulas North Sector (NNS) representing northwest-southeast Au mineralization trend.

Based on Table 5.1, NSS blocks includes average weighted grade above 1 g/t Au and are both assigned to class 1. NSS trench blocks include TH2A (315.9 t grading 2.49 g/t Au), TH3A (1825.2 t grading 1.2 g/t Au), TH4A (1774.5 t grading 1.3 g/t Au) and TH5A (3042 t grading 3.32 g/t Au). NNS blocks includes an average weighted grade of both class 1 and class 2 indicated in Table 5.1.

Table 5.1: Weighted average grade calculation for trench TH1 through TH10

Mineralisation length (**mL**) in meters(m), Depth of mineralization (**dM**) in meters (m), halfway influence (**hF)**in meters (m), Volume (**Vol.**) in cubic meters (m^3), Bulk specific gravity (**BSp. Gr.**), Block tonnage (bT (a_i -weighting factor)) in tonnes (t), G_i weighted average grade per block, Class 1 (≥ 1 g/t Au), Class 2 (≥ 0.4 g/t Au) and $\bar{G}_w$ average grade

Trench-Block	mL (m)	dM (m)	Mineralized Area (m^2)	hF (m)	Vol. (m^3)	BSp. Gr.	bT- a_i (t)	G_i (g/t)	Class	$G_i a_i$ (Class 1 & 2)	$G_i a_i$ (Class 1)
Trench TH2											
Block TH2A	0.30	10	3	27	81	3.9	315.90	2.49	1	786.59	786.59
Trench TH3											
Block TH3A	1.80	10	18	26	468	3.9	1825.20	1.24	1	2263.25	2263.25
Trench TH4											
Block TH4A	1.30	10	13	35	455	3.9	1774.50	1.3	1	2306.85	2306.85
Trench TH5											
Block TH5A	2.60	10	26	30	780	3.9	3042	3.32	1	10099.44	10099.44
Trench TH1											
Block TH1-A	3.70	5	19	22	407	2.39	972.73	0.69	2	671.18	
Trench TH6											
Block TH6A	1.20	5	6	23	138	2.39	329.82	0.78	2	257.26	
Block TH6B	1.50	5	7.5	23	173	2.39	412.27	0.78	2	321.57	
Block TH6C	0.30	5	1.5	23	34.50	2.39	82.45	0.6	2	49.47	
Trench TH7											
Block TH7A	6.40	5	32	23	736	2.39	1759.04	0.49	2	861.93	
Block TH7B	7.90	5	40	23	909	2.42	2198.57	4.60	1	10113.42	10113.42
Block TH7C	8.40	5	42	23	966	2.39	2308.74	0.47	2	1085.11	
Trench TH8											
Block TH8A	4	5	20	25	500	2.39	1195	3	1	3585	3585
Block TH8B	6.10	5	31	25	763	2.39	1822.37	0.4	2	728.95	
Block TH8C	1.60	5	2.8	25	70	2.39	167.30	2.93	1	490.19	490.19
Trench TH9											
Block TH9A	1.20	5	6	25	150	2.39	358.5	2.18	1	781.53	781.53
Trench TH10											
Block TH10A	6	5	30	22	660	2.42	1597.2	0.53	2	846.52	
Block TH10B	6	5	30	22	660	2.39	1577.4	0.57	2	899.12	
Block TH10C	6	5	30	22	660	2.42	1597.2	0.41	2	654.85	

Notes: Tonnage = Volume x Bulk Sp. Gr

1 g/t = 1 g/m^3 = 1 ppm

Scenario A

Trenches Blocks	$\sum_{i=1}^{n} G_i a_i$	$\sum_{i=1}^{n} a_i$	$\bar{G}_w$	Outcome
TH2A, TH3A, TH4A &TH5A	15456.13	6957.60	2.22	6957.6 t (1628.5 m^3) with average grade of 2.22 g/t
TH7B, TH8A, TH8C & TH9A	14970.14	3919.37	3.82	3919.37 t (1784 m^3) with average grade of 3.82 g/t
Grade (g/t)			2.79	
Tonnage (t)			10877	
Volume (6980.5 m^3) @ 2.79 g/m^3				

Adopted Equation 3.2

$$\bar{G}_w = \frac{\sum_{i=1}^{n} G_i a_i}{\sum_{i=1}^{n} a_i}$$

Scenario B

Trenches Blocks	$\sum_{i=1}^{n} G_i a_i$	$\sum_{i=1}^{n} a_i$	$\bar{G}_w$	Outcome
TH2A, TH3A, TH4A &TH5A	15456.13	6957.60	2.22	6957.6 t (1628.5 m^3) with average grade of 2.22 g/t
TH1A, TH6A, TH6B, TH6C, TH7A TH7B, TH7C, TH8A, TH8B, TH8C, TH9A, TH10A, TH10B & TH10C	21346.11	16378.61	1.30	16378.60 t (6980.5 m^3) with average grade of 1.30 g/t
Grade (g/t)			1.58	
Tonnage (t)			23336	
Volume (6980.5 m^3) @ 1.30 g/m^3				

5.2 Economic Evaluation of Nebulas Gold Resource

Large scale mining operation requires intense capital investment and the return in investments is not immediate as opposed to small scale mining technique. Small scale mining technique has been employed within the Giyani Greenstone Belt (GGB) in past. This study indicated presence of gold mineralization in the Nebulas Prospect. A study conducted by Schodde (2011) concluded that the ore grades around the world are less than 1 g/t Au at the present. Based on his conclusion, two scenarios (A and B) were presumed for resource determination in the Nebulas Prospect. Scenario A present mineralized block of Class 1 (≥ 1 g/t Au) for Nebulas South Sector (NSS) and Nebulas North Sector (NNS) while scenario B includes both class 1 and class 2 (0.4 – 0.99 g/t Au) for NNS and NSS.

In scenario A, NSS comprises total tonnage of 6957.6 t at an average weighted grade of 2.22 g/t Au and NNS with 3919.37 t with grade of 3.8 g/t Au. Scenario A establish a total resource of 10877 t at a weighted average grade of 2.79 g/t Au. In scenario B, NSS tonnage and grade remains unchanged, however, NNS comprise 16378.6 t with average weighted grade of 1.3 g/t Au. Scenario B establishes total resource of 23336 t at a weighted grade average of 1.5 g/t Au. Scenario B covers reserve which is 53.4 % more than scenario A, nevertheless, the grading (g/t Au) is 43.6 % less than scenario A.

The tonnage, geometry and grade of the orebody has been estimated using both Geosoft Target 8.4 and average weighted grade methods. Through detailed geological mapping, magnetic survey and intense trench and pit sampling, sufficient deposit information was generated to provide rationale in making a declaration of the estimate of tonnage and grade.

The location of ore body in both NNS and NSS closely spaced to confirm geological and grade continuity. The main host rocks for gold in the Nebulas Prospect are BIF, tremolite-mica schist, serpentine schist and quartz veins. The gold mineralization within these rocks in the GGB was also documented by Kramers et al. (2014), Kröner et al. (2000), McCourt and van Reenen (1992) and Sadeghi et al. (2015).

The research established a detailed and highly consistent geoscientific evidences, thereby classifying mineralized geological zone of Nebulas Prospect as measured mineral resource, in accordance to South Africa Mineral Resource Committee (SAMREC) reporting code. From the conventional classification system, the identified mineralized geological zone is classified as developed reserve because of the existence of pits marking out depth of mineralization.

5.3 Mining Method Selection for Nebulas Gold Deposit

No unique method can meet all the requirements and conditions, but relatively the appropriate mining method is the one that is technically feasible for the ore geometry and ground conditions in the area. Analytical hierarchy process (AHP) was used to prioritize the factors influencing mining method selection and ranking of potential mining method, technically appropriate for the established gold deposit in Nebulas Prospect.

5.3.1 Prioritization of factors influencing selection of mining method

The dip, ore strength, shape, thickness, grade, depth of the deposit and the strength of the host rock are the 7 factors influencing selection of an appropriate mining method for Nebulas Prospect as shown in Table 5.2. The Nebulas Prospect presents a steeply dipping, very shallow, tabular, and narrow gold deposit. With these deposit parameters, the practical alternative mining methods include but not limited to shrinkage stopping (mA_1), open pit (mA_2,) and cut and fill stopping (mA_3). The three-mining alternative have a proven record for mining steeply dipping shallow deposit with thickness less than 10 m (Gupta and Kumar, 2012). The open pit and shrinkage stoping were previously used to extract the gold ore of similar type within the belt (Billay et al., 2014; Du Plessis, 2012; Steenkamp and Clark-Mosterrt, 2012).

Table 5.2: Parameters influencing the choice method to mine the Nebulas Gold Deposit.

Intrinsic factor affecting selection method	Nebulas North Sector (NNS)	Nebulas South Sector (NSS)	Overall deposit Classification
C_1 - Dip of the deposit	80°	88°	Steep (> 45°)
C_2 - Strength of the ore	44*	48*	Moderate
C_3 - Strength of the host rock	44*	48*	Moderate
C_4 - Depth of the deposit	down to 5 m	down to 10 m	Very shallow
C_5 - Shape of the deposit	Tabular	Tabular	Tabular
C_6 - Grade of the ore	1.2 – 2.79 g/t Au	2.22 g/t Au	Erratic
C_7 - Thickness of the deposit	1.2 – 8 m	1 – 2 m	Narrow (< 10 m)
* Rock Mass Rating (RMR) computed from Rock Mass Rating System adopted from EduMine (2018)			

APH computation of pair-wise matrix comparison shown in Table 5.2, prioritized factors affecting selection of the mining method in the Nebulas Prospect and are presented in Table 5.3 with criterion priority chart. AHP revealed that depth of the deposit is the most important factor (priority = 0.282) for the selection of method for mining the Nebulas Gold Deposit, followed by dip of the deposit (priority = 0.244), deposit thickness (priority = 0.6), host rock strength (priority = 0.091), strength of the ore (priority = 0.089), shape of the deposit (priority weight = 0.071) and grade of the ore (priority = 0.054). The consistency ratio ($\boldsymbol{CR}$ = 0.035)

for all criterions was less than 10 % (0.1) and this indicates coherent judgment in specifying pair-wise comparison in the criteria.

Table 5.3: Pair-wise comparison matrix for the importance of 7 intrinsic factors.

Intrinsic Factor	C1	C2	C3	C4	C5	C6	C7
C1- Dip	1	3	3	1	3	3	2
C2- Ore strength	1/3	1	1	1/3	1	3	1/3
C3- Host rock strength	1/3	1	1	1/3	2	2	1/3
C4- Depth	1	3	3	1	3	5	3
C5- Shape	1/3	1	1/2	1/3	1	1	1/2
C6- Grade	1/3	1/3	1/2	1/5	1	1	1/3
C7- Thickness	1/2	3	3	1/3	2	3	1

Table 5.4: Analytical hierarchy process computation for prioritisation of criterions.

Criterion	Comment	Weight	Rank	Criterion Priority Chart
C1- Dip	Dip of the deposit	0.244	2	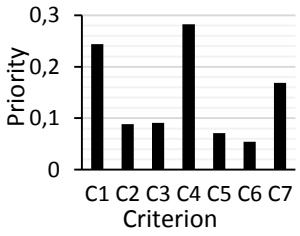
C2- Ore strength	Strength of the ore	0.089	5	
C3- Host rock strength	Strength of the host rock	0.091	4	
C4- Depth	Depth of the deposit	0.282	1	
C5- Shape	Shape of the deposit	0.071	6	
C6- Grade	Grade of the ore	0.054	7	
C7- Thickness	Thickness of the deposit	0.169	3	
$\lambda_{max} = 7.28 \quad CR = 0.035\ (3.5\%\ acceptable) \quad n = 7$				

5.3.2 Prioritization of mining method for Nebulas Gold Deposit

Mining selection method includes the interaction of various subjective criterion. The mining methods considered as possible and appropriate for Nebulas Prospect include; shrinkage stopping (mA1), open pit (mA2) and cut and fill stopping (mA3). The pairwise comparison of mining methods (denoted as mA1, mA2 and mA3) were compared in relation to weighted prioritized intrinsic factors (denoted as C1, C2,…, C7) and is shown in Figure 5.1a – g.

Based on Figure 5.1a, with consideration to dip of the deposit (C1) both mining methods are preferred and carry equal weight of priority. Regarding the ore strength (C2) shown in Figure 5.1b, cut and fill method (mA3) is more ideal amongst the shrinkage stopping (mA1) and open pit (mA2) method. However, this factor is of low priority (rank of 5) compared to other extrinsic factors. The pairwise comparison of mining methods in relation to strength of the host rock (C3) shown in Figure 5.1c prioritize cut and fill (mA3) as preferable method of mining among shrinkage stopping (mA1) and open pit (mA2).

In relation to the shape of the deposit (C5) shown in Figure 5.1e and grade of the ore (C6) shown in Figure 5.1f, shrinkage stopping is an ideal method of mining compared to shrinkage stopping and open pit mining methods. With consideration to the depth of the

deposit (C4) shown in Figure 5.1d and thickness of the deposit (C7) shown in Figure 5.1g, open pit is a high priority method for mining Nebulas Gold Deposit in comparison with shrinkage stopping and cut and fill methods.

C1	mA1	mA2	mA3	Weight	Priority Chart
mA1	1	1	1	0.333	0,5 / 0 / mA1 mA2 mA3
mA2	1	1	1	0.333	
mA3	1	1	1	0.333	

$\lambda_{max} = 3.000$ $\boldsymbol{CR} = 0.00\ (0\%)$ *acceptable*

(a) Comparison of mining methods with reference to the dip of the deposit - C1 (weight of criterion = 0.244)

C2	mA1	mA2	mA3	Weight	Priority Chart
mA1	1	4	1/2	0.333	1 / 0 / mA1 mA2 mA3
mA2	1/4	1	1/5	0.097	
mA3	2	5	1	0.569	

$\lambda_{max} = 3.025$ $\boldsymbol{CR} = 0.026\ (2.6\%)$ *acceptable*

(b) Comparison of mining methods with reference to the strength of the ore (weight of criterion C2 = 0.089)

C3	mA1	mA2	mA3	Weight	Priority Chart
mA1	1	3	1	0.405	1 / 0 / mA1 mA2 mA3
mA2	1/3	1	1/5	0.114	
mA3	1	5	1	0.481	

$\lambda_{max} = 3.029$ $\boldsymbol{CR} = 0.03\ (3\%)$ *acceptable*

(c) Comparison of mining methods with reference to the strength of the host rock – C3 (weight of criterion = 0.091)

C4	mA1	mA2	mA3	Weight	Priority Chart
mA1	1	1/5	1	0.156	1 / 0 / mA1 mA2 mA3
mA2	5	1	3	0.659	
mA3	1	1/3	1	0.158	

$\lambda_{max} = 3.029$ $\boldsymbol{CR} = 0.03\ (3\%)$ *acceptable*

(d) Comparison of methods with reference to the depth of the deposit – C4 (weight of criterion = 0.282)

C5	mA1	mA2	mA3	Weight	Priority Chart
mA1	1	5	1	0.481	1 / 0 / mA1 mA2 mA3
mA2	1/5	1	1/3	0.111	
mA3	1	3	1	0.405	

$\lambda_{max} = 3.029$ $\boldsymbol{CR} = 0.03\ (3\%)$ *acceptable*

(e) Comparison of mining methods with reference to the shape of the deposit – C5 (weight of criterion = 0.071)

C6	mA1	mA2	mA3	Weight	Priority Chart
mA1	1	5	2	0.582	1 / 0 / mA1 mA2 mA3
mA2	1/5	1	1/3	0.109	
mA3	1/2	3	1	0.309	

$\lambda_{max} = 3.004$ $\boldsymbol{CR} = 0.04\ (4\%)$ *acceptable*

(f) Comparison of mining methods with reference to the grade of the ore - C6 (weight of criterion = 0.054)

C7	mA1	mA2	mA3	Weight	Priority Chart
mA1	1	1/3	3	0.258	1 / 0 / mA1 mA2 mA3
mA2	3	1	5	0.637	
mA3	1/3	1/5	1	0.105	

$\lambda_{max} = 3.039$ $\boldsymbol{CR} = 0.04\ (4\%)$ *acceptable*

(g) Comparison of mining methods with reference to the thickness of the deposit (weight of criterion C1 = 0.169)

Indicator	Description
mA1	Shrinkage stopping
mA2	Open pit
mA3	Cut and fill
C1	Deposit dip
C2	Ore strength
C3	Host rock strength
C4	Deposit depth
C5	Deposit shape
C6	Grade of the ore
C7	Deposit thickness

Figure 5.1: (a) – (g) pair-wise comparison the mining method according to each of the criterion and (h) composite ranking of the mining methods.

Consolidated pair-wised comparison of mining methods (mA1, mA2 & mA3) in relation to weighted criterion (C1, C2,…, C7) generated composite weight for prioritizing mining methods indicated in Table 5.4. Based on Table 5.4, it is found that consistency ratio (max CR of 6%) for all parameters is less than 10 %. This validates that the integrity and objectivity of the decision-making process was well preserved. To extract this shallow deposit, multi-criterion decision making using AHP, prioritized open pit (priority = 0.375) as the most appropriate mining method in consideration of all 7 factors in the mining selection,

followed by shrinkage stopping (priority = 0.326) and cut and fill (priority = 0.2) mining methods.

Table 5.5: Aggregated pairwise comparison of mining methods (composite ranking of mining methods)

	mA1	mA2	mA3	Weight	Priority Chart
mA1	1	0.80	1.17	0.326	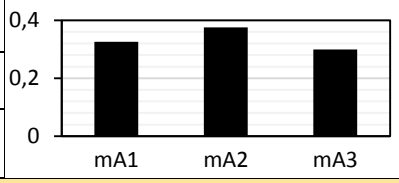
mA2	1.25	1	1.17	0.375	
mA3	0.86	0.86	1	0.299	
$\lambda_{max} = 3.005 \quad CR = 0.06\,(6\%)\ acceptable$					

CHAPTER SIX

CONCLUSION AND RECOMMENDATION

This chapter presents summary of the study. Conclusion built on discoveries of the research, linked to research objectives is presented in this section. Additionally, it gives recommendation for further investigation to support development of economic resource base.

6.1 Summary of the Study

Giyani Greenstone Belt (GGB) has not been explored to a satisfying extent. Increasing gold price in recent decade has attracted few exploration companies to explore portion of the belt with much interest on previously recognized deposits within the belt such as Klein Letaba and Louis Moore abandoned mines. Despite that, this has left potential gold prospects such as Nebulas Prospect unnoticed. Previous exploration activities such as trenches and pits which date to 1955 exist in the Nebulas Prospect, however, there is lack of information regarding gold distribution and concentration based on these activities. Feasibility sampling done as part of this study indicated significant occurrence of gold concentration ranging from 0,05 – 6.5 ppm in the Nebulas Prospect and this requires more detailed studies to establish the extent of the gold occurrence and its economic significance.

The main aim of the study was to conduct assessment of the probable gold mineralization in the Nebulas Prospect and its economic significance. The specific objectives were to define and map prospective gold mineralized zones within the Nebulas Prospect, develop a geological model showing the geometry and placement of gold in the subsurface, establish gold grade distribution and its economic implication, and selection of the most appropriate and practical mining method.

The research methods used in achieving these objectives comprised of knowledge driven predictive modelling of Nebulas Prospect to derive prospectivity map demarcating area with the potential of hosting gold mineralization. The prospectivity map generated from data integration indicated the ranks and priority for exploration target in the study area. Detailed geologic mapping program was conducted as part of the data collection for research work. The geologic map portrayed the distribution of rocks, deposits, and other geologic features in the study area. The association of gold with BIF, mafic to ultramafic rocks and quartz vein as indicated by McCourt and van Reenen (1992) allowed narrowing of target area within the study area.

Magnetic survey was conducted in geological permissive area, thereby establishing boundaries of mineralization, both lateral and vertical. Geological and geochemical investigation of the subsurface where conducted by means of trenching and pitting.

The investigation of Nebulas geological setting revealed presences of host rocks and geological structures associated with gold mineralization in the belt, which include BIF, schist and quartz veins. BIF dominates the southern part of the study area while quartz vein and schist dominates the northern part. The application of knowledge driven predictive modelling established mineral prospectivity map for Nebulas Prospect, which narrowed the potential area for further investigation. The area located outside the boundary of prospective area indicated low mineralization potential compared to highly mineralized zone within geological permissive boundary.

An inclusive geological ore body model integrating geochemical and magnetic data was developed. The model enabled estimation of grade and visualization of deposit geometry. This is useful in mine design, planning, scheduling, blending and quality control. The model enabled selection, effectively the most promising means of extracting ore both physically and economically.

The evaluation of the technical aspects of the Nebulas Gold Deposit, which include grade and tonnage was estimated using longitudinal section method. The Nebulas Gold Deposit comprise of two mineralized areas and were categorized as Nebulas North Sector (NNS) and Nebulas South Sector (NSS). The two mineralized zones which exits in the Nebulas Prospect are separated by pegmatite intrusion which was observed from magnetic data presentation. The gold mineralization in the NSS, hosted within Banded Iron Formation (BIF) comprise a measured gold resource of 6957.6 t at an average weighted grade of 2.22 g/t Au. In the NNS gold mineralization is hosted within tremolite-mica schist, serpentine schist and quartz veins. The NNS comprise a measured gold resource of 3919.37 t with grade of 3.8 g/t Au. At currently assumed economically mineable cutoff grade of 1 g/t Au, Nebulas Prospect has a measured resource of 10877 t at a weighted average grade of 2.79 g/t Au. The Nebulas Gold Deposit contain significant grade and tonnage. The highest concentration observed value of 10.65 g/t is hosted in serpentine schist and lowest significant of 1.24 g/t in BIF. Gold grades are higher in schists than in BIF and quartz veins.

No unique method can meet all the requirements and conditions, but relatively the appropriate mining method is the one that is technically feasible for the ore geometry and

ground conditions in the area. The Nebulas Prospect presents a steeply dipping, very shallow, tabular, and narrow gold deposit. Analytical hierarchy process (AHP) was used to prioritize the factors affecting mining method selection and ranking of potential mining method, technically appropriate for the established gold deposit in Nebulas Prospect. The appropriate mining methods were identified and ranked in relation to factors such as deposit dip, ore strength, deposit depth, shape and thickness that influence the selection process.

6.2 Conclusion

The geological mapping of the Nebulas Prospect revealed that the area is wholly covered by soil and has limited outcrops exposure. This barred the complete identification of host rocks (such as BIF, schists and quartz veins) associated with the gold mineralization on the surface. However, few outcrops of BIF, tremolite-mica schist were mapped. The Magnetic survey carried out to complement the continuity of host rocks exposed BIF trending east-west and northwest-southeast trending schists.

The prospectivity potential of the Nebulas Prospect was established through application of knowledge driven predictive modelling. Based on the study, it was established that 5% of the Nebulas Prospect is prospective and host significant gold mineralization with grade ranging between 1 and 10 g/t. However, areas which are outside the prospective area have low gold grade that ranges between 0.05 and 0.78 g/t. The general orebody at the Nebulas Prospect comprises a mixture of lithologies with highly erratic gold mineralization. The gold is hosted within the BIF, tremolite-mica schist, serpentine schist and quartz veins. The highest grade of gold is found within the serpentine schist while the BIF host the lowest gold grades. According to Schodde (2011) the world indicated a downward trend of gold ore grades over time, from over 2 g/t in the 1960s to 1980s to less than 1 g/t Au at the present. Thus, the gold grades above 1 g/t observed in the Nebulas Prospect are regarded as economic at the present as compared to 1980 when most mines closed in the GGB.

The developed geological model of the Nebulas Deposit showed that gold deposit type in the Nebulas Prospect resembled a steeply dipping tabular gold deposit which is very narrow (< 10 m). The distribution of gold within the Nebulas study area is continuous both laterally and vertically on the southern part. These deposit parameters supported the selection of practical alternative mining methods.

The selection of a mining method is a complex and multi-attribute decision making process. The dip, thickness, strength, grade, depth, shape of the ore body and strength of the host rock are the main factors influencing the selection of mining method to extract the

established gold deposit. The AHP model simplified the selection of mining method guided by influencing factors such as deposit dip, ore strength, deposit depth, shape and thickness. Based on the AHP method, the gold deposit in the Nebulas Prospect can be effectively mined by open pit mining method. Similar deposits, including West-59 and Frankie mines within the Giyani Greenstone Belt were mined using open pit method.

6.3 Recommendations

The study of gold evaluation is of great importance and the recommendations are elaborated in the following section for both the mining companies and researchers.

6.3.1 Recommendations for practice

Comprehensive work done in this research indicates presence of gold mineralization with grade which is sufficient in most economic case. The current study identified the gold mineralization to a depth of 10 m using pits and trenches. It is recommended that drilling program be conducted to identify potential gold mineralization beyond 10 m depth. The existence of mineralization beyond 10 m will increase the amount of gold resource in the Nebulas Prospect.

6.3.2 Recommendations for research

The selection of mining method is solely based on technical parameter of the deposit. It is recommended that research on gold metallurgy be undertaken to establish the gold recovery potential from the ore through implementation of efficient methods. This may warrant the upgrade from measured mineral resource to measured mineral reserve minable. The results from metallurgical work will support the mine feasibility studies to assess the viability of mining using small-scale open pit mining method.

REFERENCES

Anhaeusser, C.R., 2014. Archaean greenstone belts and associated granitic rocks - A review. J. African Earth Sci. 100, 684–732.

Asadi, H.H., Hale, M., 2001. A predictive GIS model for mapping potential gold and base metal mineralization in Takab area, Iran. Comput. Geosci. 27, 901–912.

Ataei, M., Jamshidi, M., Sereshki, F., Jalali, S.M.E., 2008. Mining method selection by AHP approach. J. South. African Inst. Min. Metall. 108, 741–749.

Basu, P.K., Hicks, J., Krivokapic-Skoko, B., Sherley, C., 2015. Mining operations and corporate social responsibility: A case study of a large gold mine in regional Australia. Extr. Ind. Soc. 2, 531–539.

Billay, A., Sadeghi, M., Carranza, E.J.M., 2014. Predictive Bedrock and Mineral Prospectivity Mapping in the Giyani Greenstone Belt , South Africa.

Bitarafan, M.R., Ataei, M., 2004. Mining method selection by multiple criteria decision making tools. J. South African Inst. Min. Metall. 493–498.

Bogdanovic, D., Nikolic, D., Ivana, I., 2012. Mining method selection by integrated AHP and PROMETHEE method. An. Acad. Bras. Cienc. 84, 219–233.

Bohling, G., 2005. Introduction To Geostatistics And Variogram Analysis. Earth 1–20.

Brady, B.H., Brown, E.T., 2013. Rock mechanics: For underground mining, George Allen & Unwin, London.

Brady, B.H.G., Brown, E.T., 1985. Mining methods and method selection. In: Rock Mechanics. pp. 292–315.

Bustillo Revuelta, M., 2018. Mineral Resource Evaluation. In: Mineral Resources - From Exploration to Sustainability Assessment, Springer Textbooks in Earth Sciences, Geography and Environment. Springer International Publishing, Cham, pp. 223–309.

Carbonel, D., Gutiérrez, F., Linares, R., Roqué, C., Zarroca, M., McCalpin, J., Guerrero, J., Rodríguez, V., 2013. Differentiating between gravitational and tectonic faults by means of geomorphological mapping, trenching and geophysical surveys. The case of the Zenzano Fault (Iberian Chain, N Spain). Geomorphology 189, 93–108.

Carranza, E.J.M., 2009. Geochemical Anomaly and Mineral Prospectivity Mapping in GIS, VOLUME 11. ed.

Carranza, E.J.M., Sadeghi, M., Billay, A., 2015. Predictive mapping of prospectivity for orogenic gold, Giyani greenstone belt (South Africa). Ore Geol. Rev. 71, 703–718.

Cheng, C., Thompson, R.G., 2016. Application of boolean logic and GIS for determining suitable locations for Temporary Disaster Waste Management Sites. Int. J. Disaster Risk Reduct. 20, 78–92.

Clark, I., Harper, W. V, 2007. Practical Geostatistics 2000. EcoSSe North America Llc, Ohio.

Danielson, L., 2003. Artisanal and small-scale mining from an NGO perspective. J. Clean. Prod.

de Beer, J.H., Stettler, E.H., 1992. The Deep-Structure of the Limpopo Belt From Geophysical Studies. Precambrian Res. 55, 173–186.

de Wit, M.J., van Reenen, D., Roering, C., 1992. Geologic observations across a tectono-metamorphic boundary in the Babangu area, Giyani (Sutherland) Greenstone Belt, South Africa. Precambrian Res. 55, 111–122.

Du Plessis, G.A., 2012. National Instrument 43-101 Technical Report for the Klein Letaba, Frankie, Birthday, Horseshoe and Louis Moore Projects, Limpopo Province, South Africa for Rock Island Trading 17 (Pty) Limited ("Rock Island") and Giyani Gold Corp. ("Giyani Gold"). Pretoria.

EduMine, 2018. Mining Rock Mass Rating [Web Document]. URL http://www.edumine.com/xtoolkit/tables/rmrtables.htm#d (accessed 1.25.18).

ESRI, 2017. What is geostatistics? ArcGIS Desktop [Web Document]. URL http://desktop.arcgis.com/en/arcmap/latest/extensions/geostatistical-analyst/what-is-geostatistics-.htm (accessed 2.25.17).

Gandhi, S.M., Sarkar, B.C., 2016. Essentials of Mineral Exploration and Evaluation, Essentials of Mineral Exploration and Evaluation.

Geosoft, 2004. Topics in Gridding. Tech. Work.

Geovariance, 2017. Geostatistics for Mineral Resource Estimation [Web Document]. URL http://www.geovariances.com/en/geostatistics-mineral-resource-estimation/ (accessed 2.25.17).

Goldfarb, R., Groves, D., Gardoll, S., 2001. Orogenic gold and geologic time: a global synthesis. Ore Geol. Rev. 18, 1–75.

Gupta, S., Kumar, U., 2012. An Analytical Hierarchy Process (AHP)-guided decision model for underground mining method selection. Int. J. Mining, Reclam. Environ. 26, 324–336.

Haldar, S.K., 2013. Mineral exploration : principles and applications. Elsevier.

Hartman, H.L., Britton, S.G., 1992. SME mining engineering handbook. Society for Mining, Metallurgy, and Exploration, Inc. Colorado.

Hoover, D.B., Klein, D.P., Campbell, D.C., 1994. Geophysical Methods in Exploration and Mineral Environmental Investigations. F. Geophys. 53, 1689–1699.

Huleatt, M.B., Jaques, A.L., 2005. Australian gold exploration 1976–2003. Resour. Policy 30, 29–37.

Iza, E.R.H., de F., Horbe, A.M.C., Silva, A.M., 2016. Boolean and fuzzy methods for identifying lateritic regoliths in the Brazilian Amazon using gamma-ray spectrometric and topographic data. Geoderma 269, 27–38.

Johnston, K., Ver Hoef, J.M., Krivoruchko, K., Lucas, N., 2003. The principles of geostatistical analysis. Using ArcGIS geostatistical Anal. 49–80.

Joint Ore Reserves Committee, 2012. The JORC Code 2012 Edition 1–44.

Karimnia, H., Bagloo, H., 2015. Optimum mining method selection using fuzzy analytical hierarchy process-Qapiliq salt mine, Iran. Int. J. Min. Sci. Technol. 25, 225–230.

Kassim, M., Heo, G., Kessel, D.S., 2016. A systematic methodology approach for selecting preferable and alternative sites for the first NPP project in Yemen. Prog. Nucl. Energy 91, 325–338.

Kirilin, A., Akhmetov, R., Kurenkov, V., Stratilatov, N., Abrashkin, V., Kucherov, A., Safronov, S., Yakishchik, A., 2015. Generation of Land Remote Sensing Satellites Conceptual Design Based on Regard to Required Efficiency Indices. Procedia Eng. 104, 65–75.

Kokesz, Z., 2006. Application of linear geostatistics to evaluation of Polish mineral deposits.

Kramers, J.D., Henzen, M., Steidle, L., 2014. Greenstone belts at the northernmost edge of the Kaapvaal Craton: Timing of tectonic events and a possible crustal fluid source. Precambrian Res. 253, 96–113.

Kröner, A., Jaeckel, P., Brandl, G., 2000. Single zircon ages for felsic to intermediate rocks from the Pietersburg and Giyani greenstone belts and bordering granitoid orthogneisses, northern Kaapvaal Craton, South Africa. J. African Earth Sci. 30, 773–793.

Lelubre, M., 1982. Archean greenstone belts, Precambrian Research.

Liu, C., Nie, F., Bagas, L., 2016. Geology and ore genesis of the Yu'erya gold deposit, eastern Hebei Province, China. Ore Geol. Rev. 73, 270–283.

Macdonald, E.H., 2007. Handbook of Gold Exploration and Evaluation, Handbook of Gold Exploration and Evaluation.

Marin, T., Seccatore, J., De Tomi, G., Veiga, M., 2015. Economic feasibility of responsible small-scale gold mining. J. Clean. Prod. 129, 531–536.

Marjoribanks, R., 2010. Geological Methods in Mineral Exploration and Mining. Springer, Berlin, Heidelberg.

Mathibe, B., 2012. Sustainability in the South African gold mining industry: managing a paradox. University of Pretoria.

Matthew, V., 2004. Hasn't Colorado Already Been Mapped ? Color. Geol. Surv. RockTalk 7, 1–12.

McCourt, S., van Reenen, D., 1992. Structural geology and tectonic setting of the Sutherland Greenstone Belt, Kaapvaal Craton, South Africa. Precambrian Res. 55, 93–110.

McCourt, S., Vearncombe, J.R., 1992. Shear zones of the Limpopo Belt and adjacent granitoid-greenstone terranes: implications for late Archaean collision tectonics in southern Africa. Precambrian Res. 55, 553–570.

Metelka, V., Baratoux, L., Naba, S., Jessell, M.W., 2011. A geophysically constrained litho-

structural analysis of the Eburnean greenstone belts and associated granitoid domains, Burkina Faso, West Africa. Precambrian Res. 190, 48–69.

Miller, L., Pakalnis, R., R, P., 1995. UBC Mining Method Selection, Mine Planning and Equipment Selection. In: Singhal, R.K., Poulin, R., Mehmotra, A.K., Hadjigeorgiou, J. (Eds.), Mine Planning and Equipment Selection. CRC Press.

Moon, J.C., Whateley, M.K.G., Evans, A.M. (Eds.), 2009. Introduction to mineral exploration, 2nd ed. Wily-Blackwell.

Musingwini, C., Minnitt, R.C.A., 2008. Ranking the efficiency of selected platinum mining methods using the analytic hierarchy process (AHP). Third Int. Platin. Conf. "Platinum Transform. 319–326.

Muzerengi, C., 2013. Gold-Suphide Mineralisation in the Giyani Greenstone Belt: Case Studies at Black Mountain and West 59 Targets, Limpopo Province, South Africa. University of Venda.

Nicholas, D.E., 1992. Selection Procedure. In: Hartman, H.L. (Ed.), Mining Engineering Handbook. Society for Mining , Metallurgy, and Exploration, pp. 2090–2106.

Plessis, S.J., Joubert, R., 2009. Case Study : Dighem survey for non-magnetic dyke detection ; Dorstfontein colliery , Total Coal RSA 134–142.

Porwal, A., Carranza, E.J.M., 2015. Introduction to the Special Issue: GIS-based mineral potential modelling and geological data analyses for mineral exploration. Ore Geol. Rev. 71, 477–483.

Prol-Ledesma, R.M., 2000. Evaluation of the reconnaissance results in geothermal exploration using GIS. Geothermics 29, 83–103.

Ravengai, S., Love, D., Mabvira-Meck, M., Musiwa, K., Moyce, W., 2005. Water quality in an abandoned gold mining belt, Beatrice, Sanyati Valley, Zimbabwe. Phys. Chem. Earth, Parts A/B/C 30, 826–831.

Ren, Y.-S., Chen, C., Zou, X.-T., Zhao, H.-L., Hao, Y.-J., Hou, H.-N., Hu, Z.-C., Jiang, G.-H., 2016. The age, geological setting, and types of gold deposits in the Yanbian and adjacent areas, NE China. Ore Geol. Rev. 73, 284–297.

Robert, F., Poulsen, K.H., Dubé, C.P., 1997. Gold Deposit and their Geological Classification. In: Gubins, A.G. (Ed.), Fourth Decennial International Conference on Mineral Exploration. Exploration Geochemistry, pp. 209–220.

Saaty, T.L., 1980. The Analytic Hierarchy Process: Planning, Priority Setting, Resource Allocation, 2nd ed. McGraw-Hill, New York.

Sadeghi, M., Billay, A., Carranza, E.J.M., 2015. Analysis and mapping of soil geochemical anomalies: Implications for bedrock mapping and gold exploration in Giyani area, South Africa. J. Geochemical Explor. 154, 180–193.

Saldarriaga-Isaza, A., Arango, S., Villegas-Palacio, C., 2015. A behavioral model of collective action in artisanal and small-scale gold mining. Ecol. Econ. 112, 98–109.

SAMREC, 2007. The South African code for the reporting of exploration results, mineral resources and mineral reserves 2.

Sarris, A., Galaty, M.L., Yerkes, R.W., Parkinson, W.A., Gyucha, A., Billingsley, D.M., Tate, R., 2004. Geophysical prospection and soil chemistry at the Early Copper Age settlement of Vésztó-Bikeri, Southeastern Hungary. J. Archaeol. Sci. 31, 927–939.

Schodde, R., 2011. Recent trends in gold discovery Recent trends in gold discovery. MinEx Consult. Pty Ltd 22–23.

Seccatore, J., Marin, T., De Tomi, G., Veiga, M., 2014. A practical approach for the management of resources and reserves in Small-Scale Mining. J. Clean. Prod. 84, 803–808.

Smit, C.A., van Reenen, D.D., Roering, C., 2014. Role of fluids in the exhumation of the Southern Marginal Zone of the Limpopo Complex, South Africa. Precambrian Res. 253, 81–95.

Steenkamp, N.C., Clark-Mosterrt, V., 2012. Inferred Historic Gold Mining Approaches , Giyani Greenstone Belt , South Africa. In: 9th International Mining History Congress. Johaness, pp. 1–11.

Sten, J., Lilja, H., Hyväluoma, J., Westerholm, J., Aspnäs, M., 2016. Parallel flow accumulation algorithms for graphical processing units with application to RUSLE model. Comput. Geosci. 89, 88–95.

Swash, P.M., 1988. A mineralogical investigation of refractory gold ores and their beneficiation , with special reference to arsenical ores. J. South African Inst. Min. Metall. 88, 173–179.

Telford, M.W., Geldart, L.P., Sheriff, R.E., 1990. Applied geophysics, 2nd ed. Cambridge University Press, New York.

Ugarkar, A.G., Malapur, M.A., Chandan Kumar, B., 2016. Archean turbidite hosted orogenic gold mineralization in the Gadag greenstone belt, Western Dharwar Craton, Peninsular India. Ore Geol. Rev. 72, 1224–1242.

Van Reenen, D.D., Huizenga, J.M., Smit, C.A., Roering, C., 2014. Fluid-rock interaction during high-grade metamorphism: Instructive examples from the Southern Marginal Zone of the Limpopo Complex, South Africa. Precambrian Res. 253, 63–80.

Vaughan, J.P., 2004. The process mineralogy of gold: The classification of ore types. Jom 56, 46–48.

Yamatomi, J., Okubo, S., 2009. Surface mining methods and equipment. Civ. Eng. II 2, 154.

Yavuz, M., 2015. The application of the analytic hierarchy process (AHP) and Yager's method in underground mining method selection problem. Int. J. Mining, Reclam. Environ. 29, 453–475.

Žalik, B., Mongus, D., Žalik, K.R., Lukač, N., 2017. Boolean operations on rasterized shapes represented by chain codes using space filling curves. J. Vis. Commun. Image Represent. 49, 420–432.

Zoheir, B., Emam, A., 2012. Integrating geologic and satellite imagery data for high-resolution mapping and gold exploration targets in the South Eastern Desert, Egypt. J. African Earth Sci. 66–67, 22–34.

APPENDICES

Appendix A: Location data merged with magnetic readings data

Table A-1: Magnetic Data for Survey Lines 1 -4

LINE 1					LINE 2				
X	Y	Z	Reading	STA.	X	Y	Z	Reading	STA.
271380	7433800	472.9	29716.6	203	271400	7433640	477.0	33253.1	186
271380	7433790	473.0	29698.0	202	271400	7433650	477.1	37244.1	185
271380	7433780	473.1	29729.8	201	271400	7433660	476.1	35977.4	184
271380	7433770	473.2	29915.6	200	271400	7433670	475.5	34683.6	183
271380	7433760	473.3	29967.7	199	271400	7433680	475.1	32404.8	182
271380	7433750	473.5	30209.5	198	271400	7433690	474.8	31329.5	181
271380	7433740	473.6	30145.9	197	271400	7433700	474.2	31566.8	180
271380	7433730	473.8	30180.4	196	271400	7433710	473.8	29880.5	179
271380	7433720	474.0	30179.4	195	271400	7433720	473.6	30158.0	178
271380	7433710	474.3	30520.7	194	271400	7433730	473.6	30085.7	177
271380	7433700	474.6	30840.6	193	271400	7433740	473.5	29814.9	176
271380	7433690	475.0	31353.2	192	271400	7433750	473.1	30040.5	175
271380	7433680	475.4	31517.2	191	271400	7433760	473.1	29945.9	174
271380	7433670	475.8	31821.2	190	271400	7433770	472.7	29787.2	173
271380	7433660	476.2	33221.0	189	271400	7433780	472.6	29720.9	172
271380	7433650	476.6	35718.7	188	271400	7433790	472.6	29712.9	171
271380	7433640	476.8	37762.1	187	271400	7433800	472.6	29645.6	170
LINE 3					**LINE 4**				
X	Y	Z	Reading	STA.	X	Y	Z	Reading	STA.
271420	7433800	472.2	29651.3	169	271440	7433640	477.0	31969.5	152
271420	7433790	472.3	29858.2	168	271440	7433650	476.6	22399.3	151
271420	7433780	472.4	29428.3	167	271440	7433660	475.7	34234.9	150
271420	7433770	472.5	30335.5	166	271440	7433670	475.0	32458.2	149
271420	7433760	472.7	29580.6	165	271440	7433680	474.5	31655.0	148
271420	7433750	472.9	29708.6	164	271440	7433690	474.2	30777.0	147
271420	7433740	473.1	30031.6	163	271440	7433700	473.7	30684.6	146
271420	7433730	473.1	29954.9	162	271440	7433710	473.3	30151.7	145
271420	7433720	473.4	30029.0	161	271440	7433720	473.0	30022.5	144
271420	7433710	473.6	30055.7	160	271440	7433730	472.8	30166.7	143
271420	7433700	473.9	30590.1	159	271440	7433740	472.6	30309.6	142
271420	7433690	474.4	31096.8	158	271440	7433750	472.3	29772.3	141
271420	7433680	474.9	31488.7	157	271440	7433760	472.3	30241.9	140
271420	7433670	475.5	32046.7	156	271440	7433770	472.2	29704.9	139
271420	7433660	476.1	33200.6	155	271440	7433780	472.1	29607.7	138
271420	7433650	476.7	34841.7	154	271440	7433790	472.0	29257.8	137
271420	7433640	477.1	26057.8	153	271440	7433800	471.8	29596.0	136

Table A-2: Magnetic Data for Survey Lines 5-9

LINE 5	LINE 6

X	Y	Z	Reading	STA.
271460	7433800	471.4	29603.0	135
271460	7433790	471.7	29683.0	134
271460	7433780	471.8	29735.0	133
271460	7433770	471.8	29741.1	132
271460	7433760	471.5	29744.2	131
271460	7433750	471.8	29828.8	130
271460	7433740	471.9	29960.0	129
271460	7433730	472.0	30120.9	128
271460	7433720	472.3	30158.8	127
271460	7433710	472.6	29979.3	126
271460	7433700	472.9	30437.0	125
271460	7433690	473.3	31051.9	124
271460	7433680	473.4	31947.9	123
271460	7433670	474.1	32548.4	122
271460	7433660	474.9	32542.7	121
271460	7433650	475.6	34550.6	120
271460	7433640	476.3	34326.5	119

X	Y	Z	Reading	STA.
271480	7433640	474.8	32539.1	118
271480	7433650	473.9	26068.7	117
271480	7433660	473.3	36444.6	116
271480	7433670	472.7	34271.8	115
271480	7433680	472.2	33457.6	114
271480	7433690	471.7	32107.6	113
271480	7433700	471.3	31185.0	112
271480	7433710	471.0	31516.7	111
271480	7433720	470.8	30032.1	110
271480	7433730	470.8	29994.0	109
271480	7433740	470.8	30170.5	108
271480	7433750	470.9	29908.9	107
271480	7433760	470.7	29736.1	106
271480	7433770	471.0	29657.0	105
271480	7433780	471.0	29575.2	104
271480	7433790	470.9	29531.5	103
271480	7433800	470.8	29694.6	102

LINE 7				
X	Y	Z	Reading	STA.
271500	7433800	470.3	29649.1	101
271500	7433790	469.8	29521.7	100
271500	7433780	470.2	29695.5	99
271500	7433770	469.9	29406.0	98
271500	7433760	470.2	29646.3	97
271500	7433750	470.3	29708.0	96
271500	7433740	470.2	29693.0	95
271500	7433730	470.0	29629.5	94
271500	7433720	469.9	29329.0	93
271500	7433710	469.9	30055.7	92
271500	7433700	470.2	30143.4	91
271500	7433690	470.0	30663.1	90
271500	7433680	470.6	31397.1	89
271500	7433670	471.1	31998.8	88
271500	7433660	471.8	32231.8	87
271500	7433650	472.7	25959.1	86
271500	7433640	473.0	34991.3	85

LINE 4				
X	Y	Z	Reading	STA.
271520	7433640	471.1	31711.7	84
271520	7433650	470.6	32480.9	83
271520	7433660	469.9	28042.2	82
271520	7433670	469.4	30937.4	81
271520	7433680	469.0	31184.3	80
271520	7433690	468.8	30059.6	79
271520	7433700	468.9	30594.3	78
271520	7433710	468.9	29467.2	77
271520	7433720	468.9	30001.1	76
271520	7433730	468.8	29751.3	75
271520	7433740	468.7	29914.6	74
271520	7433750	468.6	29586.3	73
271520	7433760	468.5	29537.3	72
271520	7433770	468.4	29530.2	71
271520	7433780	468.3	29500.0	70
271520	7433790	468.1	29456.7	69
271520	7433800	467.8	29173.1	68

Table A-1: Magnetic Data for Survey Lines 9 -4

LINE 9	LINE 10

X	Y	Z	Reading	STA.
271540	7433800	465.7	29492.3	67
271540	7433790	465.7	29394.5	66
271540	7433780	466.1	29490.8	65
271540	7433770	466.4	29405.3	64
271540	7433760	466.8	29434.8	63
271540	7433750	467.0	29488.4	62
271540	7433740	467.1	29578.5	61
271540	7433730	467.5	29466.6	60
271540	7433720	467.9	29606.4	59
271540	7433710	468.0	30020.9	58
271540	7433700	468.0	29584.9	57
271540	7433690	468.0	29693.9	56
271540	7433680	468.1	29958.1	55
271540	7433670	468.2	29993.5	54
271540	7433660	468.3	29914.4	53
271540	7433650	468.5	26072.0	52
271540	7433640	468.8	30061.4	51

X	Y	Z	Reading	STA.
271560	7433640	467.7	29114.8	50
271560	7433650	467.7	29067.0	49
271560	7433660	467.7	29661.9	48
271560	7433670	467.7	31248.9	47
271560	7433680	467.7	28560.7	46
271560	7433690	467.7	29604.4	45
271560	7433700	467.7	29513.1	44
271560	7433710	467.6	29544.8	43
271560	7433720	467.3	29477.5	42
271560	7433730	466.9	29524.3	41
271560	7433740	466.5	30089.4	40
271560	7433750	466.1	29384.1	39
271560	7433760	465.7	29561.7	38
271560	7433770	465.4	29438.8	37
271560	7433780	465.1	29221.2	36
271560	7433790	464.7	29191.1	35
271560	7433800	464.7	29247.9	34

LINE 11

X	Y	Z	Reading	STA.
271580	7433800	464.4	29183.9	33
271580	7433790	464.5	29210.9	32
271580	7433780	464.7	29223.1	31
271580	7433770	465.0	29234.2	30
271580	7433760	465.3	29297.6	29
271580	7433750	465.7	29310.9	28
271580	7433740	466.1	29354.3	27
271580	7433730	466.4	29496.4	26
271580	7433720	466.8	29386.7	25
271580	7433710	467.0	29373.0	24
271580	7433700	467.2	29214.9	23
271580	7433690	467.3	29509.1	22
271580	7433680	467.4	30426.6	21
271580	7433670	467.4	29143.0	20
271580	7433660	467.4	29188.3	19
271580	7433650	467.3	29276.7	18
271580	7433640	467.3	29377.8	17

LINE 12

X	Y	Z	Reading	STA.
271600	7433640	467.0	29280.0	16
271600	7433650	467.1	28995.2	15
271600	7433660	467.1	29476.0	14
271600	7433670	467.1	29277.0	13
271600	7433680	467.1	29180.3	12
271600	7433690	467.0	29238.6	11
271600	7433700	466.8	29202.4	10
271600	7433710	466.6	29209.2	9
271600	7433720	466.4	29306.4	8
271600	7433730	466.1	29241.8	7
271600	7433740	465.8	29208.3	6
271600	7433750	465.5	29188.0	5
271600	7433760	465.2	29006.0	4
271600	7433770	464.9	29154.6	3
271600	7433780	464.7	29103.1	2
271600	7433790	464.5	29100.5	1
271600	7433800	464.4	29176.3	0

Appendix B: Gold assay results and average weighted grade calculation per trench

The Following Equation was used to calculated average weighted gold in grams per ton (g/t) for different mineralisation intervals

$$\bar{G}_w = \frac{Ga_1 + G_2a_2 + G_na_n}{a_1 + a_2 + \cdots a_n} = \frac{\sum_{i=1}^{n} G_i a_i}{\sum_{i=1}^{n} a_i}$$

$\boldsymbol{G_1}$ to $\boldsymbol{G_n}$ are the values (gold grade in g/t) whose weighted average is to be determined, $\boldsymbol{a_1}$to $\boldsymbol{a_n}$ are the weighting factors (mineralization length, volume or block tonnage), $\bar{\boldsymbol{G}}_{\boldsymbol{w}}$ is the weighted average Grade.

Table AP 1. 1: Trench No 1 Gold Assay Results (Au (g/t)- $\boldsymbol{G_i}$) and Weighted Grade Calculations ($\bar{\boldsymbol{G}}_{\boldsymbol{w}}$- Au g/t)

SAMPLE NO	Sample Length (m)- $\boldsymbol{a_i}$	**From (m)**	**To (m)**	Au (g/t)- $\boldsymbol{G_i}$
TH1-1	1.8	8.5	10.3	0.93
TH1-2	1.9	10.3	12.2	0.47
Total Trench Length	3.7	Average Grade Au (g/t) - $\bar{\boldsymbol{G}}_{\boldsymbol{w}}$		0.69g/t for 3.7m

Table AP 1. 2: Trench No 2 Gold Assay Results (Au (g/t)- $\boldsymbol{G_i}$) and Weighted Grade Calculations ($\bar{\boldsymbol{G}}_{\boldsymbol{w}}$- Au g/t)

SAMPLE NO	Sample Length (m)- $\boldsymbol{a_i}$	**From (m)**	**To (m)**	Au (g/t)- $\boldsymbol{G_i}$
TH2-1	0.3	3.7	4	2.49
Total Trench Length	4	Average Grade Au (g/t) - $\bar{\boldsymbol{G}}_{\boldsymbol{w}}$		2.49g/t for 0.3m

Table AP 1. 3 Trench No 3 Gold Assay Results (Au (g/t)- $\boldsymbol{G_i}$) and Weighted Grade Calculations ($\bar{\boldsymbol{G}}_{\boldsymbol{w}}$- Au g/t)

SAMPLE NO	Sample Length (m)- $\boldsymbol{a_i}$	**From (m)**	**To (m)**	Au (g/t)- $\boldsymbol{G_i}$
TH3-1	1.8	1.8	3.6	1.24
Total Trench Length	3.6	Average Grade Au (g/t) - $\bar{\boldsymbol{G}}_{\boldsymbol{w}}$		1.24 g/t for 1.8 m

Table AP 1. 4: Trench No 4 Gold Assay Results (Au (g/t)- G_i) and Weighted Grade Calculations ($\bar{G}_w$- Au g/t)

SAMPLE NO	Sample Length (m)- a_i	From (m)	To (m)	Au (g/t)- G_i
TH4-1	3.7	0	3.7	0.23
TH4-2	3.7	3.7	7.4	0.23
TH4-3	2.4	7.4	9.8	0.28
TH4-4	2.1	9.8	11.9	1.3
TH4-5	2.6	11.9	14.5	0.5
TH4-6	3.7	14.8	18.5	0.09
Total Trench Length	18.2	Average Grade Au (g/t) - $\bar{G}_w$		0.37 g/t for 18 m
TH4-4 only	2.1	Average Grade Au (g/t) - $\bar{G}_w$		1.3 g/t for 2.1 m

Table AP 1. 5: Trench No 5 Gold Assay Results (Au (g/t)- G_i) and Weighted Grade Calculations ($\bar{G}_w$- Au g/t)

SAMPLE NO	Sample Length (m)- a_i	From (m)	To (m)	Au (g/t)- G_i
TH5-1	0.9	2.3	3.2	1.4
TH5-2	1	3.2	4.2	3.11
TH5-3	0.7	4.2	4.9	6.07
TH5-4	0.6	4.9	5.5	0.31
(TH5-1 To TH5-4)	3.2	Average Grade Au (g/t) - $\bar{G}_w$		2.75 g/t for 3.2 m
(TH5-1 To TH5-3)	2.6	Average Grade Au (g/t) - $\bar{G}_w$		3.32 g/t for 2.1 m
(TH5-2 To TH5-3)	1.7	Average Grade Au (g/t) - $\bar{G}_w$		4.33 g/t for 1.7 m

Table AP 1. 6: Trench 6 Gold Assay Results (Au (g/t)- G_i) and Weighted Grade Calculations ($\bar{G}_w$- Au g/t)

SAMPLE NO	Sample Length (m)- a_i	From (m)	To (m)	Au (g/t)- G_i
TH6-1	1.2	5.5	6.7	0.78
TH6-2	1.5	6.7	8.2	0
TH6-3	1.6	8.2	9.8	0
TH6-4	1.5	9.8	11.3	0
TH6-5	1.2	11.3	12.5	0.16
TH6-6	1.5	12.5	14	0.78
TH6-7	1.6	14	15.6	0
TH6-8	1.5	15.6	17.1	0
TH6-9	1.8	22.3	24.1	0
TH6-10	1.2	25.8	27	0
TH6-11	0.3	27	27.3	0.62
TH6-12	1.2	27.3	28.5	0.16
TH6-13	1.6	28.5	30.1	0.16
TH6-14	1.5	30.1	31.6	0
TH6-1	1.2	Average Grade Au (g/t) - $\bar{G}_w$		0.78 g/t for 1.2 m
TH6-5 To TH6-6	2.7	Average Grade Au (g/t) - $\bar{G}_w$		0.50 g/t for 2.7 m
TH5-11 To TH6-13	3.1	Average Grade Au (g/t) - $\bar{G}_w$		0.20 g/t for 1.7 m

Table AP 1. 7: Trench 7 Gold Assay Results (Au (g/t)- G_i) and Weighted Grade Calculations ($\bar{G}_w$- Au g/t)

SAMPLE NO	Sample Length (m)- a_i	From (m)	To (m)	Au (g/t)- G_i	Au (g/t) - $\bar{G}_w$
TH7-1	1.2	0	1.2	0	
TH7-2	1.2	1.2	2.4	0	
TH7-3	1.3	2.4	3.7	0	
TH7-4	1.2	3.7	4.9	0	
TH7-5	1.2	4.9	6.1	0	
TH7-6	1.2	6.1	7.3	0.16	
TH7-7	1	7.3	8.3	0.08	0.26 (g/t) Au for 4.2 m
TH7-8	0.8	8.3	9.1	0.08	
TH7-9	1.2	9.1	10.3	0.62	
TH7-10	1.8	10.3	12.1	0	
TH7-11	1.9	12.1	14	0	
TH7-12	1.5	14	15.5	0	
TH7-13	1.5	15.5	17	0	
TH7-14	1.5	17	18.5	0	
TH7-15	1.6	18.5	20.1	0	
TH7-16	1.5	20.1	21.6	1.09	
TH7-17	1.5	21.6	23.1	0.31	0.49 (g/t) Au for 6.4 m
TH7-18	1.5	23.1	24.6	0.31	
TH7-19	1.9	24.6	26.5	0.31	
TH7-20	0.9	26.5	27.4	2.03	
TH7-21	0.3	27.4	27.7	4.03	
TH7-22	1.5	27.7	29.2	6.34	
TH7-23	1.5	29.2	30.7	3.6	4.6 (g/t) Au for 7.9 m
TH7-24	0.9	30.7	31.6	10.65	
TH7-25	0.6	31.6	32.2	6.45	
TH7-26	1.1	32.2	33.3	2.54	
TH7-27	1.1	33.3	34.4	2.49	
TH7-28	0.8	34.4	35.2	0.78	
TH7-29	0.9	35.2	36.1	0.47	
TH7-30	1.5	36.1	37.6	0.47	
TH7-31	0.6	37.6	38.2	0.62	0.47 (g/t) Au for 8.4 m
TH7-32	1.5	38.2	39.7	0.16	
TH7-33	1.6	39.7	41.3	0.93	
TH7-34	1.5	41.3	42.8	0.08	
TH7-35	1.5	42.8	44.3	0	
TH7-36	1.7	44.3	46	0	

Table AP 1. 8: Trench 8 Gold Assay Results (Au (g/t)- G_i) and Weighted Grade Calculations ($\bar{G}_w$- Au g/t)

SAMPLE NO	Sample Length (m)- a_i	From (m)	To (m)	Au (g/t)- G_i	Au (g/t) - $\bar{G}_w$
TH8-1	1.4	2	3.4	2.34	3 g/t for 4 m
TH8-2	0.7	3.4	4.1	0.44	
TH8-3	1.9	4.1	6	4.44	
TH8-4	1.5	6	7.5	0.4	0.4 g/t for 6.1 m
TH8-5	1.6	7.5	9.1	0.53	
TH8-6	1.5	9.1	10.6	0.35	
TH8-7	1.5	10.6	12.1	0.34	
TH8-8	1.6	12.1	13.7	2.93	2.93 g/t for 1.6

Table AP 1. 9: Trench 9 Gold Assay Results (Au (g/t)- G_i) and Weighted Grade Calculations ($\bar{G}_w$- Au g/t)

SAMPLE NO	Sample Length (m)- a_i	From (m)	To (m)	Au (g/t)- G_i	Au (g/t) - $\bar{G}_w$
TH9-1	1.2	11	12.2	0.62	0.374 g/t for 3 m
TH9-2	0.6	12.2	12.8	0.31	
TH9-3	1.2	12.8	14	0.16	
TH9-4	1.8	14	15.9	0	
TH9-5	1.2	15.9	17.1	0	
TH9-6	1.1	17.1	18.2	0.16	0.16 g/t for 1.1 m
TH9-7	1.4	18.2	19.5	0	
TH9-8	0.9	19.5	20.4	0	
TH9-9	1.8	20.4	22.3	0	
TH9-10	1.8	22.3	24.1	0	
TH9-11	1.8	24.1	25.9	0	
TH9-12	1.2	25.9	27.2	2.18	2.18 g/t for 1.2m
TH9-13	1.2	27.2	28.4	0.02	0.06 g/t for 1.1 m
TH9-14	1.8	28.4	30.2	0.08	

Table AP 1. 10: Trench 10 Gold Assay Results (Au (g/t)- G_i) and Weighted Grade Calculations ($\bar{G}_w$- Au g/t)

SAMPLE NO	Sample Length (m)- a_i	From (m)	To (m)	Au (g/t)- G_i	Au (g/t) - $\bar{G}_w$
TH10-1	1.2	0	1.2	0.31	
TH10-2	1.2	1.2	2.4	0.16	
TH10-3	1.2	2.4	3.7	0.93	0.53 g/t for 6 m
TH10-4	1.2	3.7	4.9	0.78	
TH10-5	1.2	4.9	6.1	0.47	
TH10-6	1.2	6.1	7.3	0	
TH10-7	1.2	7.3	8.5	0.62	
TH10-8	1.2	8.5	9.8	0.93	
TH10-9	1.2	9.8	11	0.47	0.57 for 6 m
TH10-10	1.2	11	12.2	0.54	
TH10-11	1.2	12.2	13.4	0.31	
TH10-12	0.7	13.4	14.1	0.16	
TH10-13	0.5	14.1	14.6	0.31	
TH10-14	0.6	14.6	15.2	0.31	0.31 for 6 m
TH10-15	0.8	15.2	15.9	0.62	
TH10-16	0.6	15.9	16.6	0.16	
TH10-17	1.2	16.6	17.8	0.31	
TH10-18	1.2	17.8	19	0.78	
TH10-19	1.2	19	20.2	0.47	0.41 for 6 m
TH10-20	1.2	20.2	21.4	0.31	
TH10-21	1.2	21.4	22.6	0.16	
TH10-22	1.2	22.6	23.9	0.16	
TH10-23	1.2	23.9	25.1	0.31	
TH10-24	1.2	25.1	26.3	0.08	0.14 for 6 m
TH10-25	1.2	26.3	27.5	0	
TH10-26	1.5	27.5	29	0.16	
Total Length	6.3	Average Grade Au (g/t)		0.42 g/t Au	

Table AP 1. 11 Pit 1 and 2 gold assay results

SAMPLE NO	Sample Length (m)	Depth (m)	Description	Au (g/t)
TH7-1	1.2	1	Pit opening	3.8
TH7-2	1.2	5	Pit bottom	4.2
TH7-3	1.2	1	Pit opening	1.2
TH7-4	1.2	10	Pit bottom	1.9